Rubisco and inorganic carbon assimilation

Katia Wostrikoff, Luke C M Mackinder

Chapter 7
Rubisco and inorganic carbon assimilation
Katia Wostrikoff[1] and Luke C.M. Mackinder[2]
[1]Sorbonne Université, CNRS, Paris, France
[2]University of York, UK

Key Words: Rubisco, CO_2 concentrating mechanism, CCM, photosynthesis

Abstract:

Ribulose-1,5-bisphosphate carboxylase/oxygenase (Rubisco) is the entry point of CO_2 into the Calvin- Benson Cycle (CBC), connecting the inorganic carbon and organic carbon realms making it arguably one of the most important enzymes on Earth. Chlamydomonas has proven to be a powerful model for understanding Rubisco biogenesis, function, regulation and engineering with this chapter highlighting the core findings in the field of Chlamydomonas Rubisco biology over the last several decades. In addition to performing carboxylation, Rubisco also performs an energy wasteful oxygenation reaction that results in photorespiration. To minimize photorespiration Chlamydomonas operates a highly effective CO_2 concentrating mechanism (CCM) that increases the CO_2: O_2 ratio at the active site of Rubisco reducing oxygenation of the ribulose-1,5-bisphosphate substrate. The CCM involves an interplay between carbonic anhydrases, inorganic carbon transporters and structural components to move inorganic carbon against its concentration gradient from the external environment to a specialized sub-chloroplast structure called the pyrenoid. Rapid advances in understanding CCM function highlighted in this chapter, including recent discoveries concerning the importance of Rubisco structure for its condensation into the pyrenoid, has merged the Rubisco and CCM fields and laid the groundwork for what is expected to be an exciting decade for Rubisco and CCM research.

Table of content

I. Introduction

The Calvin- Benson Cycle (CBC) links the inorganic carbon and organic carbon worlds. The CBC, driven by ATP and NADPH produced via the light reactions of photosynthesis (see Chapters 8, 15-19), fixes carbon dioxide (CO_2) into organic carbon that forms the basis of energy flow into the biosphere and drives the global carbon cycle. At the heart of the CBC is the enzyme Ribulose-1,5-bisphosphate carboxylase/oxygenase (Rubisco), that catalyzes the initial fixation of CO_2 to ribulose-1,5-bisphosphate (RuBP). In chlorophytes, Rubisco is an hetero-oligomeric enzyme, composed of a plastid encoded large subunit (LS) and a nuclear encoded small subunits (SS) that assemble into the so-called form I LS_8SS_8 holoenzyme, which has been crystallized from *Chlamydomonas* (Taylor et al., 2001; Mizohata et al., 2002). Combining genetics with the ability to modify both the plastid encoded LS and introduce variants for the nuclear encoded SS has led to the establishment of *Chlamydomonas* as a robust model for studying Rubisco function, expression, regulation, assembly (section II) and engineering strategies (sections III). Beside its essential role in CO_2 fixation, the high intracellular Rubisco abundance (section V.A) and the ability cell's to rapidly remobilized it under nutrient stress conditions makes it

an important amino-acid reservoir (section IV). Lastly, LS displays a moonlighting function in RNA metabolism (section V.B) that may be physiologically important under oxidative stress conditions, whereas SS has multiple roles in Rubisco holoenzyme stabilization, catalysis and condensation in the pyrenoid (section VI.D).

In addition to performing carboxylation, Rubisco performs an energy wasteful oxygenation reaction that results in photorespiration. To minimize the Rubisco oxygenation reaction *Chlamydomonas* operates an effective CO_2 concentrating mechanism (CCM) that maintains a high level of CO_2 at the active site of Rubisco even under severe CO_2 limiting conditions. *Chlamydomonas* has the most intensively studied eukaryotic algal CCM with an accumulation of research over the past four decades that has identified the core components, their structural and functional importance and how the CCM integrates with other cellular processes (section VI). Recent tools and technical advances in the last decade including the availability of a large mapped mutant library, high resolution transcriptomics and proteomics, and large-scale localization approaches have accelerated our understanding of CCM function. Combined with detailed biochemical, cell biology and structural studies, researchers have identified many additional CCM components, revealing novel regulatory roles and the importance of the pyrenoid in CCM function. This new wealth of data on CCM function, including discoveries concerning the importance of Rubisco structure for its condensation in the pyrenoid, has merged the Rubisco and CCM fields and laid the groundwork for what is expected to be an exciting decade for Rubisco research.

II. Rubisco biogenesis

In *Chlamydomonas* as in all chlorophytes, genes encoding Rubisco subunits no longer cluster within an operon, as is the case in cyanobacteria and plastids of non-green algae (Martin et al., 1998). While the *rbcL* gene encoding LS is still plastid-encoded, *RBCS* genes are nucleus-encoded. The splitting of the LS-SS operon allows novel regulations (section I) but also introduces additional challenges for the stoichiometric production of Rubisco subunits, which ultimately assemble into the LS_8SS_8 functional holoenzyme (section I.B).

A. *rbcL* and *RBCS* gene organization and expression

In *Chlamydomonas*, the chloroplast *rbcL* gene lies within the small single-copy region, immediately upstream of *trnG2*. It is transcribed divergently from *atpA* (Maul et al., 2002) and located in a region of the plastid genome where DNA superhelicity responds to light (Salvador et al., 1998), which may have regulatory implications. The *rbcL* promoter contains a canonical -10 Pribnow box and is one of the two most active promoters in the chloroplast genome (Blowers et al., 1990; Klein et al., 1994). Transcription occurs over the entire cell cycle (Herrin et al., 1986; Salvador et al., 1993a) and generates a triphosphorylated primary transcript (first mapped by (Dron et al., 1982)) that is not further processed (Johnson et al., 2010; Cavaiuolo et al., 2017), and has cis-regulatory elements within the UTRs (described below).

1. cis- regulatory elements within the *rbcL* transcript:

a- *Maturation element within rbcL 3' UTR:*

The *rbcL* 3' UTR contains two stem-loop structures designated IR1 and IR2. The transcript ends two nucleotides after IR2, generating an 87 nucleotide-long 3'UTR (Goldschmidt-Clermont et al., 2008). The stem-loops are not able to promote efficient termination of transcription (Rott et al., 1996). Instead, *rbcL* mRNA 3' end maturation was shown to depend on a two-step process involving endonucleolytic cleavage and 3' exonucleolytic resection, as modeled for *atpB* (Stern and Kindle, 1993), where the endonucleolytic cleavage destabilizes downstream sequences (Hicks et al., 2002; Rymarquis et al., 2006). A genetic screen using a chimeric gene fused to the *rbcL* 3' UTR identified a sequence specific element in IR2 and two nuclear loci, *TAS1* and *TAS2,* involved in 3'UTR processing (Goldschmidt-Clermont et al., 2008). These findings suggested a model in which the IR2 specific element recruits an endonuclease to induce downstream cleavage. The TAS1 and TAS2 proteins could be involved either directly through binding to IR2, or indirectly. Interestingly, in the absence of the TAS1 and TAS2 transcripts, the *rbcL* transcript still accumulates and is processed, which makes the exact functions of TAS1 and TAS2 uncertain. Furthermore, the IR1 and IR2 cis-elements act redundantly to stabilize the transcript against exonucleolytic decay since *rbcL* mRNA stabilization was only impaired when both elements were deleted (Goldschmidt-Clermont et al., 2008).

b- The *rbcL 5'UTR contains a stabilizing element*

The 92 nt long *rbcL* 5' UTR is highly structured with two experimentally confirmed stem-loop (Anthonisen et al., 2001) (Figure 1) and a third predicted stem-loop that traps the initiation codon (Dron et al., 1982). Interestingly, an RNA-stabilizing element that maps to the base of the first stem-loop and the single-stranded region that connects the first and second stem-loop was identified (nucleotides +38 to +47 with respect to the +1 transcriptional start site). Mutations within this element dramatically alter the stability of a chimeric *rbcL-gus* transcript in which part of the *rbcL* 5'UTR (1-63) is fused to the *gus* coding sequence (CDS) (Anthonisen et al., 2001). Although the first stem loop structure is required for *rbcL* transcript stabilization, neither its sequence nor its length constitutes key determinants. Rather the loop structure itself is required to confer the proper conformation to the downstream stabilizing element (Suay et al., 2005). Based on the instability of chimeric *rbcL-gus* transcripts bearing extensions longer than 6 nucleotides at the 5' end of the mature transcript, an additional factor involved in transcript stability has been proposed: some RNA stability could be conferred through shielding the *rbcL* triphosphorylated first nucleotide from a 5' to 3' ribonuclease by trapping it in the first stem loop structure (Salvador et al., 2011). The involvement of 5'-to-3' ribonucleases in *rbcL* transcript decay became apparent from the stability conferred by a polyG cage added to the *rbcL* 5' terminus (Salvador et al., 2011).

2. MRL1, an organellar trans-regulatory factor for *rbcL* expression

a. MRL1 is a pentatricopeptide repeat (PPR) protein, conserved in higher plants

A common feature to most, if not all, chloroplast-encoded transcripts is their long half-lives conferred by RNA stabilizing proteins (Chapter 13). A single organellar

trans-acting factor, MRL1, is required for *rbcL* mRNA stabilization. MRL1 belongs to the small family of PPR proteins in *Chlamydomonas* and bears 12 PPR motifs that would fold in an alpha solenoidal structure allowing its specific binding to a 12 nt target within the *rbcL* 5'UTR, whose tentative localization is indicated in Figure 1 (Johnson et al., 2010)(Cre06.g298300, Table 1). MRL1 possesses a second conserved domain, the "C-domain", that is predicted to fold into α helices (Tourasse et al., 2013) and is required for function. Whether it participates in conferring the overall helicoidal structure to the 140 kDa MRL1 or has additional roles in RNA binding is unknown. Binding of MRL1 to the *rbcL* 5'UTR protects the transcript from 5'-to-3' exonucleolytic degradation. Interestingly, MRL1 is one of the few examples of organellar trans-acting factors that are conserved throughout the green lineage, but absent from Rhodophyta, Cyanophora and secondary symbionts (Tourasse et al., 2013). Although conserved within the green lineage, the phenotypes of *mrl1* mutants differ slightly between species. In Arabidopsis, where the *rbcL* mRNA is processed, the *mrl1* mutant lacks only the processed transcript (Johnson et al., 2010), while *rbcL* transcripts are completely missing in *Chlamydomonas mrl1* mutants. MRL1 in *Chlamydomonas* belongs to a high molecular weight complex whose accumulation depends on the presence of the *rbcL* transcript. Recently, MRL1 was identified by proteomics as part of the ribosome interactome. It preferentially interacts with the 30S ribosome subunit but is also present in the 50S ribosome interactome (Westrich et al., 2021), suggesting that it remains bound to the *rbcL* transcript during translation, although it is not known whether MRL1 is required for translation ***per se***.

b. MRL1 footprint?

So far, MRL1's binding site has not been unambiguously identified. One obvious binding target would be the stabilizing element identified by (Anthonisen et al., 2001), even though this sequence is shorter than MRL1's predicted target. According to the generally accepted model, MRL1 binding would generate a small RNA footprint by protecting the mRNA binding target from degradation. Bioinformatic approaches based on the sRNA miner program (Ruwe et al., 2016) applied to high-throughput sequenced sRNA libraries generated in two independent studies (Loizeau et al., 2014; Cavaiuolo et al., 2017) identified two distinct protected fragments in the *rbcL* 5'UTR. One maps to the first stem-loop of the *rbcL* transcript (Cavaiuolo et al., 2017), which is unlikely to represent MRL1's target since the role of this stem-loop is not sequence specific (Suay et al., 2005). Protection of this sequence may result from an overall higher stability conferred by the stem loop. The second protected fragment identified by (Loizeau et al., 2014) encompasses the stabilizing element and extends between the first and the second stem loop (Figure 1). Whether this region is indeed MRL1's target awaits further experimental validation.

c. MRL1, a regulator of rbcL gene expression?

If MRL1 is in limiting amounts, then its level of expression may define the level of accumulation of *rbcL* transcripts. This is seemingly the case: complementation of *mrl1* null mutants by random insertion of an *MRL1* transgene allowed recovery of photosynthetic strains with varying levels of *rbcL* transcript and LS protein accumulation (Johnson, 2011). Use of a tagged version of MRL1 established a link between the levels of the *rbcL* transcript, the LS proteins and accumulation of the MRL1 protein (Wietrzynski, 2017). Thus, manipulating MRL1 levels may be used to

manipulate carbon metabolism (Johnson, 2011). It is not yet known if and how MRL1 levels and/or activity are themselves regulated. Interestingly, MRL1 is part of the *Chlamydomonas* phosphoproteome (Wang et al., 2014) and displays at least four confidently mapped phospho-sites of unknown significance.

d. MRL1 expression

MRL1 expression appears to be upregulated in high CO_2 conditions (Phytozome/GeneAtlas2.0). In synchronized cultures exposed to a 12 h light-12 h dark diurnal cycle, MRL1 transcript peaks soon after the onset of light before decreasing until reaching midday, and then increasing again during the second part of the day and into the night (Strenkert et al., 2019). This pattern is somewhat paralleled by that of the *rbcL* mRNA in the same cultures (Strenkert et al., 2019), in agreement with the idea that the MRL1 level dictates *rbcL* mRNA accumulation levels. However, it should be noted that the amplitude of *rbcL* mRNA cycling appears to be lower than other photosynthetic genes (Herrin et al., 1986; Idoine et al., 2014). Curiously, in non-synchronized cultures, *MRL1* transcript accumulation is lower under phototrophic than mixotrophic conditions, while the level of the *rbcL* mRNA is similar between the two conditions (Cavaiuolo et al., 2017). This is not in accord with the observation that in mixotrophically grown cultures MRL1 levels dictate the accumulation of *rbcL* mRNA, unless the MRL1 protein stability is itself affected by the culture conditions; the MRL1 protein could be more stable under phototrophic conditions, compensating for lower of RNA levels.

3. Localized *rbcL* translation

rbcL translation has long been shown to be upregulated in the light versus the dark period in synchronized cells (Herrin et al., 1986; Sun and Zerges, 2015). While in most cases, there is a good correlation between *rbcL* mRNA accumulation and LS translation levels (Trosch et al., 2018), examination of the rifampicin-independent rate of LS synthesis, either in the light phase of synchronized cells or in non-synchronized mixotrophically grown cultures (Herrin et al., 1986; Eberhard et al., 2002) helped establish chloroplast translation as a major regulatory step in its accumulation in *Chlamydomonas* (Eberhard et al., 2002). How LS synthesis varies according to environmental fluctuations is further developed in section A.5 with an in-depth discussion of chloroplast translation in Chapter 14. Nonetheless, it is interesting to note that the pyrenoid, whose major constituent is Rubisco (section VI.D), has been proposed to behave as a structural organizing center for translation. *In situ* observations using fluorescent probes have revealed that light induces *rbcL* transcripts to localize to regions at the outer perimeter of the pyrenoid, but that are distinct from the T-zones, which are on the pyrenoid's lateral sides and defined by the presence of some chloroplast encoded transcripts (Uniacke and Zerges, 2007). *rbcL* mRNA localization was shown to depend on its translation (Uniacke and Zerges, 2009), with newly synthesized LS fractionating with the pyrenoid (Zhan et al., 2018). As the plastid ribosome S21 translation marker itself is not detected in the pyrenoid (Sun et al., 2019), LS synthesis probably occurs in close proximity to the pyrenoid, which results in entrapment of newly synthesized LS during pyrenoid purification. Noteworthy, the pyrenoid is not required for LS synthesis, as evidenced by unaltered Rubisco levels in several pyrenoid deficient CCM mutants (exemplified for EPYC1 mutant in (Mackinder et al., 2016)). Whether and to what extent LS translation is associated with biogenic

membranes is unclear. While LS translation has been linked to membrane-bound polysomes in isolated barley chloroplast (Muhlbauer and Eichacker, 1999), more recent work in maize has indicated that *rbcL* ribosome footprints come largely from the stromal fraction (Zoschke and Barkan, 2015).

4. *RBCS* gene regulation

Chlamydomonas RBCS genes encoding Rubisco small subunit (SS) constitute a small multigene family composed of two genes, *RBCS1/2* (Cre02.g120100 and Cre02.g120150, table 1), which are adjacent on the genome. The close proximity of these genes has allowed the isolation of null mutants in which both genes were inactivated (Khrebtukova and Spreitzer, 1996; Dent et al., 2005). The two RBCS proteins differ by only four amino acids (Goldschmidt-Clermont, 1986) and are functionally redundant since both genes can rescue a *RBCS* deletion mutant (Khrebtukova and Spreitzer, 1996), even though the mRNA from the *RBCS2* gene is about four-fold higher than that of *RBCS1* (Goldschmidt-Clermont, 1986; Zones et al., 2015; Strenkert et al., 2019). *RBCS* genes respond to light and culture medium at the transcriptional level, and are more highly expressed in phototrophic than in mixotrophic conditions (Goldschmidt-Clermont, 1986). In synchronous cultures grown phototrophically, *RBCS* transcripts increase upon the onset of light, with *RBCS1* peaking slightly later in the day than *RBCS2* (Zones et al., 2015; Strenkert et al., 2019). *RBCS* transcripts then decrease at the end of the day (Strenkert et al., 2019). Curiously*, RBCS2* exhibits a more pronounced decrease in the dark over a 12 h warm day/12 h cold night rhythm, which mimics the growth of *Chlamydomonas* in its natural environment (Strenkert et al., 2019), compared to growth at constant temperature (Zones et al., 2015) where *RBCS2* expression remained high during the dark period. Whether this reflects a temperature effect or differences in light fluences is unknown.

Apart from being regulated by light, medium composition and diurnal cycles, *RBCS* genes were described as targets of retrograde signaling, which leads to down-regulation of nuclear-encoded genes in response to altered chloroplast metabolism or impaired chloroplast translation (reviewed in (Johanningmeier, 1988; Nott et al., 2006)). A differential effect on *RBCS1/2* has been observed, with *RBCS1* being more responsive than *RBCS2* (Johanningmeier, 1988). Furthermore, it has been suggested that some mRNAs encoded by nuclear genes could undergo a localized translation next to the chloroplast envelope, but this is not the case for *RBCS* genes since *RBCS2* transcripts were not enriched in the vicinity of the chloroplast (Uniacke and Zerges, 2009).

Noteworthy, *RBCS* regulatory elements have been widely used for robust transgene expression in *Chlamydomonas*, as described in Vol 1, Chapter 12. The features of the gene being used include the *RBCS2* promoter, either in its original configuration (Fuhrmann et al., 2001) or as the more efficient hybrid *HSP70A-RBCS2* promoter fusion (Schroda et al., 1999), the *RBCS2* first intron (reviewed in (Schroda, 2019)), shown to contain a transcriptional enhancer (Lumbreras and Purton, 1998), the sequence encoding the transit peptide, engineered to contain the *RBCS1/2* intron enhancing element (Genkov et al., 2010), and the *RBCS2* terminator, although the latter does not confer strong expression (reviewed in (Schroda, 2019)). Most of these parts are available as compatible ‘biobricks’ for modular cloning from the *Chlamydomonas* MoClo Toolkit (Crozet et al., 2018).

5. Changes in gene expression in response to environmental cues

In response to changes in the environment, *Chlamydomonas* cells undergo both transcriptional and post-transcriptional regulation of the Rubisco-encoding genes, which helps balance the production of Rubisco subunits. Translation is a key regulated step for *rbcL*, which is discussed below and in the Chapters 14 and 19.

a. Expression changes in response to trophic conditions

Contrary to *RBCS*, *rbcL* expression is not dramatically influenced by whether the cells are cultured in nutrient replete minimal or acetate- supplemented medium: comparable levels of *rbcL* RNA accumulation (Cavaiuolo et al., 2017) and translation rates were observed under mixotrophic (includes acetate) and phototrophic conditions (Eberhard et al., 2002; Trosch et al., 2018), even if in some cases LS synthesis can be uncoupled from *rbcL* mRNA levels (Herrin et al., 1986; Eberhard et al., 2002). Furthermore, *rbcL* expression is not strongly influenced by the light intensity (Uniacke and Zerges, 2009). Nonetheless, in synchronized cultures, light has been shown to trigger degradation of untranslatable chimeric transcripts generated by fusing part of the *rbcL* promoter and 5'UTR to the *gus* coding sequence (the chimeric transcript is stable in the dark) (Salvador et al., 1993b). This behavior is not observed for endogenous *rbcL* transcripts, indicating that a second sequence element, mapped to the *rbcL* coding sequence (Singh et al., 2001), is counteracting the photo-activated transcript decay. Furthermore, this degradation is not prevented by polyG addition to the *rbcL* 5' end (Salvador et al., 2011), implying that endonucleases and not solely 5'-to-3' exonucleases are involved in the degradation process. Other chimeric genes, such as a *rbcL* 5'UTR-cytochrome *f* fusion, do not show this light-instability in cultures maintained in continuous light (Johnson et al., 2010). Whether the instability depends on the culture conditions or on the chimeric gene context is not known. Curiously a decrease in *rbcL* mRNA accumulation induced by rifampicin treatment has a different outcome for the LS synthesis rate depending on the culture conditions. While the rate of LS synthesis is unaffected in mixotrophic conditions, a marked decrease is observed for cells grown phototrophically in continuous light (Eberhard et al., 2002). Whether this difference is correlated to a decrease in MRL1 expression or its stability during the rifampicin treatment under phototrophic conditions, or to the decreased stability of the mRNA stability for other transcripts involved in chloroplast gene expression is unknown.

Nutrient stress on the other hand, notably sulfur and nitrogen starvation, result in a rapid decrease within the first 24 hours of deprivation in *RBCS* (Schmollinger et al., 2014; Majeran et al., 2019) and/or *rbcL* transcript levels (Irihimovitch and Stern, 2006; Majeran et al., 2019). In response to sulfur starvation, the latter was shown to be in partly due to a rapid global repression of chloroplast transcription, resulting from the decreased availability of the chloroplast SIG1 sigma factor, which is mediated by the SAC3 (*SNRK2.2*) kinase (Irihimovitch and Stern, 2006). Furthermore, while LS synthesis is not significantly affected during the first 48 hours of sulfur deprivation (Majeran et al., 2019), the Rubisco is actively degraded (see IV.B).

b. Circadian changes in synchronized cells.

In synchronous cultures, *rbcL* is one of the first photosynthetic genes induced, with its transcript peaking after a few hours of illumination (1 h after onset of light in (Strenkert et al., 2019) and 4 h after the onset of light in (Herrin et al., 1986)); *RBCS*

induction follows shortly after that of *rbcL*. The rate of LS synthesis is low in the dark, but peaks early in the light compared to other photosynthetic genes, and then declines after 2 h of illumination and resumes after an additional 8 h (Sun et al., 2019). Whether light-induced LS synthesis is due to a release of inhibition exerted at the translation elongation step, as proposed for land plants (Kim and Mullet, 2003), remains unknown.

c. Changes in expression depending on CO_2 concentration

Shifting cells from high to low CO_2 results in a transitory decline of both LS and SS synthesis rates, which returns to the original rate after 8 h (Winder et al., 1992). Notably, the shift does not affect *rbcL* or *RBCS* transcript accumulation, suggesting post-transcriptional regulation potentially associated with induction of the carbon concentrating mechanism (CCM).

d. Changes in expression after a shift to high light

Within 15 min of exposing *Chlamydomonas* to high light (HL, ~700 µmol photons m^{-2} s^{-1}), there is a transient decrease in LS translation without a concomitant decrease in *rbcL* or *RBCS* mRNA. After ~6 h in HL the LS synthesis rate rebounds to the level observed for low light grown cells (Shapira et al., 1997). The mechanism associated with this translation inhibition has been characterized in-depth. It is triggered by an imbalance in the reduced/oxidized glutathione pool (GSS/GSSG), a low molecular mass thiol having a regulatory role in algae and plants and associated with the generation of reactive oxygen species (Irihimovitch and Shapira, 2000). The decline in the rate of LS synthesis and decreased holoenzyme assembly stems from inhibition of translation early in the elongation phase (Cohen et al., 2005), as deduced from the observation that *rbcL* mRNA becomes associated with smaller sized polysomes. Translational inhibition upon oxidative stress is proposed to occur through autoregulation by LS, which would no longer be able to dimerize, either because of oxidative induced structural changes or because of altered binding of LS to an oxidized chaperone (Yosef et al., 2004; Cohen et al., 2005; Cohen et al., 2006). As a result of this inability to dimerize, the LS N-terminal domain, which under reducing conditions is buried in the holoenzyme at the intradimeric interface, would be unmasked and free to bind to *rbcL* mRNA, resulting in translation inhibition. Whether the mechanisms associated with inhibition of *rbcL* translation in response to oxidative stress and as a consequence of the Control by Epistasy of Synthesis (CES) (Chapter 19 and section B.4) are shared is uncertain. However, in the case of oxidative stress, translational inhibition would rely on altering the dimer interface which would expose the RbcL RNA Recognition Motif, while in the case of CES, repression has been shown to require accumulation of the LS octamer (Cohen et al., 2006; Wietrzynski et al., 2021).

B. Rubisco holoenzyme assembly

Since the last edition of the Chlamydomonas Sourcebook, tremendous progress in our understanding of the Rubisco assembly pathway has been obtained. Strikingly, although the composition of the Rubisco complex is simple, its assembly, and especially LS core subunit folding and oligomerization, is an assisted process involving several chaperones. Rubisco has thus emerged as a paradigm of chaperone-assisted assembly based on the characterization of plant mutants that has revealed various auxiliary factors that act as chaperones, in-depth characterizations of these factors by recombinant co-expression with cyanobacterial LS, and co-crystallization of assembly

products. These studies culminated in the recombinant production of plant Rubisco (in *E. coli*), an unachieved goal for more than two decades (Aigner et al., 2017). Several recent reviews highlight these findings (Bracher et al., 2017; Vitlin Gruber and Feiz, 2018; Hayer-Hartl and Hartl, 2020), and therefore we will focus on the association of the assembly pathway as it applies to *Chlamydomonas*, as diagrammed in Figure 1.

1. Folding of LS requires the CPN60 chaperonin

Nascent LS requires the CPN60 chaperonin for folding. The nanocage formed by the CPN60A and CPN60B subunits is arranged in two stacked hetero-heptameric rings topped by a hetero-oligomeric heptamer-formed by the CPN11/20/23 cofactor proteins. The chaperonin encapsulates LS, creating the specific hydrophilic environment required for folding and for preventing unproductive hydrophobic contacts leading to aggregation. A more in-depth description of the function of CPN60, whose major but not sole substrate is LS, is provided in Chapter 20. Importantly, the GroEL bacterial homolog of CPN60 does not fold plant LS, indicating that CPN60A/B has acquired features to promote the recruitment of plant nascent LS (Aigner et al., 2017). In plants, mutations in one of the CPN60A encoding paralogs abolishes LS accumulation, which suggests a specific recruitment of LS by this isoform (Feiz et al., 2012; Kim et al., 2013). Similarly, the *Chlamydomonas* CPN60A isoform has been found to recognize LS more efficiently than the CPN60B isoforms (Zhang et al., 2016), leading to a model in which CPN60A would recruit LS while CPN60B would allow oligomerization of the nanocage (reviewed in (Vitlin Gruber and Feiz, 2018)). Additional substrate-specificity may also be conferred by varying the composition of the CPN11/20/23 cofactor ring (Zhao et al., 2019). Copurification of CPN60A with affinity-tagged ribosomes suggests that nascent LS delivery to the chaperonin occurs co-translationally (Westrich et al., 2021).

2. LS oligomerization is a chaperone-assisted process

Folded LS rapidly dimerizes, as free LS monomers are not detected under native conditions (Wietrzynski et al., 2021). The dimer forms through the interaction of two LS subunits in a head-to-tail configuration and involves hydrogen bonding, salt bridges and polar interactions. Among the many residues at the LS dimeric interface (van Lun et al., 2011), two pairs of conserved amino-acids (E109-R253 and E110-R213 in *Chlamydomonas*) are critical for dimerization of Rubisco form I. LS dimerization is followed by a second oligomerization step, yielding LS octamers in the form of tetramers of antiparallel dimers. Adjacent LS dimers form two different interfaces stabilized by hydrogen bonds (van Lun et al., 2011).

a- The RBCX and RAF1 chaperones

Two unrelated chaperones, RBCX and RAF1 are involved in the LS dimerization step. They may either promote dimerization and/or stabilize the resulting dimers. Interestingly, both chaperones are conserved in photosynthetic organisms as distantly related as cyanobacteria and vascular plants. Even though RBCX and RAF1 are seemingly involved in the same process, their respective binding sites on LS differ, as observed in structures obtained after co-crystallization of cyanobacterial LS with RBCX or RAF1 expressed in *E. coli* (Bracher et al., 2011; Hauser et al., 2015; Huang et al., 2020; Xia et al., 2020), which hints at a different mode of action. In cyanobacteria, RbcX is a 15 kDa protein functioning as a boomerang-shaped dimer (Bracher et al.,

2011) that binds to a conserved motif at LS-C-terminus and also to residues in the intradimeric adjacent LS N-terminal domain. Two orthologous genes are found in plants, but *Chlamydomonas* only has the *RBCX2* orthologue, for which there are two paralogs (Bracher et al., 2015). Noteworthy, RBCX2A might be the dominant functional form as its transcripts are 20 to 50 times more abundant than those for RBCX2B. RBX2B is not a canonical RBCX isoform as it bears a long protein extension at its C-terminus. RBCX2A knock-down strains in *Chlamydomonas* showed reduced Rubisco accumulation (Hauser, 2016), suggesting a role of RBCX in Rubisco assembly. Similarly, partial inactivation of the *rbcX* gene located within the Rubisco operon of the cyanobacterium *Synechococcus* PCC 7002 led to a severe reduction in Rubisco abundance, although a polar effect of the lesion on the downstream *rbcS* gene cannot be excluded (Onizuka et al., 2004). On the other hand, deleting *rbcX* had no apparent effect on the cyanobacterium *Synechococcus* PCC7942. However *rbcX* in this cyanobacterium is no longer localized within the Rubisco operon (Emlyn-Jones et al., 2006); this makes it unclear whether RbcX is required for assembly. The current model places RBCX as a facilitator of Rubisco assembly, as yields of expression of plant recombinant LS are higher in its presence (Aigner et al., 2017). Interestingly, RBCX2A has been identified in *Chlamydomonas* as one of the chaperones induced in a ClpP deficient strain as part of the chloroplast unfolded response (Ramundo and Rochaix, 2014).

The second chaperone involved in LS oligomerization is the RAF1 factor (Rubisco Accumulation Factor 1). RAF1 is a 50 kDa protein in *Chlamydomonas*, slightly larger than its cyanobacterial or plant counterparts. It functions as a dimer, which brackets the LS dimer at the top and bottom by binding extensively across LSs (Hauser et al., 2015). In *Chlamydomonas*, $RAF1_2$-LS_2 dimers are detected in wild-type strains, suggesting that they constitute true assembly intermediates. Yet dimers without RAF1 could also be observed under conditions in which LS is translated at high rates while assembly is impaired. Therefore, RAF1 is not required for LS dimerization but rather for dimer stabilization and appears to be in limiting amounts (Wietrzynski et al., 2021). Interestingly, RAF1 displays a binding interface to an adjacent LS dimer, as observed in cyanobacterial $RAF1_8$-LS_8 structures (Huang et al., 2020; Xia et al., 2020), and may hence have a further role in the tetramerization of LS dimers. In *Chlamydomonas* SS mutants, LS and RAF1 comigrate in a LS_8-RAF1 complex, which could constitute a second assembly intermediate *in vivo* (Wietrzynski et al., 2021).

b- The RAF2 chaperone

Beside the extensively characterized RBCX and RAF1 chaperones, a third conserved chaperone in plants and algae is the RAF2 factor (Rubisco accumulation 2, Feiz et al., 2014), which encodes an inactive form of Pterin Carbinolamin Dehydratase, also known as CGL31. Knock-outs of RAF2 in maize accumulate 10% of the wild type levels of Rubisco, while the phenotype is less severe in Arabidopsis (Fristedt et al., 2018). The mode of RAF2 action remains poorly understood. Does it serve as a SS chaperone, as suggested by its interaction with SS in co-immunoprecipitation experiments in maize (Feiz et al., 2014), or is it involved in LS core stabilization as suggested by the fact that RAF2 is required for recombinant production of plant LS (Aigner et al., 2017) in the absence of SS? Further experiments are needed to better understand its function in the assembly pathway.

c- *Is there a Chlamydomonas orthologue for the plant BSD2 chaperone?*

A fourth auxiliary factor, BSD2, is required for Rubisco assembly in plants (Brutnell et al., 1999). BSD2 is a small DNA-J like protein of ~10 kDa containing zinc-finger binding motifs. The crescent-shaped protein, arranged in a hairpin around two zinc ions, has been crystallized in a $BSD2_8$-LS_8 complex, in which BSD2 monomers bind to either side of the LS_2 dimer (Aigner et al., 2017). An *in vivo* interaction with LS is suggested by comigration of Rubisco and BSD2 in tobacco chloroplast extracts (Conlan et al., 2019). Interestingly, BSD2 is not present in cyanobacteria containing Rubisco Form IB, and as such, may represent a post-endosymbiotic innovation. It is tempting to speculate that it might fulfill a function related to the decoupled SS production occurring in eukaryotes from the green lineage. Interestingly, a $BSD2_8$-LS_8 complex was observed when SS amounts were limiting, which may suggest that in plants a $BSD2_8$-LS_8 complex is the end-state intermediate before SS binding. Based on the BSD2 binding interface and insertion into the RuBP substrate binding pocket, it has been proposed that BSD2 may stabilize LS in an open conformation preventing RuBP binding before the formation of mature Rubisco (Aigner et al., 2017). In *Chlamydomonas*, two proteins containing zinc-finger motifs have been proposed to represent BSD2 orthologues: ZNJ2 (Cre03.g201050), which has chaperone activity and comigrates with polysomal fractions associated with *rbcL* transcripts (Doron et al., 2014), although its role in Rubisco biogenesis has not been established, and ZNJ6 (Cre06.g251716) (Doron et al., 2018). The latter is not likely involved in Rubisco biogenesis since it is a thylakoid associated DNAJ-like chaperone that may participate in the unfolded chloroplast response during temperature stress (Amiya and Shapira, 2021).

3. SS-binding to LS octamer confers structural stability

a- *Formation of Rubisco holoenzyme*

The ultimate assembly step in Rubisco maturation requires binding of SS to the chaperone-protected LS_8 core, yielding Rubisco LS_8SS_8, where four SS subunits cap both the top and bottom of the LS octamer (see Fig. 2). In *Chlamydomonas*, SS binding probably occurs by displacement of RAF1 from a RAF1-LS octamer. *In vitro* work showed that both RBCX and RAF1 interactions with cyanobacterial LS are very dynamic and easily dislodged from their respective $RbcX_8$-LS_8 and $RAF1_8$-LS_8 complexes upon SS addition (Liu et al., 2010; Hauser et al., 2015; Kolesinski et al., 2017). Interestingly, cyanobacterial RAF1 was able to displace $RBCX_8$ in $RBCX_8$-LS_8 complexes yielding $RAF1_8$-LS_8, which suggests sequential action of RBCX followed by RAF1 (Kolesinski et al., 2017). Furthermore, cyanobacterial tripartite RAF1-LS-SS complexes have been obtained and crystallized with either 4 or 8 SS bound to $RAF1_8$-LS_8 (Xia et al., 2020). Comparing the $RAF1_8$-LS_8 and RAF1-LS-SS structures reveals a SS-induced shift in RAF1 position, explaining the dynamic and sequential nature of RAF1 displacement. Whether SS also requires interaction with chaperones, such as the RAF2, is still unknown.

b- *Hybrid Rubisco assembly reveals a relaxed requirement for SS assembly*

SS assembly within the holoenzyme appears to be a less constrained process compared to LS core assembly. LS and its assembly chaperones show strong

coevolution, leading to difficulties in generating Rubisco hybrid enzymes in vivo using non-native LS (Kanevski et al., 1999; Whitney and Andrews, 2001), unless the cognate RAF1 chaperone is co-expressed (Whitney et al., 2015). In contrast, expression of plant SS (spinach, Arabidopsis and sunflower) with the native *Chlamydomonas rbcL* gene yielded functional hybrid Rubisco that accumulated to WT levels in Chlamydomonas and supported photosynthetic growth comparable to that of WT cells, provided that the cultures were grown in a high CO_2 environment; in the strains with the plant-*Chlamydomonas* hybrid enzyme were impaired for the CCM (and therefore required high CO_2) because no pyrenoid could form in the absence of Chlamydomonas SSU ((Genkov et al., 2010) and VI.D). Similarly, *Chlamydomonas* SS could complement Arabidopsis *RBCS* knock-down plants that express the Arabidopsis LS core (Atkinson et al., 2017). These relaxed assembly constraints are also congruent with the fact that SS is far more divergent among clades than LS, although their structure is well conserved.

c- SS binding confers stability to the LS core

One of the main functions of Rubisco SS is its indisputable contribution to holoenzyme stability. In *Chlamydomonas*, this is evidenced by the phenotype of SS-lacking mutants that express LS with a 5' *psaA* UTR: in this strain LS synthesis remains high in the absence of SS, but it only accumulates to trace amounts (Khrebtukova and Spreitzer, 1996; Wietrzynski et al., 2021).

Rubisco stability is usually assessed by measuring the level of Rubisco accumulation at either 25°C or 35°C, a more restrictive condition. A second proxy consists in assaying the thermal stability of the purified enzyme as a function of activity along a temperature gradient. Taking advantage of the impressive mutagenesis studies performed on *Chlamydomonas* Rubisco over the years, mostly in Spreitzer's laboratory, important SS regions involved in holoenzyme stability were defined which, not unexpectedly, map to the LS/SS interface regions (van Lun et al., 2011). It should be noted however that mutations of individual amino acids within SS that alter stability do not prevent Rubisco assembly. These residues are:

i) The conserved L18, Y32 and E43 residues of SS in contact with the LS α-helix 8 region, a structural element of the α/β barrel contributing to the active site (see Figure 2). Alanine substitutions of these residues induce a large decrease in Rubisco accumulation even though the strains may still be phototrophic (Genkov and Spreitzer, 2009). The Y32 residue in particular has been proposed to shield LS charged amino acids (R431 and N432) from the solvent. Noticeably, the E43 residue provides additional stabilizing contact with the LS α-helix 1 through an ionic bond with LS R187,

ii) The βA/βB loop (aa 46-73; see Fig. 2), which early on was referred to as an assembly domain (Wasmann et al., 1989). This loop is located between the βA and βB strands and is at the entrance of the solvent channel where it contacts LS at two interfaces (van Lun et al., 2011). This region of SS shows the highest divergence among species, largely because of its variable length: it consists of 28 amino acids in *Chlamydomonas* but only 22 in land plants (Spreitzer, 2003). Noteworthy, the loop size is not an essential determinant for assembly but contributes to stability as indicated by the differential phototrophic phenotypes of hybrid enzymes with a *Chlamydomonas* LS core and cyanobacterial SS, which has a loop of only 10 aa. While phototrophic at 25°C, mutants in the βA/βB loop display a strong decrease in Rubisco levels at 35°C concurrent with a loss of phototrophy (Karkehabadi et al., 2005). Similarly, mutations

N54S, A57V and C65S were isolated as suppressors of the temperature-sensitive LS mutant L290F by restoring holoenzyme stability (Du et al., 2003; Genkov et al., 2006). Alanine- scanning mutagenesis within the βA/βB loop also identified the conserved R71 residue as contributing to stability: the mutant displays both a reduction in the enzyme's thermal stability and in Rubisco accumulation at 35°C (Spreitzer et al., 2001). This phenotype may result from disruption of one of the six ionic bonds between the LS and SS subunits. Furthermore, a cluster of tyrosine residues (Y67, Y68, Y72) provides stability through aromatic interactions with LS residues. Alanine substitution mutants were photoautotrophic, but the modified Rubisco was inactivated at a lower temperature than the wild type enzyme and showed up to a 90% decrease in holoenzyme accumulation at 35°C for the Y67A and Y72A mutants. This decrease results from conformational changes, followed by changes in the kinetics of subtilisin-induced proteolysis (Esquivel et al., 2006). The aromatic interactions also contribute positively to the stabilization of Rubisco against accelerated turnover under oxidative conditions –all mutants of SS in the tyrosine residues of the loop cluster were shown to degrade faster than the wild type Rubisco in cells experiencing oxidative stress (Esquivel et al., 2006).

4. Checkpoints/misassembly

Productive assembly of Rubisco with correctly folded proteins is controlled at multiple steps, allowing the concerted accumulation of both subunits. Invariably, in the absence of its assembly partner, neither the LS nor SS accumulate to significant levels due to processes involving either proteolysis or regulation of synthesis (Figure 1), as detailed below.

Proteolysis plays an important role in Rubisco homeostasis. Unassembled SS has been shown to undergo rapid degradation, with a half-life of less than 7.5 minutes, as observed in ribosomal mutants displaying impaired LS synthesis or in the presence of a chloroplast translation inhibitor (Mishkind and Schmidt, 1983; Schmidt and Mishkind, 1983). Degradation of unassembled SS is mediated by the Clp protease (Majeran et al., 2019).

On the other hand, a reduction or absence of SS leads to inhibition of LS synthesis (Khrebtukova and Spreitzer, 1996). This regulation of translation - known as the CES process and described in more detail in Chapter 19 - relies on regulation of translation initiation by unassembled LS. Recent work indicates that the repressor form would consist of a high molecular weight LS_8 complex in association to some extent with RAF1 (Wietrzynski et al., 2021). Interestingly, translation inhibition yields reduced LS synthesis rates that are still higher than the rates needed to produce the trace amounts of LS that accumulate. Thus, in the absence of SS, LS accumulation levels are determined both by the CES process and by degradation of unassembled LS. Furthermore, the extent of degradation of LS is inversely correlated to the amount of LS that can be stabilized by the limiting RAF1 chaperone (Wietrzynski et al., 2021).The importance of proteolysis of unassembled LS is further illustrated in some LS assembly-incompetent mutants that escape CES regulation and display a high rate of LS synthesis, and yet hardly accumulate either LS or SS. These results indicate that both subunits are prone to degradation, even though mutated LS undergoes, to some

extent, the folding process, since they are found associated with the CPN60 chaperone (Majeran et al., 2019; Wietrzynski et al., 2021). The inability to reduce the ClpP content in these LS mutants indirectly indicates that removal of unassembled LS by the Clp protease is essential for the cell homeostasis and survival (Majeran et al., 2019). In some instances, insoluble aggregates of unassembled LS and SS were observed (Wietrzynski, 2017), perhaps due to overloading the protease capacity of the chloroplast. Together, these results suggest that in the absence of ClpP, LS/ SS aggregates become too burdensome for the cell, thereby eliciting an autophagy-like response that leads to cell death (Ramundo and Rochaix, 2014).

5. Post-translational modifications: which, when and why?

Protein N-termini are proposed to be an important determinant of protein stability in chloroplasts, by a process termed the N-end rule, which states that specific amino-acids at the N-terminal will target proteins for degradation (Rowland et al., 2015; Bouchnak and van Wijk, 2019). After LS-N-formyl methionine at position 1 is deformylated and excised, residue S2 is further processed and P3 is acetylated (Houtz et al., 1992). These N-terminal modifications occur co-translationally and in a sequential manner. Actinonin, which inhibits peptide deformylases (PDF), prevents N-terminal processing, which indicates that deformylation precedes M1 excision (by Methionine aminopeptidase, MAP) and other N-terminal modifications. Surprisingly, Chlamydomonas strain in which LS N-terminal processing is blocked (actinonin treatment) still assembleRubisco (Giglione et al., 2003). Dual organellar-targeted orthologues of PDF1b and MAP1D have been identified in Chlamydomonas, but the enzymes specifically involved in LS N-terminal serine removal and proline acetylation are still unknown. While seven aminopeptidases, among which is a serine aminopeptidase, have been identified in the *Arabidopsis* chloroplast proteome, their substrate specificity, and more specifically their involvement in LS N-terminal processing have not been experimentally tested (Zybailov et al., 2008). Additionally, 8 members of the N-acetyltransferases encoding gene family (GNAT) have been shown to be chloroplast-localized and characterized in plants (Bienvenut et al., 2020). Although all GNATs exhibited broad substrate specificity, a single member, GNAT7, was found to be able to acetylate proline residues (Bienvenut et al., 2020; Giglione and Meinnel, 2021). Interestingly, a GNAT7-homologous N-acetyltransferase, cpNAT1 (Cre14.g614750), has recently been identified in *Chlamydomonas* and shown to be ribosome associated (Zybailov et al., 2008; Westrich et al., 2021), but its role inRubisco N-terminal acetylation is yet to be experimentally assessed. Noteworthy, N-acetylation has generally been linked to an increase in protein stability (Bienvenut et al., 2011).

Rubisco SS, on the other hand, might be the sole chloroplast protein that starts with a methionine which gets post-translationally methylated (Taylor et al., 2001; Rowland et al., 2015). This methylation may help the mature SS that is generated after cleavage of its chloroplast transit peptide (cTP), escape the NME rule. Noteworthy, the methylated-M, which interacts with LS-W411, may have a role in catalysis, potentially stabilizing interactions of the RuBP substrate with LS (van Lun et al., 2011). *Chlamydomonas* mutants in the annotated SS-Rubisco methyltransferase *RMT2* gene (Cre12.g524500) display altered photosynthetic growth (Li et al., 2019), yet whether RMT2 truly plays a role in SS methylation has not been determined.

Another methyltransferase - the Large Subunit Methyl transferase or LSMT - has been implicated in trimethylation of LS-K14 in some plant Rubisco's (Solanaceae and

Cucurbitaceae), which is not observed in *Chlamydomonas*, although *Chlamydomonas* does have a gene encoding a putative LSMT (*RMT1*). This paradox has been recently solved through the discovery that LSMT specificity towards Rubisco is a recent acquisition leading to a bifunctional enzyme whose primary function is trimethylation of Fructose Bisphosphate Aldolase (FBA, (Ma et al., 2016)). Moreover, while the function of the K14 trimethylation is still elusive from the lack of phenotypes observed in tobacco mutants, the analysis of CryoEM images of the Rubisco-LSMT complex revealed a large surface binding area that engages with the LS dimer, suggesting that trimethylation most likely occurs post-translationally (Raunser et al., 2009).

One of the surprises of the crystallographic structures obtained for *Chlamydomonas* Rubisco (Taylor et al., 2001; Mizohata et al., 2002) is the presence of other LS post-translational modifications (PTM) that are less commonly observed. These consist of 4-hydroxyprolination of the conserved residues P104 and P151 and methylation of C256 and C369. Hydroxyprolination was hypothesized to increase the rate of LS folding following translation (Mizohata et al., 2002) but is not essential for Rubisco assembly and function: photosynthesis could be restored by complementation of an *rbcL* deletion mutant with mutated versions bearing proline to alanine mutations, which prevent further hydroxylation. However, Rubisco catalysis was significantly altered in the P104A mutant, which displayed a decreased carboxylation rate accompanied by a decreased growth rate (Rasineni et al., 2017). The effect on catalysis in the P104A mutant might be due to the lack of the PTM, rather than to the P-to-A substitution as hydroxyl groups from the hydroxyP104 residue provide contacts with residues from LS 60's catalytic loop (Rasineni et al., 2017). The prolyl 4-hydroxylase responsible for this modification has not been identified, although several prolyl 4-hydroxylases are predicted to be chloroplast localized, with at least one, Cre10.g443050, experimentally associated with the chloroplast (Terashima et al., 2010). Likewise, it remains unknown whether hydroxylation occurs prior or post-assembly: P104 is exposed to solvent in the dimer, but P151 is relatively buried.

Regarding methylation of the cysteine residues, a C256A mutation resulted in decreased Rubisco accumulation at 35°C, leading to a non-photosynthetic phenotype together with a strong impact on the catalytic properties of the enzyme. This phenotype was not observed in a strain harboring a C256F substitution of LS; the F residue at this position is conserved in land plants. These findings indicate that the C256 methylation is functionally important, likely by extending the contact region between LS and SS, thereby mediating the change in catalysis (Rasineni et al., 2017). This modification likely precedes Rubisco assembly as C256 is not solvent accessible in the assembled enzyme (Taylor et al., 2001). In contrast, no functional role has yet been ascribed to C369 (Rasineni et al., 2017).

Noteworthy, Rubisco cysteine residues are not involved in disulfide bonds under 'standard' growth conditions (Taylor et al., 2001). However, an intradimer disulfide bond involving C247 residues of opposing LS subunits can form under some conditions. This was observed when *Chlamydomonas* experienced oxidative stress induced by cupric ion exposure (Mehta et al., 1992). It was also occasionally in purified spinach and cyanobacterial Rubisco (Ranty et al., 1991). Another study reported C247 to be reduced and insensitive to its redox environment (Garcia-Murria et al., 2018).

Apart from the non-enzymatic carbamylation of K201 by a non-substrate CO_2, which is an absolute prerequisite for Rubisco function (Lorimer and Miziorko, 1980), the functional significance of most Rubisco PTMs remains poorly understood (Houtz et al.,

2008). Noteworthy, expression of Rubisco subunits in *E. coli* did not prevent Rubisco assembly or reduce its activity even though various PTMs did not occur in the heterologous system (Aigner et al., 2017). The future identification of the enzymes responsible for Rubisco PTM will probably enable a better understanding of their role in Rubisco assembly and function.

6. Is Rubisco assembly a pyrenoid localized process?

Recent breakthrough discoveries (Mackinder et al., 2016) revealed the essential role of Rubisco SS and the EPYC1 protein in Rubisco supramolecular organization within the pyrenoid, an essential feature commonly found in many green algae, but also in hornworts, to cope with limiting CO_2 concentrations (Barrett et al., 2021), see section VI.D. Since LS translation may occur close to the pyrenoid, this raises the question of whether Rubisco assembly and the processes leading to its supramolecular organization are coupled or not. Two observations indicate that Rubisco assembly is not a pyrenoid localized process i) Rubisco localization to the pyrenoid requires fully assembled Rubisco, with a prominent role for SS in localization (developed in section VI.D), ii) Rubisco chaperones were not identified in pyrenoids based on proteomics (Zhan et al., 2018) and fluorescent tagging (Mackinder et al., 2017).

III. Catalysis

A. Rubisco chemistry

Chlamydomonas Rubisco shares typical Rubisco catalytic attributes. The active site is formed at the interface between the LS C-terminal α/β barrel domain of one LS subunit and the N-terminal of an adjacent LS, yielding two active sites per dimer, and thus 8 active sites per LS_8SS_8 holoenzyme. Conservation of the catalytic residues and universal structural features support a similar mode of catalysis among all Rubiscos.

Catalysis of Rubisco requires prior activation by a Mg ion and a non-substrate CO_2 molecule involved in carbamylation of the conserved LS-K201. Carbamylation is followed by interaction of the enzyme with RuBP in its extended conformation. This interaction results in movement of loop 6, tighter binding of RuBP and subsequent rigid body movement of the enzyme that involves both the N- and C-terminal domains of the intradimeric adjacent LS subunits and the movement of the flexible LS C-terminus towards loop 6, which shields RuBP from the solvent. These structural rearrangements, characterized by a strong increase in hydrogen bonding (van Lun et al., 2011), lead Rubisco to adopt its closed conformation state, which provides the proper environment for the fixation of a CO_2 with the generation of an unstable 6 carbon intermediate that is hydrolytically cleaved. The exact roles of the residues forming the active site in the 5-step carboxylation reaction are still being investigated (Cummins et al., 2018, 2019). Upon cleavage, two phosphoglycerate molecules are released (reviewed in (Andersson, 2008)) that enter the CBC (see Chapter 8). As indicated by its name, Rubisco poorly discriminates CO_2 from O_2 and, in addition to carboxylation, catalyzes RuBP oxygenation in a competing counterproductive reaction. However, the oxygenase activity in *Chlamydomonas* is greatly alleviated by the development of a

CO_2 concentrating mechanism (CCM) in which the formation of the pyrenoid, which is packed with Rubisco, is critical (see section VI.D).

B. Gas specificity and carboxylation rates are dictated by the active site environment

Rubisco is known to be a slow catalyst (median value of 3.3 s^{-1} (Flamholz et al., 2019)), with a reported catalytic efficiency (kcat) of about 2.3 CO_2 molecules fixed per second in *Chlamydomonas* (Spreitzer et al., 2005), even though recent work indicates that some Rubisco form II enzymes may exhibit much faster carboxylation rates (Davidi et al., 2020). The efficiency with which CO_2 out-competes O_2 is described by the Ω specificity factor, which takes into account the maximal velocity of the carboxylation (V_c) and oxygenation (V_o) reactions, as well as the affinities of the two gas (K_c and K_o) ($\Omega = V_c/V_o \times K_o/K_c$) (Spreitzer and Salvucci, 2002). Ω values range from <50 to >90 (Flamholz et al., 2019; Poudel et al., 2020). Generally low for form II containing organisms, Ω increases in form I-containing organisms, with the highest values observed in non-green algae. Yet, specificity alone is not sufficient to ascribe a higher carboxylation rate (reviewed in (Spreitzer and Salvucci, 2002)) and, in fact, an inverse correlation between specificity and carboxylation rate has been observed suggesting a trade-off between specificity and the turn-over rate of the enzyme (Tcherkez et al., 2006; Savir et al., 2010; Studer et al., 2014). A higher specificity factor was suggested to be associated with tighter binding of the carboxylated intermediates. Their delayed release from the enzyme results in a lower turn-over rate. Nonetheless, Ω has been used as a diagnostic parameter indicating overall efficiency (Parry et al., 2003). Recent structural comparisons among various Rubisco's showed a correlation of higher substrate specificity associated with Rubisco form I, with positively charged cavities around the active site. These cavities represent gas substrate binding channels that would enhance electrostatic interactions with CO_2 rather than O_2 (Poudel et al., 2020). Interestingly, this feature of the form I enzyme likely reflects its evolution in CO_2 depleted environments. Furthermore, the active site plasticity required to generate increased specificity towards CO_2 might have been acquired at the expense of structural stability, as recently suggested (Banda et al., 2020). This instability might have driven the evolution of the small subunit, a stabilizing component of the enzyme.

C. *Chlamydomonas*, a historical model to develop a “better” enzyme

With the development in the 1990s of chloroplast transformation allowing for site-directed mutagenesis of Rubisco LS (see Chapter 19) and the ease of performing classical forward genetic studies, *Chlamydomonas* has emerged as a model system in “Rubiscology”. Two aims were pursued: i) a better understanding of the contribution to catalysis of the LS and SS subunits, ii) the long-term goal of deciphering how to improve Rubisco efficiency with a specificity factor mirroring that typical of land plants (~ about 20% higher). Multiple approaches using classical genetics, phylogenetics and more recently computational molecular dynamics have allowed the identification of important domains in addition to the resides of the *Chlamydomonas* LS active site (reviewed more extensively in (Andersson, 2008; Andersson and Backlund, 2008)). From a phylogenetic perspective, one would infer that the differences in the catalytic properties and slight modifications of Rubisco structure can be ascribed to residues

not conserved among species, allowing differential stabilization of the transition states of the enzyme. In *Chlamydomonas*, this has led to a directed scrutiny of some of the 34 amino acids not conserved in land plants. Structures of *Chlamydomonas* native, mutant, revertant and hybrid Rubisco enzymes (see Table 2) have led to the elaboration of hypotheses to account for the mutations' effects and to guide additional mutagenesis studies (tables 3 and 4). These experiments have revealed functionally important residues in the LS subunit in the vicinity of the active sites such as the loop 6 V331 residue and T342 (Chen and Spreitzer, 1989; Chen et al., 1991; Karkehabadi et al., 2007), but also long-range interactions (L290, D473).

1. Contribution of various LS and SS domains

a. LS N-termini contribution

In addition to the two active site residues E60 and N123, which are critical for the catalytic properties of the enzyme (Zhu and Spreitzer, 1994), the conserved K128 residue has been proposed to lock the closed conformation of the enzyme upon ligand binding through interaction with the adjacent LS (van Lun et al., 2011). Plant-like substitutions affecting the non-conserved M42 and C53 residues of *Chlamydomonas* LS exhibited only minor effects on catalysis, suggesting that the N-terminal domain does not contribute substantially to differences in the catalytic properties of the *Chlamydomonas* and land plant enzymes (Du et al., 2003).

b. LS Loop 6 (331-338)

Loop 6 flexibility is essential, as its movement allows the transition from an open to a closed active site during catalysis. The conserved K334 is known to orient and stabilize the transition state intermediate. K334 also interacts with E60 and T65 of an adjacent N-terminal (Knight et al., 1990) and is presumed to form hydrogen bonds with CO_2 (Andersson and Backlund, 2008). The importance of loop 6 has been highlighted in *Chlamydomonas* through the analysis of the V331 residue. V331 is part of the hinge on which loop 6 moves and has proven essential: a V331A mutant is non-photosynthetic and exhibits a strong reduction in Ω and carboxylation efficiency (Chen and Spreitzer, 1989), as it was unable to bind the 2'-carboxyarabinitol bisphosphate (CABP) transition analog (Chen et al., 1991). Mutations within or close to loop 6 restored tighter binding of CABP and increased concomitantly Ω, as apparent in the second site revertants T342I and G344S (Karkehabadi et al., 2007). Residues V331 and T342 were shown to be codependent and to establish a hydrophobic pocket around K334. The decreased specificity in the V331A mutant was further linked to an altered interaction between S379 and CABP through a lengthened hydrogen bond, indicating its probable contribution to differences in kinetic constants. This was also apparent from the decreased rate of carboxylation and altered Ω value observed in a S379A mutant (Zhu and Spreitzer, 1994). Together, these results indicate that the environment around the active site is an important determinant in the catalytic properties of the enzyme, although the effect of mutations has been difficult to predict (Karkehabadi et al., 2007).

c. LS C-terminal extension (aa463-475)

The LS C-terminal extension is present only in Rubisco form I and is involved in the stabilization of the catalytically active closed state by packing it against loop 6. Special attention has been given to the D473 residue, which has been suggested to

serve as a latch in this movement (Duff et al., 2000; Satagopan and Spreitzer, 2004), and more generally to 4 amino-acids surrounding D473, which are divergent between *Chlamydomonas* and the consensus sequence found in most flowering plants (Satagopan and Spreitzer, 2008). While the D473 residue does not appear to be critical for catalysis, it does contribute to the conformation of the active site and substrate binding since a D473E mutant enzyme was active but exhibited a decreased Ω and carboxylation efficiency (Satagopan and Spreitzer, 2004). The enzyme structure in this mutant showed subtle alterations in the active site that resulted in an altered interaction between L335 and CABP. Additionally, the C-terminus was found to be disordered, indicating that D473 might influence loop 6 dynamics and ultimately the catalytic site (Karkehabadi et al., 2007). Introducing plant-like substitutions within the 4 amino acids in the direct vicinity of D473 increased the specificity, but at the expense of the carboxylation rate (Satagopan and Spreitzer, 2008).

d. LS/SS interface

Although far from the active site, the LS/SS interface at the surface of the enzyme critically impacts both catalytic parameters and enzyme stability (see section B.3). Characterization of the LS L290F temperature-sensitive mutant was instrumental in demonstrating that long range interactions can affect the catalytic site. This lesion caused both decreased enzyme stability (Chen et al., 1988) and a 13% reduction in Ω. These altered characteristics were restored in the LS-A222T and V262L suppressor mutants (Hong and Spreitzer, 1997). Interestingly, the highly conserved L290, A222, and V262 LS residues surround the βA/βB loop of Rubisco SS and the same L290F mutant could be suppressed by mutations affecting SS residues, such as the N54S, A57V (Du et al., 2000) and C65S (Genkov et al., 2006). Additionally, the single C65S mutant was shown to enhance catalysis. These three residues are part of the SS βA/βB loop, which underscores its importance in catalysis through long-range effects.

e. SS βA/βB loop (aa 46-73)

The previous experiments indicate that the SS βA/βB loop not only contributes to Rubisco stability, but also to differences in Rubisco catalytic features. As the βA/βB loop shows strong divergence among species, it was examined with respect to its impact on differences in the catalytic features of the enzyme. As apparent from Table 4, most of the βA/βB loop mutations negatively influenced the specificity factor and the carboxylation efficiency. Y67A and Y72A showed strong effects on the specific activity, decreasing Ω to 5% of the wild-type level (Esquivel et al., 2006). Replacing the C65 amino-acid in Chlamydomonas by a P, found at that position in plant SS, had a deleterious effect on specificity and carboxylation efficiency (Genkov et al., 2006). Importantly, changes in catalysis are in some cases uncoupled from adverse effects on stability.

The βA/βB loop further defines the width of the central solvent channel which could potentially impact catalysis. Restricting the channel width through the replacement of I58 with three tryptophan residues yielded mutants exhibiting a decrease in both stability and Ω, and yet Rubisco was still able to transition from the closed to open states (Esquivel et al., 2013). It was suggested that CO_2 and O_2 gas partitioning could be altered in this mutant, thereby accounting for the decreased carboxylation rates observed (Esquivel et al., 2013).

f. Hybrid Rubisco with altered catalytic properties

A comparative mutagenesis approach was undertaken to explore whether the divergence in SS and LS sequences could account for the different specificities towards CO_2/O_2 specificity observed for algae and plants, with particular attention to residues at the LS/SS interface. Additionally, hybrid enzymes were generated by replacing the *Chlamydomonas* SS βA/βB loop with ones from either spinach or *Synechococcus* (Karkehabadi et al., 2005). In the case of spinach, the hybrid enzyme showed a decreased carboxylation rate, without affecting Ω. Rather than eliciting marked structural alterations, these changes in catalysis were attributed to changes in the dynamics of the enzyme.

To explore the functional importance of the LS/SS interface, the LS divergent C256, K258, I265, V221 and V235 residues were mutated to the residues found in land plant counterparts, generating the C256F, K258R, I265V, V221C and V235I variants. Single, double or triple mutants had either no or negative effects on Rubisco accumulation, growth, Ω, and carboxylation efficiency (Du et al., 2003). Yet, combining the plant-like substitutions in a pentamutant restored Ω to the level observed in Chlamydomonas wild type cells (Spreitzer et al., 2005). Only when the SS plant βA/βB loop was expressed in the *Chlamydomonas* LS pentamutant did the hybrid enzyme acquire plant-like properties, with a higher specificity and decreased carboxylation rate (Spreitzer et al., 2005). Even though these parameters would result in a decrease in net CO_2 fixation at physiological concentrations of CO_2 and O_2, this study shows that mutagenesis of residues at the LS/SS interface could lead to an improvement in certain Rubisco catalytic properties.

Other hybrid enzymes composed of plant SS from spinach, Arabidopsis and sunflower-and *Chlamydomonas* LS were generated (Genkov et al., 2010). They exhibited a slightly increased Ω without alteration of the carboxylation rate, but these features were still more closely aligned to those of algae than of plants, further indicating the complexity of using rational design strategies, given our current state of knowledge, to catalytically improve Rubisco. Conversely, hybrid Rubisco expressed in Arabidopsis with the SS stemming from *Chlamydomonas* are functional, even though they exhibit lower kcat and specificity values (Atkinson et al., 2017).

g. Role of SS as a clamp

It is not completely understood how the SS βA/βB loop interaction with the LS interface strongly influences the catalytic properties of Rubisco, even though it is at the opposite end of the α/β barrel that forms the catalytic site. Alanine substitutions of the SS E43 and W73 conserved residues led to a decrease in the Ω, likely through altered contacts with the LS alpha1 helix, and may explain the long range effects observed in other βA/βB loop mutants on catalysis (Genkov and Spreitzer, 2009). Similarly, mutations of the SS Y32, L78 and F81 residues strongly decreased the carboxylation rate and were identified as important for interactions of SS with LS helix 8 and the LS αB-βC loop (Genkov and Spreitzer, 2009). Computational analysis of protein dynamics further suggested that the catalytic parameters depend on the proper positioning of SS at three critical points: i) the βA/βB loop, ii) the SS-MethylM1 with L-W411, and iii) SS-helix A (involving Y32) with LS-helix 8 (van Lun et al., 2011). These three regions would act as a clamp that fixes LS in the proper position for stabilization of the ligand.

h. SS may function as CO_2 reservoirs

In an alternative approach, molecular dynamics simulations were performed to model migration of the CO_2 and O_2 gases at the enzyme's surface (van Lun et al., 2014). At variance with the hypothesis proposed by (Esquivel et al., 2013), the Rubisco central solvent channel does not appear to play a major role in partitioning CO_2 to the active sites. Rather, a CO_2 path may involve the LS/SS interface, the groove between two LS dimers and the entry region of the active site. Notably, SS residues would contribute more significantly to CO_2 binding than LS residues through their interactions with CO_2 that involves small hydrophobic amino acid side chains or sulfur-containing residues, although CO_2 binding usually involves basic residues, which are highly represented on the LS surfaces (Poudel et al., 2020). This led to the proposal that SS subunits may have evolved as CO_2 reservoirs in response to depleted environmental CO_2, with an in vivo role on catalysis as suggested by altered catalytic parameters in strains with mutagenized SS residues at the LS/SS interface, which were shown to be part of the CO_2 binding region (Genkov and Spreitzer, 2009; van Lun et al., 2014).

2. Limits and conclusions about Rubisco design

Tables 3 and 4 summarize the catalytic properties of mutant/variant Rubiscos that have been generated. These studies have allowed identification of residues that influence catalysis and specificity. They have been instrumental in demonstrating that SS is not exclusively dedicated to stabilizing the holoenzyme, but also influences catalysis through long-range effects, as well as having a role in CO_2 local enrichment, and led to the realization that the SS was responsible for the supramolecular organization of Rubisco and more generally of the pyrenoid (Meyer et al., 2012; He et al., 2020).

Nonetheless, mutagenic approaches for studying the catalytic features of Rubisco are complicated because they also can have a negative effect on Rubisco biogenesis, and so building a 'better' LS would be constrained because of the impact of such changes on folding and assembly (Durao et al., 2015), as demonstrated by low substitution rates within *rbcL* chloroplast sequences compared to those of prokaryotes (Andersson, 2008). It also became apparent that single or a limited number of substitutions do not dramatically improve catalysis, and that Rubisco evolution is constrained by the limits of CO_2/O_2 discrimination. More recently, research on carboxylation rate improvement has focused on other experimental approaches. Directed evolution using Rubisco-dependent *E. coli* screens (RDE) (Wilson et al., 2018; Zhou and Whitney, 2019) or exploiting synthetic biology approaches to establish CO_2 dependent autotrophic *E. coli* strains (Antonovsky et al., 2016; Gleizer et al., 2019) can now be envisioned for algae and plants since the genes encoding LS and SS subunits from some plant species can be expressed in *E. coli* (Aigner et al., 2017; Wilson et al., 2019; Lin et al., 2020), even though the requirement for compatible interactions with the chaperones may hamper these approaches in some cases. A second route for improving the carboxylation rate of Rubisco involves increasing the CO_2 concentration in the vicinity of the enzyme. This would involve coupling expression of hybrid Rubisco with that of an engineered CCM. Recently a hybrid Rubisco composed of Arabidopsis LS and *Chlamydomonas* SS was successfully condensed into a protopyrenoid structure (which also required expression of the EPYC1 protein, see section VI.D), (Atkinson et al., 2020); this is a first important step in the development of a modular, transferrable CCM.

D. Maintenance and control of Rubisco activity.

1. Requirement of Rubisco activase for metabolic repair

a. An alleviated requirement for RCA in Chlamydomonas due to an efficient CCM

Rubisco activity becomes inhibited by binding of RuBP analogs or when RuBP binds to the enzyme prior to its activation by carbamylation of LS K201 amino-acid. Rubisco activase (RCA), a chaperone of the AAA+ family, is involved in the maintenance and repair of Rubisco by releasing the inhibitory sugar phosphates from the active sites, thereby coupling ATP hydrolysis to the remodeling of inhibited Rubisco into an active state. In *Chlamydomonas*, RCA1 encodes a protein with approximately 65% identity with higher plant orthologues (Roesler and Ogren, 1990), which typically encode both an α and a shorter β isoform. *Chlamydomonas* RCA1 is closer to the plant beta isoform (Gontero and Salvucci, 2014). In accord with its function, RCA colocalizes with Rubisco to the pyrenoid, as shown by immunolocalization studies (McKay and Gibbs, 1991), fluorescence fusion protein localization (Mackinder et al., 2017) and its presence in the pyrenoid associated proteome (Zhan et al., 2018). Compared to plants in which RCA knock-outs aren't viable at air CO_2 concentrations (Somerville et al., 1982; Portis and Salvucci, 2002), an *rca1* mutant of *Chlamydomonas* only displays a strong photosynthetic impairment at air levels of CO_2 when in a CCM deficient background (*cia5*, (Pollock et al., 2003)), indicating that the CCM can partly mitigate the inefficiency of Rubisco operating in the absence of the activase. Interestingly, a second gene (*RCA2*) encoding an RCA-like protein is present in the *Chlamydomonas* genome, predicted to be chloroplast localized and fractionates with the pyrenoid (Zhan et al., 2018). However, this *RCA2* gene is expressed at a low level and whether it fulfils a role in Rubisco metabolic repair is not known. *RCA1* expression is under circadian control, with mRNA peaking near the end of the dark period, asynchronous with the accumulation of the RCA1 protein, which accumulates to higher levels in the light period (Rawat and Moroney, 1995). These expression data are confirmed by a recent transcriptomic study (Strenkert et al., 2019). Rubisco activase expression is also slightly induced upon transfer from high CO_2 conditions to air (Rawat and Moroney, 1995; Pollock et al., 2003), with the mRNA increasing approximately two-fold (Im et al., 2003). RCA activity itself may be regulated through phosphorylation events and relocalization according to the metabolic state of the cell ((McConnell et al., 2018) and see Chapter 8).

b. RCA mode of action

Structures of green-type RCA have been obtained for tobacco (Stotz et al., 2011), Arabidopsis (Hasse et al., 2015) and creosote (Henderson et al., 2011) (reviewed in (Bhat et al., 2017)), but not yet for *Chlamydomonas*. RCA subunits comprise an N-terminal domain, an AAA+ core with an α/β nucleotide-binding domain adopting a Rossman fold, a sub-helical domain, and a C-terminal domain. RCA subunits undergo dynamic oligomerization. Only the hexameric form, when bound to ATP, is thought to be active (Stotz et al., 2011), with higher order oligomers hypothesized to constitute a storage form (Serban et al., 2018).

A long-standing question has been to understand how RCA interacts with Rubisco to promote structural remodeling. Alternative models of either a side-on

binding mode or a top-on binding mode have been proposed (Wachter et al., 2013). An intriguing observation has been the specificity observed for Solanaceous RCA towards Rubisco, which does not activate non-solanaceous Rubisco (Wang et al., 1992). Earlier work using *Chlamydomonas rbcL* mutants indicated that the solvent accessible LS βC-βD loop, found close to loop 6 and to the C-terminal domain shielding the active site, is an important determinant for Rubisco activation as P89R and D94K substitutions within this loop rendered *Chlamydomonas* Rubisco susceptible to activation by solanaceous RCA (Larson et al., 1997; Ott et al., 2000). Structural comparisons of these two groups of Rubisco have identified a few divergent residues that all cluster on the equatorial axis of the enzyme. Conversely, RCA residues at position 311 and 314 were found to interact with the βC-βD LS loop, thereby defining RCA's helix 9 as the so-called specificity helix (Li et al., 2005). Further studies have indicated that the size of the solvent channel is not critical in the activation process as a *Chlamydomonas* SS I58W mutant, which strongly decreases solvent channel access, can still be fully activated (Esquivel et al., 2013). Furthermore, hybrid Rubiscos composed of tobacco SS and Chlamydomonas LS did not alter RCA specificity, indicating that SS is not a major determinant of the species-specific RCA interaction (Wachter et al., 2013).

Recently, experimental evidence in Arabidopsis and for the cyanobacterial RCA-like protein in Nostoc (Flecken et al., 2020; Ng et al., 2020) have provided support for the side-on binding model (Portis et al., 2008). The green-type RCA hexamer pore has been shown to be positioned over the Rubisco catalytic site, allowing the repair of one site at a time. An ATP-driven threading mechanism involving non-canonical pore loops compared to the conserved ones generally used by AAA+ chaperones transiently pulls the Rubisco LS conserved N-terminus (first 20 amino acids), thereby disrupting interaction with LS 60s loop and releasing the inhibitory sugar phosphate.

2. Control of Rubisco activity in the CBC cycle

Rubisco activity itself can be tuned accordingly to the *Chlamydomonas* metabolic status, either directly or through regulation of Rubisco activase. The redox model and the regulatory role of post-translational modifications, such as lysine acetylation, S-glutathionylation, nitrosylation, tyrosine nitration for LS, or phosphorylation of Rubisco Subunits or RCA, involved in these regulatory processes are described in Chapter 8.

IV. Rubisco catabolism during nutrient and oxidative stresses

A. The degradation of Rubisco holoenzyme under nutrient stress and senescence is ClpP-dependent

Because of its high abundance, Rubisco sequesters high levels of both nitrogen and sulfur amino acids. Under nutrient stress or during senescence, these reserves are mobilized through a global remodeling of the chloroplast apparatus that involves Rubisco catabolism. In *Chlamydomonas*, Rubisco degradation has been observed both under nitrogen-depletion (Majeran et al., 2001; Schmollinger et al., 2014; Wei et al., 2014) and sulfur-depletion (Zhang et al., 2004; De Mia et al., 2019; Majeran et al., 2019). Interestingly, Rubisco catabolism induced by nutrient deprivation was shown to be triggered by NO accumulation (Wei et al., 2014; De Mia et al., 2019) and leads ultimately to Rubisco proteolysis through an incompletely characterized cascade of events. While in land plants extra-plastidial degradation of Rubisco mediated by

autophagy-dependent Rubisco containing bodies or autophagy-independent senescence-associated vesicles has been observed during stress and senescence (reviewed in (Izumi and Nakamura, 2018)), the role of autophagy in the Rubisco degradation in *Chlamydomonas* is unknown. Rubisco degradation appears to occur mainly in the stroma, as deduced from the major role played by the Clp protease under nutrient stress (see figure 1 and also Chapter 20), (Wei et al., 2014; De Mia et al., 2019; Majeran et al., 2019).

B. Oxidative modifications, Rubisco fragmentation and aggregation accompany the degradation process

Rubisco degradation is thought to start with Rubisco inactivation followed by fragmentation, leading to enzyme disassembly and proteolysis (Sugiyama et al., 1968). Oxidative modifications have a prominent role in these processes as they were shown to inactivate Rubisco and induce structural weakness leading to fragmentation or increased access to proteolysis (reviewed in (Moreno et al., 2008)). Oxidative modifications may also tag Rubisco for degradation. Possible modifications include cysteine-thiol to disulfide oxidation, S-glutathionylation and S-nitrosylation. Interestingly, Rubisco undergoes cysteine S-nitrosylation under abiotic stress in plants (Abat and Deswal, 2009; Vanzo et al., 2014; Grabsztunowicz et al., 2017) and it is tempting to speculate that such a modification could represent a degradation tag. In *Chlamydomonas*, C247 and C172 of Rubisco LS and C84 of Rubisco SS have been shown to be potential targets of S-glutathionylation (Zaffagnini et al., 2012), but whether this is the case *in vivo* and during stress is still unknown. Interestingly, no significant change was detected in the oxidation state of Rubisco cysteine residues during early responses to N starvation (Smythers et al., 2020), but the enzyme was shown to be oxidatively modified upon exposure to high light for 2 h or upon H_2O_2 treatment (Cohen et al., 2005).

Beside these PTMs, non-enzymatic hydrolysis following hydroxyl ROS ($OH^{\cdot}$) attack of Rubisco in the presence of metal ions (reviewed in (Feller et al., 2008)) has been proposed to trigger Rubisco fragmentation, with protein cleavage mostly occurring at the N-terminal region. Fragmentation has been observed in oxidative conditions both *in vivo* in plants submitted to stresses (such as very high light, hypoxia or a shift from moderate to low light) and *in vitro* with purified Rubisco (Desimone et al., 1996; Feller et al., 2008; Grabsztunowicz et al., 2015), yielding fragments of diverse sizes that depend on the specific plants and conditions. In *Chlamydomonas* the S61-T68 loop of LS has been identified as a redox-sensitive proteolytic cleavage site (Marin-Navarro and Moreno, 2003). Located at the intradimeric interface, this loop would become exposed under oxidative conditions. Furthermore, Rubisco fragmentation in *Chlamydomonas* has been observed *in vivo* upon strong oxidative stress induced by high light (Cohen et al., 2005), methyl viologen (Knopf and Shapira, 2005), hydrogen peroxide (Esquivel et al., 2006) or upon salt stress (Marin-Navarro and Moreno, 2006). Fragmentation occurs prior to degradation, as the fragments remain associated with the Rubisco holoenzyme instead of being released upon cleavage (Knopf and Shapira, 2005). Yet, these fragments are observed only under strong oxidizing conditions, and not upon nutrient stress (Wei et al., 2014; De Mia et al., 2019; Majeran et al., 2019). This may indicate different mechanisms leading to degradation or that fragment accumulation reveals a limitation of the proteolytic capabilities of the cell that can ultimately lead to cell toxicity. Interestingly, aggregation

of Rubisco subunits is observed concomitantly with Rubisco fragmentation (Knopf and Shapira, 2005; Esquivel et al., 2006; Marin-Navarro and Moreno, 2006). Aggregate formation, involving mostly LS subunits, is somewhat paralleled by a decrease in Rubisco SS accumulation. Depending on the situation, these aggregates result in part from cross-linking that involves disulfide or non-disulfide bridges (Marin-Navarro and Moreno, 2006) or from hydrophobic interactions (Knopf and Shapira, 2005). Aggregation is thought to be required for further recruitment of oxidized Rubisco to the membranes, which has been described in *Chlamydomonas* both under cupric ion treatment (Mehta et al., 1992) and salt stress (Marin-Navarro and Moreno, 2006), but not upon exposure to methyl viologen (Knopf and Shapira, 2005). In the latter case, the abundance of Rubisco aggregates correlated with viability loss, indicating proteocytotoxicity of the aggregates. The recruitment of Rubisco aggregates to membranes may stimulate the formation of Rubisco autophagic vesicles, suggesting that under some conditions *Chlamydomonas* Rubisco degradation could occur through autophagy, as observed for Rubisco-Containing Bodies (RBCs) in plants (Ishida et al., 2008).

C. Roles of cysteine oxidation in the degradation process

The roles of nine Rubisco cysteines conserved throughout the green lineage have been extensively studied in *Chlamydomonas* as they may transduce a redox signal into conformational changes that determine the catabolic fate of the enzyme. A model in which sequential oxidation of specific cysteines displaying different redox potentials leads to Rubisco inactivation and proteolytic susceptibility has been proposed (Moreno et al., 2008; Garcia-Murria et al., 2018). The first cysteines undergoing oxidation in LS are C427 and C192. Their oxidation to thiolate would provide a protective charged environment that would, in turn, delay the oxidation of the respective nearby C459 and C172. As the oxidation state progresses and impacts the C449–C459 cysteine pair, Rubisco undergoes inactivation (Marin-Navarro and Moreno, 2006). Oxidation of the C449–C459 pair would enhance Rubisco degradation under saline stress, but retard Rubisco cross-linking, aggregation and membrane association, as evidenced by the behavior of C-to-S substitution mutants (Marin-Navarro and Moreno, 2006). Moreover, the double C-to-S mutant depicts a stronger phenotype than the single mutants, thereby discarding the possibility of disulfide bond formation with either of the cysteines of this pair (Garcia-Murria et al., 2008). The increased protease susceptibility linked to C oxidation of the wild-type enzyme might result from a conformational change leading to exposure of the S61–T68 loop, which when cleaved in the two LS dimer subunits, leads to unrestricted proteolysis (Marin-Navarro and Moreno, 2003; Moreno et al., 2008).

Lastly, the C172 residue can be oxidized, which results in increased protease susceptibility. The involvement of this modification in stress-related proteolysis has been shown in early studies; the C172S mutant strongly reduces, but does not prevent, Rubisco proteolytic susceptibility *in vivo* under oxidative conditions (Moreno and Spreitzer, 1999; Moreno et al., 2008). Importantly, premature oxidation of C172 is mitigated by the oxidation of the C192 (Garcia-Murria et al., 2018). The conservation of the seemingly C172 ‘unfavorable’ residue may be explained by its proximity to important residues of the catalytic site, as suggested by the decreased catalytic parameters observed in the C172S mutant (Garcia-Murria et al., 2008).

For *Chlamydomonas* Rubisco SS, the sequential oxidation of the thiols groups

of its 4 C residues likely occurs as well, as evidenced in vitro by the gradual shift in SS electromobility upon incubation with increased oxidized glutathione (Cohen et al., 2005).

V. Non-catalytic aspect of Rubisco-Moonlighting function of LS

A. Rubisco quantification and excess LS

In several studies the relative (Mastrobuoni et al., 2012) and absolute amount of Rubisco in *Chlamydomonas* have been measured (Wienkoop et al., 2010; Recuenco-Munoz et al., 2015; Hammel et al., 2018). Experimental biases and culture conditions have been invoked to account for differences in quantification. In the latest report using the Qconcat technology, which is based on comparisons with known amounts of concatenated peptides, Rubisco LS was shown to represent 6.6 % of the cell protein content for mixotrophically grown *Chlamydomonas*, which represents 25.2 attomol/cell. Noteworthy, a small excess of LS relative to SS (ratio of 1.56:1) has been observed (Hammel et al., 2018). This ratio is somewhat surprising since a concerted accumulation of Rubisco subunits predicts a 1:1 ratio, and an unassembled LS pool would exert a negative feed-back on its own translation by the CES process. It is not clear how this observation can be reconciled with the dogma of stoichiometric accumulation of Rubisco subunits, other than suggesting the existence of a non-holoenzyme LS pool in an assembly form that escapes the CES process. Since the CES repression would be due to the accumulation of the last assembly intermediate RAF-LS before LS-SS assembly, it is conceivable that an escape route via LS aggregation, as observed in stress-related situations, would lead to an excess of LS vs SS.

A. A moonlighting function is associated to LS RNA-binding activity in oxidative stress

In light of the excess of LS observed in *Chlamydomonas* cells, it is interesting to note that a specific role of LS - independent of the CO_2 fixation function of the holoenzyme - has been described in several instances, as discussed below. Yet, a unifying model that integrates these different observations still needs to be developed and tested.

1. LS has an unspecific RNA-binding activity

Rubisco LS has been isolated as a *rbcL* mRNA binding protein under oxidative conditions (Yosef et al., 2004). LS RNA binding activity was subsequently shown to be non-specific (Yosef et al., 2004) and not restricted to *Chlamydomonas* oxidized LS, but conserved in land plants and even in the more distantly related form II Rubisco from *R. rubrum* (Yosef et al., 2004; Cohen et al., 2006). The binding activity has been localized to the LS N-terminal domain, which harbors structural similarity to an RNA-recognition motif by adopting a ferredoxin-like fold. LS RNA binding activity has been proposed to be mediating the translation inhibition triggered by oxidative stress, as mentioned in the section A. 5 (Yosef et al., 2004; Cohen et al., 2005; Cohen et al., 2006).

2. LS assembles within cp RNA granules upon stress

Rubisco oxidation has been shown to trigger Rubisco reorganization: Under oxidative stress SS dissociates from the holoenzyme with the concomitant formation of LS aggregates (Knopf and Shapira, 2005). Accordingly, Rubisco LS-rich punctuate foci are detected by in situ immunofluorescence around the pyrenoid under oxidative stress conditions (Uniacke and Zerges, 2008). Distinct from the T-zones, they would appear as stroma bulges in close proximity to the pyrenoid-associated membrane tubular network (Uniacke and Zerges, 2007, 2008). As the foci appear under stress and colocalize with mRNA, these structures were called chloroplast stress granules (cpSG) by analogy to mammalian systems. Zerges and coworkers hypothesized that Rubisco LS acts as a SG-assembly factor through RNA interaction and self-aggregation. Interestingly, cpSG disappear in the presence of chloramphenicol, which is used to block translation in the chloroplast by preventing polysome dissociation, but not in the presence of lincomycin, a translational inhibitor allowing mRNA run-off from polysomes. This suggests that LS aggregation depends on the presence of RNA released from polysomes. A model has been proposed, in which cpSG would facilitate mRNA fluxes for translation in the oxygen-depleted environment provided by the pyrenoid. Whether *rbcL* mRNA is present in these structures, and whether the cpSG could provide the physical link that accounts for the inhibition of translation previously observed (Irihimovitch and Shapira, 2000; Yosef et al., 2004; Cohen et al., 2005; Cohen et al., 2006), awaits further characterization.

3. Moonlighting function of LS in oxidized RNA management

A pool of SS-free insoluble LS could be involved in the management of oxidized RNA (Zhan et al., 2015). The physiological relevance of this moonlighting activity is revealed under stress; an absence of LS leads to increased cell death upon oxidative treatments, while the presence of a small amount of unassembled LS, such as in a SS-deficient mutant, correlated with enhanced resistance. Contrary to stress granules, the RNA management activity would occur constitutively and be represented by a small, dedicated pool of LS - LS aggregates in the vicinity of the oxygen-depleted pyrenoid that would capture RNA, thereby preventing RNA oxidation and damage. Whether cpSG formation involves further aggregation of stress-released oxidized LS from these preexisting clusters remains to be determined.

VI. The CO_2-concentrating mechanism

A. Inorganic carbon acquisition in aquatic environments

Rubisco is the enzymatic gatekeeper between the inorganic carbon (Ci) and organic carbon realms. Ci in the atmosphere is almost exclusively CO_2, resulting in terrestrial plants relying on CO_2 diffusion from the atmosphere into the cellular environment. However, when CO_2 dissolves in water it takes on a range of forms, CO_2, HCO_3^-, CO_3^{2-} - (collectively Ci) that are in a pH dependent equilibrium (Figure 3), and whose ratio and availability can rapidly change. This means that while only CO_2 can be the Ci substrate for Rubisco; aquatic photosynthetic organisms are not solely limited to using CO_2 from their external environment but can access a range of Ci sources and then convert them to CO_2 intracellularly at the site of Rubisco activity. Although multiple Ci forms may be available, aquatic photosynthetic organisms can face several challenges associated with the uptake of Ci from their environment. These include the rapid

depletion of CO_2 in aquatic environments due to the slow equilibrium of CO_2 from the atmosphere into water, the slow diffusion of CO_2 in water (~10 000X slower than air) and the slow dehydration of HCO_3^- to CO_2 relative to the photosynthetic fixation of CO_2 (Badger, 1994). In addition, and of specific relevance to *Chlamydomonas* biology, freshwater is typically poorly buffered, so pH changes through respiratory release of CO_2 or photosynthetic CO_2 removal can be rapid and result in a dramatic shift between Ci species availability. Individually or collectively, the above challenges can lead to local CO_2 depletion at the cell surface and the bulk medium/environment resulting in photosynthetic related growth reduction.

The above "Ci chemistry" challenges associated with CO_2 assimilation by aquatic photosynthetic organisms have led to the evolution of CO_2-concentration mechanisms (CCMs) that enable the use of both CO_2 and HCO_3^-, and the ability to both rapidly and specifically acclimate to changing Ci availability and speciation. Importantly CCMs enable the scavenging of Ci from the external environment when it starts to become rate limiting for photosynthesis, thus resulting in higher cellular levels of Ci than the external environment (Badger et al., 1980). CCMs are found in nearly all aquatic organisms and have been extensively studied in cyanobacteria and *Chlamydomonas* (Giordano et al., 2005). As well as enabling sustained growth under limiting CO_2, CCMs minimize photorespiration by maintaining a relatively high CO_2/O_2 ratio at the active site of Rubisco (see section III) and allow high CO_2 fixation rates to be achieved with less Rubisco. Thus, the CCM frees up energy and resources for cellular growth.

B. CCM induction and multiple acclimation states

At replete (high) CO_2 levels, CO_2 diffusion is sufficient to support photosynthetic rates in cells having a low affinity (high $K_{1/2}$) for CO_2, similar to the affinity of Rubisco for CO_2 (Jordan and Ogren, 1981; Moroney and Tolbert, 1985). As CO_2 becomes limiting *Chlamydomonas* induces its CCM which in turn increases the cell's affinity for Ci; the $K_{1/2}$ for Ci decreases by 10-120 fold relative to high CO_2 grown cells (Moroney and Tolbert, 1985). This increased affinity results in an approximate 10- to 40-fold increase in the intracellular Ci concentration relative to the external environment (Badger et al., 1980; Spalding et al., 1983b; Moroney and Tolbert, 1985). CCM induction results in a broad range of physiological, structural and metabolic responses that coincide with dramatic transcriptome (Brueggeman et al., 2012; Fang et al., 2012), proteome (Küken et al., 2018; Strenkert et al., 2019) and metabolome (Küken et al., 2018; Strenkert et al., 2019) changes . A subset of these changes is directly related to increased Ci uptake, Ci flux to Rubisco and CO_2 fixation, however, a large proportion appear to be related to adapting and sustaining a new metabolic status of the cell (Brueggeman et al., 2012; Fang et al., 2012).

Chlamydomonas has three distinguishable CO_2 acclimation states (Figure 4A-C). These include one high (replete) CO_2 (0.5-5%) where there is minimal CCM induction, and two limiting CO_2 acclimation states: 'low CO_2' (0.04-0.5%) and 'very low CO_2' (<0.04%). The exact CO_2 concentration that distinguishes these acclimation states varies depending on the aeration rate, cell density, light intensity, light quality and temperature. Furthermore, we note that the terminology related to the CO_2 concentration has not been standardized, and that CO_2 draw down during cell growth can result in very low CO_2 conditions in air grown (i.e. low CO_2) cultures (Wang et al.,

2015). In addition, pH is critical in determining dissolved CO_2 levels, i.e. two culture both grown at 0.04% CO_2 but at pH 7 vs pH 8 will have very different dissolved CO_2 and HCO_3^- levels and could potentially be in different limiting CO_2 acclimation states (Figure 3). For the rest of this chapter, limiting CO_2 will refer collectively to low CO_2 and very low CO_2 or be used if the exact limiting CO_2 concentration is unclear.

An accumulation of recent evidence indicates that there are large physiological changes between Ci uptake at low and very low CO_2, with very low CO_2 leading to a clear increase in Ci affinity, decrease in growth rate and decrease in maximum photosynthetic rate (Wang and Spalding, 2006; Yamano et al., 2010; Duanmu and Spalding, 2011; Wang and Spalding, 2014a; Wang et al., 2015; Yamano et al., 2015; Kono and Spalding, 2020). However, at the transcript level there is very little change between the two limiting CO_2 acclimation states (Fang et al., 2012). At low CO_2, a CO_2 uptake system based on the stromal/chloroplast carbonic anhydrase LCIB (Low CO_2 Induced (LCI) protein B) is dominant (Wang and Spalding, 2006; Wang and Spalding, 2014a), most likely driven by photosynthetic stromal alkalization, cyclic electron flow (CEF) and pseudo CEF (PCEF) (See below; Burlacot et al., 2021; Fei et al., 2021). At very low CO_2, an active HCO_3^- uptake system based on the plasma membrane and chloroplast envelope HCO_3^- transporters High Light Activated 3 (HLA3) and LCIA becomes increasingly important (Mariscal et al., 2006; Duanmu et al., 2009b; Wang and Spalding, 2014a; Yamano et al., 2015). This very low CO_2 active HCO_3^- uptake system appears, at least to some extent, to be driven by mitochondrial produced ATP (Burlacot et al., 2021). However, acclimation states are not mutually exclusive and there is most likely considerable overlap of states during transitions between them (Figure 4).

C. CCM operation – inorganic carbon shuttling

As discussed above, for the fixation by Rubisco by the CBC, Ci has to pass from the external environment across at least the plasma membrane and the chloroplast envelope to Rubisco in the chloroplast stroma. At high CO_2 levels, Rubisco is predominantly diffuse in the stroma so will have direct access to stromal CO_2, however under limiting CO_2 conditions Rubisco is packaged into the pyrenoid (Borkhsenious et al., 1998) and additional Ci transport steps are involved (see below).

1. At high CO_2

At high CO_2, CO_2 diffusion alone from the external environment to the active site of Rubisco is thought to be sufficient to sustain the required CO_2 flux to maintain Rubisco carboxylation rates. However, two proteins have been implicated in CO_2 uptake at high CO_2, the high CO_2 expressed periplasmic alpha carbonic anhydrase CAH2 (Rawat and Moroney S; Fujiwara et al., 1990) and Rhesus protein 1 (RHP1) (Soupene et al., 2004). Periplasmic carbonic anhydrase could help minimize boundary layer effects at the cell surface (Reinfelder, 2011) where reduced mixing and the slow diffusion of CO_2 can be overcome through replenishing CO_2 from HCO_3^-. RHP1 is proposed to function as a CO_2 channel that could minimize CO_2 resistance across the plasma membrane. Collectively, these may help maintain a high inward CO_2 gradient with reduced membrane resistance to increase diffusion rates to support Rubisco carboxylation rates (Figure 4A).

2. Periplasmic space

In addition to CAH2, CAH1 is also found in the periplasmic space (Fujiwara et al., 1990). CAH1 and CAH2 are adjacent to each other on chromosome 4 and share 92% conservation at the amino acid level (Fujiwara et al., 1990). However, in contrast to CAH2, CAH1 is low CO_2 induced (Fujiwara et al., 1990; Fang et al., 2012). In line with CAH2 function, the role of CAH1 is most likely to maintain Ci equilibrium at the cell surface that compensates for to the slow uncatalyzed conversion between CO_2 and HCO_3^-. As discussed above, the pH would determine the CO_2:HCO_3^- ratio and the CO_2 acclimation state may determine whether Ci uptake is predominantly CO_2 based, HCO_3^- based or a balance of both. In a low CO_2 LCIB-based uptake cell state, CAH1 could predominantly replenish CO_2 at the cell surface, whereas under a very low CO_2 state CAH1 may replenish HCO_3^- for HLA3 mediated HCO_3^- uptake (Figure 4B and C). Although, CAH1 has been widely implicated in the CCM, a *cah1* mutant had no discernible reduction in Ci affinity across a broad pH range (Van and Spalding, 1999). This was in contrast to studies in which the addition of cell-impermeable carbonic anhydrase inhibitors resulted in a significant decrease in Ci affinity (Badger et al., 1980; Moroney et al., 1985). In the *cah1* mutant, carbonic anhydrase activity could be through residual CAH1, CAH2 or CAH8 activity. CAH8 has been localized to the plasma membrane, however whether the active site is orientated towards the cytosol or the periplasmic space is unknown (Ynalvez et al., 2008).

3. Transport across the plasma membrane

At limiting CO_2 two key plasma membrane localized Ci uptake proteins have been identified, LCI1 and HLA3. Both are upregulated at limiting CO_2 at the transcriptional (Im and Grossman, 2002; Brueggeman et al., 2012; Fang et al., 2012) and protein (Gao et al., 2015; Yamano et al., 2015) levels. HLA3 is an ABC (ATP-binding cassette) transporter belonging to the ABCC subfamily (Im and Grossman, 2002; Meyer and Griffiths, 2013). It contains two globular domains associated with ATP binding and hydrolysis connected by multiple long transmembrane helices associated with substrate recognition and transport across the plasma membrane (Im and Grossman, 2002; Meyer and Griffiths, 2013). Collectively, data strongly supports a role in HCO_3^- transport at very low CO_2 (Duanmu et al., 2009b; Gao et al., 2015; Yamano et al., 2015; Atkinson et al., 2016). Indirect HCO_3^- transport activity has been shown through heterologous *Xenopus* oocyte expression of HLA3 that resulted in a 2.7-fold increase in ^{14}C HCO_3^- uptake (Atkinson et al., 2016) and increased Ci affinity in the very low CO_2 range in high CO_2 grown cells over expressing HLA3 (Gao et al., 2015). In addition, a *hla3* mutant showed reduced Ci affinity at very low CO_2 at high pH (pH 9) where HCO_3^- is the dominant Ci species (Yamano et al., 2015). However, a severe CCM phenotype is only observed in a *hla3/lcia* double mutant indicating that HLA3 is not the only route for transporting Ci across the plasma membrane at very low CO_2 (see below; (Yamano et al., 2015)).

LCI1 over expression (Ohnishi et al., 2010) supported a role for this protein in Ci uptake that has recently been confirmed (Kono et al., 2020; Kono and Spalding, 2020). LCI1 has no clear evolutionary origin and is apparently unique to *Chlamydomonas* and closely related green algae (Meyer and Griffiths, 2013). A recent crystal structure resolved to 3.19 Å shows that it has four transmembrane domains that assemble into a homotrimer. Each of the subunits form an electronegative channel that

contained extra electron density at the cytoplasmic side, consistent with the presence of a CO_2 molecule (Kono et al., 2020). The transport of CO_2 instead of HCO_3^- was further supported by molecular dynamics simulations (Kono et al., 2020) and extensive O_2 evolution data using the *lci1* mutant across a wide range of Ci and pH levels (Kono et al., 2020; Kono and Spalding, 2020). Reduced photosynthetic O_2 evolution of *lci1* at lower pH, where CO_2 is favored, and investigation into the Ci affinity of *lci1* double mutant combinations that also have lesions defective for CO_2 driven uptake (*lci1*/*lcib*) and HCO_3^- uptake *(lci1*/*lcia*) support a role in CO_2 transport specifically at above air levels of CO_2 (> 0.04% CO_2), with minimal involvement at very low CO_2 (Kono and Spalding, 2020).

HLA3 and LCI1 potentially form a complex with ACA4 (Mackinder et al., 2017). ACA4 is a P-type ATPase most likely functioning in H^+ pumping into the periplasmic space. Localized regulation of periplasmic pH could help determine HCO_3^-:CO_2 ratios to support the supply of substrate to HLA3 and LCI1, depending on external Ci levels (Figure 4B and C). Likewise, regulation of cytosolic pH at the plasma membrane inner surface could help generate the Ci inward gradient and trap incoming CO_2 in the form of HCO_3^- (Moroney et al., 2011).

4. In the cytosol

After crossing the plasma membrane (PM), Ci has to move through the cytosol prior to transport across the chloroplast envelope and into the chloroplast. However, due to the structural organization of the *Chlamydomonas* cell, transit through the cytosol maybe minimal as transmission electron microscopy and cryo-electron tomography (cryo-ET) data indicate that the vast majority of the PM is tightly apposed to the chloroplast envelope (Ohad et al., 1967; Engel et al., 2015). CAH9 has been proposed to be a cytosolic carbonic anhydrase (Moroney et al., 2011). Localization of CAH9 to the cytosol was shown via fluorescent protein tagging, however it should be noted that an old and potentially incorrect gene model of *CAH9* was used to generate the clones for these studies making it necessary to further validate the localization (Mackinder et al., 2017). Whether a carbonic anhydrase is required in the cytosol is unclear; with cytosolic pH expected to be ~7, the presence of a carbonic anhydrase could be detrimental to HCO_3^- accumulation and result in increased CO_2 leakage from the cell, especially when the dominant Ci transport occurs via HCO_3^- at very low CO_2 levels. This has been shown to be the case in cyanobacteria where cytosolic expression of an exogenous carbonic anhydrase led to a severe disruption of the CCM (Price and Badger, 1989).

5. Transport across the chloroplast envelope

LCIA, also known as NAR1.2 (Nitrate assimilation-related; NAR), is the main Ci transporter associated with the chloroplast envelope (Mariscal et al., 2006; Wang and Spalding, 2014a; Yamano et al., 2015). It belongs to the formate-nitrite transporter (FNT) family (Mariscal et al. 2006), a family associated with the transport of a diverse range of small anionic molecules (Lü et al., 2013). Unlike other members of the *Chlamydomonas* NAR family, LCIA is regulated by CO_2 levels and not the nitrogen source (Mariscal et al., 2006). Electrophysiological measurements in *Xenopus* oocyte expressing the LCIA protein indicated that it could support both HCO_3^- and nitrite permeability (Mariscal et al., 2006), and ^{14}C HCO_3^- uptake in *Xenopus* oocytes was

also later shown (Atkinson et al., 2016). However, the exact function and regulation of LCIA is unknown. Interestingly, it appears that FNT members typically function as H^+ coupled symporters via transient protonation of their substrate to allow passage through a hydrophobic barrier (Lü et al., 2013; Atkovska and Hub, 2017; Wiechert and Beitz, 2017). This raises the potential that LCIA could actively drive HCO_3^- into the chloroplast due to the increased proton electrochemical gradient across the chloroplast envelope through photosynthetic driven alkalization of the stroma.

Supporting the role of LCIA in HCO_3^- uptake at very low CO_2 over that of low CO_2, is that decreased Ci affinity and growth is only seen in an *lcia* mutant at very low CO_2 and at high pH, where HCO_3^- is the predominant Ci species (Wang and Spalding, 2014a; Yamano et al., 2015). This phenotype is similar to that seen for HLA3 deficient strains (Duanmu et al., 2009b; Yamano et al., 2015). Interestingly, the *lcia* mutant has severely reduced *HLA3* transcript and subsequently HLA3 protein (Yamano et al., 2015). In contrast, in the *hla3* mutant, *LCIA* transcript and protein is unaffected (Yamano et al., 2015). These results potentially indicate a retrograde signaling event from the chloroplast to the nucleus that is dependent on correct LCIA function (see below for further discussion). A *hla3*/*lcia* double mutant showed a considerably lower Ci affinity than the *hla3* mutant at both pH 7.8 and pH 9, whilst it had a comparable Ci affinity to *lcia* at pH 7.8 but a lower sustained (i.e. 12 hours after exposure to very low CO_2 conditions) affinity at pH 9, potentially explained by the complete absence of HLA3 (Yamano et al., 2015). Due to reduced HLA3 in the *lcia* mutant it is hard to distinguish the different contributions of LCIA and HLA3, however, increased Ci affinity is only seen in high CO_2 grown WT cells when both are overexpressed, indicating that both are required for significant Ci uptake (Yamano et al., 2015). Collectively this data supports cooperative HCO_3^- uptake by HLA3 and LCIA at very low CO_2.

Further support that LCIA plays a critical role in the CCM at very low CO_2 is the phenotype of a *lcia*/*lcib* double mutant. A strain null for both LCIA and LCIB results in a severe CCM growth phenotype, fails to grow at both low and very low CO_2 and exhibits reduced Ci affinity regardless of the pH (Wang and Spalding, 2014a). In the same study and in line with other data, the *lcia* mutant only showed reduced Ci affinity at a high pH and with no reduced growth in spot tests at both low and very low CO_2. In contrast, the *lcib* mutant fails to grow at low CO_2 but showed close to WT growth at very low CO_2. This data provides convincing evidence for the role of two complementary acclimation states (Figure 4B and C), with LCIA/HLA3 involved in HCO_3^-uptake and LCIB in “active” CO_2 uptake (see below).

Other proteins that have been associated with Ci uptake across the chloroplast envelope are chloroplast envelope membrane protein A (CemA; formerly Ycf10) (Rolland et al., 1997), CIA8 (Machingura et al., 2017) and CCP1/2 (Chen et al.; Ramazanov et al., 1993; Pollock et al., 2004). CemA is encoded in the chloroplast genome with mutants showing severely reduced Ci affinity, although this analysis was performed at high light and the strain is high light sensitive. The similarity of CemA to pxcA, a cyanobacterial proton extrusion protein (Ohkawa et al., 1998), indicates a potentially similar role in maintaining the chloroplast pH and the H^+ electrochemical gradient. An over acidified stroma could potentially reduce HCO_3^- accumulation by shifting the HCO_3^-: CO_2 ratio towards CO_2, which wouldincrease leakage out of the chloroplast. It could also potentially reduce HCO_3^- import if LCIA functions as a H^+ symporter. A disrupted pH would also be expected to have non-CCM related

chloroplast functioning and photosynthetic defects that could explain the range of phenotypes seen in *cemA* mutants (Rolland et al., 1997).

In addition to LCIA, CIA8 (Ci accumulation mutant 8) has been proposed to be involved in Ci uptake potentially at the chloroplast envelope (Machingura et al., 2017), however definitive localization is still lacking. A *cia8* mutant was identified in an insertional mutagenesis screen where it failed to grow at very low CO_2. The *cia8* mutant showed a reduced affinity for Ci at both pH 7.3 and pH 9 for low CO_2 grown cells, but also a reduced Ci affinity in high CO_2 grown cells (Machingura et al., 2017). CIA8 belongs to the conserved solute carrier 10 (SLC10) family of proteins. Classically shown to be Na^+/bile acid symporter members, they have now been shown to have diverse transport and regulatory functions (Da Silva et al., 2013). Interestingly, the *cia8* mutant potentially has reduced transcription of other Ci transport related genes including *HLA3* (Machingura et al., 2017).

The strongly induced CCM proteins CCP1/2 were initially proposed to be localized to the chloroplast envelope, however fluorescent protein tagging has shown both to be mitochondrial localized, forming a typical mitochondrial network pattern that co-localizes with a mitochondrial marker dye (Atkinson et al., 2016; Mackinder et al., 2017). Initial biochemical localization to the chloroplast envelope (Ramazanov et al., 1993) could be explained by the tight association of mitochondria with the chloroplast upon low CO_2 induction (Geraghty and Spalding, 1996). CCP1/2 knock-down lines have an interesting phenotype; they show poor growth at low CO_2 with no reduction in Ci affinity, indicating that they have a role in longer-term adaption to limiting CO_2 (Pollock et al., 2004).

6. In the stroma

LCIB plays a central role in the *Chlamydomonas* CCM (Spalding et al., 1983a; Wang and Spalding, 2006; Wang and Spalding, 2014b). Under specific conditions, *lcib* mutants show an intriguing “air-dier” phenotype where they fail to grow at air-levels of CO_2 but show close to WT growth at very low CO_2 (Wang and Spalding, 2006). Importantly, although *lcib* mutants grow at very low CO_2 compared to low CO_2, this growth is slightly reduced compared to that of the WT and they have a reduced Ci affinity compared to very low CO_2 grown WT cells (Duanmu et al., 2009a), indicating that LCIB also plays a role in the CCM at very low CO_2. This is further supported by both *lcia/lcib* and *hla3/lcib* double mutants, which have more severe growth defects and a further decrease in Ci affinity at very low CO_2 relative to the individual single mutants (Duanmu et al., 2009b; Wang and Spalding, 2014a). Also of note, the *lcib* air-dier phenotype is suppressed by inactivation of the thylakoid lumen carbonic anhydrase CAH3 (see below), with *lcib*/*cah3* double mutants failing to grow at very low CO_2 but showing improved growth relative to *lcib* at low CO_2 levels (Duanmu et al., 2009a). Exactly how this data can be reconciled with the current model of the CCM is still unclear (Duanmu et al., 2009a).

LCIB forms a predicted heterohexameric complex with its homolog LCIC that shows dynamic localization (Yamano et al., 2010). *LCIB/C* transcripts and proteins are highly up regulated upon limiting CO_2. At low CO_2 LCIB/C are diffuse throughout the stroma but also seen forming puncta of varying sizes. Upon transfer into very low CO_2 they relocalize to the pyrenoid periphery where they form tight puncta that appear to fuse to form a more evenly dispersed layer around the pyrenoid (Yamano et al., 2010;

Mackinder et al., 2017). Although predominantly at the pyrenoid periphery, LCIB can also form puncta within the pyrenoid, most likely associated with the pyrenoid tubules (Yamano et al., 2010). Whereas *lcib* mutants have a clear CCM phenotype, no mutants in LCIC have been characterized to date and its functional importance remains unclear. LCIB has been proposed to be a unidirectional carbonic anhydrase that could drive HCO_3^- accumulation in the stroma (Wang and Spalding, 2014b). Structural studies indicate that LCIB belongs to the beta carbonic anhydrase family and LCIB homologs isolated from diverse algae showed carbonic anhydrase function in vitro, although carbonic anhydrase activity could not be demonstrated for LCIB (Jin et al., 2016). A recent diffusion-reaction model of the *Chlamydomonas* CCM indicates that if LCIB functions as a carbonic anhydrase it would not need to be directional and that the high pH of the stroma maintained during photosynthesis would allow LCIB driven HCO_3^- accumulation by rapidly converting membrane permeable CO_2 to membrane impermeable HCO_3^- (Fei et al., 2021). At very low CO_2, where a HLA3/LCIA HCO_3^- based uptake system dominates, the relocalization of LCIB to the pyrenoid periphery would minimize HCO_3^- to CO_2 conversion of imported HCO_3^- and potentially enable recapture of CO_2 leaking out of the pyrenoid (see below). There are two additional LCIB/C homologs, LCID and LCIE. Both *LCID* and *LCIE* are low CO_2 induced genes with *LCIE* only expressed at low levels (Fang et al., 2012). Both require further investigation into their function, if any, in the CCM.

In addition to LCIB, CAH6 was proposed to be stromal localized. However, both fluorescence protein fusion data (Mackinder et al., 2017) and flagella proteome data (Pazour et al., 2005; Engel et al., 2012) support its localization in flagella and not the chloroplast.

7. Transport across the thylakoid lumen

At both low and very low CO_2, accumulated stromal HCO_3^- is proposed to passively enter the thylakoid lumen via three bestrophin-like homologs BST1-3. BST1-3 have been localized to thylakoids with enrichment in the thylakoids located at the pyrenoid periphery (Mukherjee et al., 2019). Bestrophins are typically linked to Cl^- channeling, however they have also been shown to be HCO_3^- permeable (Qu and Hartzell, 2008; Yu et al., 2010). RNAi knockdown lines of BST1-3 showed reduced growth at very low CO_2, reduced Ci affinity and Ci accumulation (Mukherjee et al., 2019). This data is further corroborated in a recent membrane inlet mass spectrometry (MIMS) study that also indicates reduced Ci uptake in the BST1-3 knock-down lines upon Ci addition and that this corresponds to only a small reduction in the proton motive force (*pmf*) compared to a large *pmf* drop in WT (Burlacot et al., 2021). These results indicate that BST1-3 are potentially using the *pmf* to drive HCO_3^- uptake, most likely by supplying protons for the conversion of HCO_3^- to CO_2 via CAH3 within the thylakoid lumen (see below). In the same study Burlacot et al. (2021) showed that a *pgrl1/flvB* double mutant perturbed in both CEF and PCEF has a severe CCM defect at both low and very low CO_2. Providing strong evidence that *pmf* generation via CEF/PCEF energizes the CCM (Burlacot et al., 2021) most likely by driving HCO_3^- dehydration to CO_2 within the thylakoid tubules that traverse the pyrenoid, but could also support HCO_3^-uptake into the stroma via LCIA if LCIA functions as a HCO_3^-/H^+ symporter (see above).

Affinity purification followed by mass spectrometry indicates that BST1 and BST3 interact with LCIB and LCIC (Mackinder et al., 2017). This potentially enables LCIB

mediated HCO_3^- accumulation to be in close proximity to HCO_3^- channeling into the thylakoid lumen via BST1-3. These identified interactions require further confirmation via complementary approaches. Evidence for direct HCO_3^- transport by BST1-3 is still lacking and should be a priority of future work. It is unknown if BST1-3 forms pentamers similar to other characterized bestrophins (Kane Dickson et al., 2014; Yang et al., 2014; Owji et al., 2020), and if such putative assembled complexes are homo- or heteromeric.

8. CO_2 release and fixation by Rubisco in the pyrenoid

Several mutants that failed to grow in atmospheric CO_2 but over-accumulated Ci up to five times that of WT cells were identified through mutagenesis screens (Spalding et al., 1983b; Moroney et al., 1986). These were later identified as having mutations in the *CAH3* gene (Funke et al., 1997). The over accumulation of Ci in the absence of a thylakoid localized CAH3 strongly supports the functional importance of a carbonic anhydrase in accelerating HCO_3^- dehydration to CO_2 and that the *pmf* and thylakoid acidification through CEF may drive the CCM, as proposed by (Raven, 1997) and (Pronina and Borodin, 1993), and further supported via experimental data (Burlacot et al., 2021) and reaction diffusion modelling (Fei et al., 2021). CAH3 has also been associated with PSII function, potentially by H^+ removal via HCO_3^- dehydration at the electron donor side of PSII, however the exact function is unclear (Villarejo et al., 2002; Benlloch et al., 2015; Terentyev et al., 2019). During CCM induction there is evidence that CAH3 moves within the thylakoid lumen from thylakoids outside of the pyrenoid to the thylakoid tubules traversing the pyrenoid (termed pyrenoid tubules) (Markelova et al., 2009; Sinetova et al., 2012). Modelling also supports the requirement for CAH3 accelerated CO_2 release within the pyrenoid tubules for efficient CCM function (Fei et al., 2021). The dynamic movement of CAH3 from potentially PSII to the PSII lacking pyrenoid tubules during CCM induction is interesting and could explain both PSII and CCM related phenotypes (Sinetova et al., 2012), however conclusive evidence for this is still lacking. As CAH3 is present at both high and low CO_2, regulation is most likely post-translational. There is evidence that CAH3 undergoes phosphorylation during CCM induction (Blanco-Rivero et al., 2012b), however whether this is the trigger for relocation or activity is unclear.

Once CO_2 is released within the pyrenoid tubules it is proposed to leak across the pyrenoid tubule membranes into the pyrenoid matrix for fixation via Rubisco.

D. Pyrenoid structure and function

At the heart of the *Chlamydomonas* CCM is the pyrenoid. Failure to assemble the pyrenoid (Meyer et al., 2012; Mackinder et al., 2016) or incorrect assembly (Ma et al., 2011; Itakura et al., 2019) results in a severe high CO_2 requiring phenotype. Pyrenoids are widespread throughout diverse algae and are strongly associated with efficient CCM function (Badger et al., 1998; Meyer et al., 2020a; Barrett et al., 2021).

1. Spatial organization of the pyrenoid

The *Chlamydomonas* pyrenoid is a phase-separated assembly of Rubisco around membrane tubules (pyrenoid tubules) that are continuous with the thylakoids. A single pyrenoid assembles at a central position within the cup of the chloroplast. Three clear

pyrenoid sub-regions are visible via electron microscopy: pyrenoid tubules, pyrenoid matrix and starch sheath (Ohad et al., 1967). However, using fluorescence fusion proteins at least 8 protein sub-regions can be distinguished (Mackinder et al., 2017; Meyer et al., 2020b). Cryo-ET of the pyrenoid highlighted the intricate structure of the pyrenoid tubules and the dramatic structural changes that thylakoids undergo as they converge and change from flat stacked assemblies to tubular structures at the pyrenoid periphery (Engel et al., 2015). At the centre of the pyrenoid several pyrenoid tubules converge to form the pyrenoid tubule knot. Within the pyrenoid tubules are ~4-6 minitubules that provide direct channels between the stroma and the pyrenoid matrix (Figure 4D) (Engel et al., 2015). The molecular basis underpinning pyrenoid tubule formation is unknown and whether this predates or postdates pyrenoid matrix assembly or whether pyrenoid tubule formation and matrix assembly are a co-dependent process is unclear. It is also unclear if pyrenoid tubule formation is required for pyrenoid positioning and CCM function. Several proteins have been specifically localized to the pyrenoid tubules including CAH3 (Markelova et al., 2009; Blanco-Rivero et al., 2012b), CAS (Wang et al., 2016), Rubisco binding membrane protein (RBMP) 1, which is found throughout the tubules (Meyer et al., 2020b), RBMP2, which is enriched at the pyrenoid tubule knot (Meyer et al., 2020b), and PSBP4, which is found at the thylakoid convergent sites at the pyrenoid periphery (Mackinder et al., 2017). The functions of RBMP1/2 are unknown, although they could be involved in pyrenoid assembly (see below). A *psbp4* mutant is acetate requiring and light sensitive (Wakao et al., 2021) and through homology to an Arabidopsis PSBP4 protein most likely has a role in PSI assembly (Liu et al., 2012; Mackinder et al., 2017). Also, PSI components, PSAH (Mackinder et al., 2017) and PSAF (Emrich-Mills et al., 2021) have been shown to be good markers for pyrenoid tubules; unlike some other photosystem proteins they appear not to be excluded from them (Mackinder et al., 2017). However, it is still unclear if fully assembled and functional PSI, PSII and cytochrome b_6f have access to the pyrenoid tubules.

Surrounding the pyrenoid tubules is the pyrenoid matrix. The matrix is formed through liquid-liquid phase separation via the condensation of Rubisco and Essential Pyrenoid Component 1 (EPYC1) (Mackinder et al., 2016; Freeman Rosenzweig et al., 2017; Wunder et al., 2018). EPYC1 is a predominantly disordered protein that contains four nearly identical ~60 amino acid repeats each containing a Rubisco Binding Motif (RBM) with an additional C-terminal RBM. Via weak but multivalent interactions of the RBM with the eight available binding sites on the Rubisco holoenzyme (He et al., 2020) complex coacervation takes place resulting in a dense phase-separated Rubisco assembly that can be mimicked *in vitro* (Wunder et al., 2018) and also in plant chloroplasts (Atkinson et al., 2020). The phase-separated Rubisco matrix has liquid-like properties demonstrated through continual internal mixing, pyrenoid growth via coalescence of discrete Rubisco droplets, fission during division and short order Rubisco distribution that resembles that of a liquid (Freeman Rosenzweig et al., 2017). Under CCM induced conditions, >80% of Rubisco is condensed into the pyrenoid. In contrast, at high CO_2 and in the dark the pyrenoid undergoes partial dissolution by an unknown mechanism resulting in a pyrenoid with <40% of the Rubisco (Borkhsenious et al., 1998; Mackinder et al., 2016). Fluorescence protein tagging (Mackinder et al., 2017; Meyer et al., 2020b), pyrenoid proteomics (Mackinder et al., 2016; Zhan et al., 2018) and affinity purification followed by mass spectrometry (Mackinder et al., 2017) has identified over 100 high-confidence pyrenoid components. Whilst some appear to

be solely localized to the pyrenoid, a large number are either enriched in the pyrenoid but also within the stroma or equally distributed throughout the pyrenoid and stroma (Mackinder et al., 2017).

Under CCM induced conditions a tightly packed starch sheath of a varying number of plates is assembled around the pyrenoid matrix (Kuchitsu et al., 1988; Ramazanov et al., 1994). In addition to carbohydrate storage, the starch appears to act as a diffusion barrier to prevent CO_2 leakage from the pyrenoid matrix (Toyokawa et al., 2020). Although the role of the starch sheath in the CCM has been questioned (Villarejo et al., 1996), both experimental data (Itakura et al., 2019; Toyokawa et al., 2020) and modelling data (Fei et al., 2021) indicate an important role in efficient CCM operation. Modelling supports the importance of the starch sheath as a CO_2 diffusion barrier to increase CO_2 within the pyrenoid matrix (Fei et al., 2021). However, experimental data using mutants deficient in the starch synthesis proteins isoamylase1 (ISA1) and a-1,4 glucanotransferase (STA11) that lack an intact starch sheath indicate that phenotypes associated with the absence of starch may be more complicated (Toyokawa et al., 2020). Both *isa1* and *sta11* mutants showed a CCM related growth defect at very low CO_2, however both also had perturbed LCIB localization, with LCIB forming a single large punctum at the pyrenoid periphery instead of an even peripheral pyrenoid layer (Toyokawa et al., 2020). This mislocalization of LCIB makes it difficult to determine whether the reduced CCM efficiency is a consequence of the absence of a CO_2 diffusion barrier or the perturbed function of LCIB.

Several other starch synthesis proteins have also been localized to the starch sheath including STA2 and SBE3 (Mackinder et al., 2017). Of interest is the localization pattern shown by LCI9 that is enriched at the junctions between starch plates and forms a clathrin-like structure around the pyrenoid matrix (Mackinder et al., 2017). A CCM mutant in Starch Granule Accumulation 1 (SAGA1) that appears to be localized at the pyrenoid matrix/starch sheath interface has a highly perturbed starch sheath and formed multiple pyrenoids (Itakura et al., 2019), however its exact role in starch formation and pyrenoid assembly is unclear. Pyrenoid starch is degraded at high CO_2 and during the dark. Break down in the dark most likely provides ATP to support cellular processes, however high CO_2 disassembly of the starch sheath may be required for Rubisco to diffuse out of the pyrenoid and into the surrounding stroma, enabling increased access to CO_2 in the absence of active Ci uptake (Figure 4A).

2. A Conserved Rubisco Binding Motif Organizes the Pyrenoid

As outlined above, the pyrenoid matrix is formed via Rubisco condensation through EPYC1. Each of the five RBMs on EPYC1 form both electrostatic and hydrophobic interactions with the Rubisco interface formed by the two alpha helical domains of the Chlamydomonas SS (Meyer et al., 2012; He et al., 2020). This explains the atomic basis for the inability of *Chlamydomonas* LS -plant SS hybrid Rubisco's to form a pyrenoid (Meyer et al., 2012). Additionally, the short EPYC1 RBM was shown to be present across several additional pyrenoid localized proteins and is responsible for targeting proteins to the pyrenoid (Meyer et al., 2020b). Disruption of the RBM in a pyrenoid localized protein results in the inability of the protein to accumulate in the pyrenoid, whilst the addition of a 3xRBM to a non-pyrenoid enriched stromal protein or thylakoid protein resulted in targeting to the pyrenoid. Proteins containing RBMs also contain a range of other domains including the carbohydrate binding module 20

(CBM20; seen in SAGA1, SAGA2), extended coiled-coil domains (SAGA1) and transmembrane domains (RBMP1 and RBMP2). This led to the proposal that the RBM may guide pyrenoid assembly, with RBMP1/2 linking the pyrenoid matrix to the pyrenoid tubules and SAGA1/2 linking the starch sheath to the matrix. However, an alternative explanation, or a co-function of the RBM, could be the precise targeting of proteins to pyrenoid sub regions to perform a specific function.

E. CCM regulation and Ci sensing

Full CCM induction requires both light and limiting CO_2 (Wang et al., 2015), however at least a subset of CCM genes can be induced at very low CO_2 levels in the dark (Ruiz-Sola et al., 2021). The CCM also appears to be under tight circadian control with increased Ci affinity and a subset of CCM gene transcripts and proteins up-regulated prior to the onset of light in synchronized cultures (Mitchell et al., 2014; Tirumani et al., 2014; Strenkert et al., 2019). How *Chlamydomonas* senses Ci, integrates it with light-driven processes and the circadian rhythm is unclear. Transcriptomics during low CO_2 acclimation and between cells grown at high and limiting CO_2 identified between 2000-5500 genes that are transcriptionally regulated by CO_2 availability (Brueggeman et al., 2012; Fang et al., 2012). The signal sensing Ci limitation required for CCM induction could be due to direct sensing of a change in Ci, could be through sensing specific metabolites (i.e. photorespiratory intermediates), the redox poise or energy status of the cell, or be a combination of the above.

Whilst guanylate/adenylate cyclases and cAMP signaling has been implicated in CO_2 sensing in diverse organisms including diatoms (Harada et al., 2006; Cummins et al., 2014), there is currently no evidence for their role in Ci sensing in *Chlamydomonas* although they have been linked to hypoxia (Düner et al., 2018) and carbon monoxide (Horst et al., 2019) sensing. Of note is the chemotactic behaviour of *Chlamydomonas* towards Ci (Choi et al., 2016), indicating the directional sensing of Ci. Whether this is linked to or separate from CCM induction is yet to be explored. It has been proposed that CAH6 within the flagella could play a role in this chemotactic behaviour, however this is still lacking substantial support.

Whilst little is known about the genetic basis of sensing a change in Ci availability, there are several genes implicated in the transcriptional control of the CCM. Dubbed as the “master regulator”, CIA5 (also known as CCM1) appears to exert transcriptional control over most limiting CO_2 induced genes associated with the CCM (Fang et al., 2012). The *cia5* mutant has a severely defective CCM and lacks considerable control over CCM induction, particularly at the transcriptional level (Moroney et al., 1989; Fukuzawa et al., 2001; Xiang et al., 2001; Miura et al., 2004; Fang et al., 2012). Although the function of CIA5 is still not fully resolved, it most likely acts as a transcription factor or transcription co-activator. It contains two zinc binding domains (Kohinata et al., 2008) and a transcriptional activation domain (Chen et al., 2017). *CIA5* is constitutively expressed across CO_2 levels but very little is known about how CIA5 is activated and what target genes it directly interacts with. Transcriptional response comparisons between WT and the *cia5* mutant across CO_2 levels (Miura et al., 2004; Fang et al., 2012) indicate that over 2700 genes (~15% of genes) are under the control of CIA5 with approximately half of these showing no CO_2 response. This finding indicates that CIA5 most likely plays a critical role in the regulation of cellular processes outside of the CCM (Fang et al., 2012). Approximately 14% of detected genes were

CO_2 regulated, of which over two-thirds were under some form of CIA5 regulation (Fang et al., 2012). The finding that ~4% of detected genes were CO_2 regulated independent of CIA5 indicates that other regulatory genes either working in parallel or upstream of CIA5 are yet to be identified. Supporting the diverse function of CIA5 is the role it plays in photoprotection control, through its transcriptional regulation of energy dependent quenching (qE) components LHCSR3 (Light Harvesting Complex-Stress Related protein 3) and PSBS (Photosystem II Subunit S). Interestingly, photoprotective gene regulation appears to respond to intracellular CO_2 levels independent of light. With light having an indirect affect by driving photosynthetic electron flow that produces ATP and NADPH for CO_2 fixation in the CBC and in turn reducing intracellular CO_2. This is supported by CIA5 dependent photoprotection and CCM gene induction at very low CO_2 levels in the dark and repression by CO_2 release via acetate metabolism or inhibiting photosynthetic electron flow (Ruiz-Sola et al., 2021).

Downstream and regulated by CIA5 is the Myb-type transcription factor LCR1. LCR1 is upregulated when CO_2 becomes limiting and directly regulates a subset of CCM genes including *LCI1* and *CAH1* (Yoshioka et al., 2004). LCR1 has been shown to directly interact with the CAH1 promoter (Yoshioka et al., 2004), however CAH1 activation (and most likely other LCR1 target genes) is likely more complex than just LCR1 regulation as the CAH1 promoter region contains both enhancer and silencing regions that bind multiple nuclear proteins (Kucho et al., 1999; Kucho et al., 2003) and there is still transient but unsustained expression of CAH1 in the *lcr1* mutant (Yoshioka et al., 2004).

CO_2 enters the CBC through fixation via Rubisco. As CO_2 becomes limiting the CO_2:O_2 ratio at the active site of Rubisco decreases resulting in a transient increase in photorespiration until full induction of the CCM (Brueggeman et al., 2012; Wang et al., 2015). In parallel to an increase in the flux through the photorespiratory pathway there is a decrease in CBC flux during the initial period of acclimation to limiting CO_2, resulting in a reduction in NADPH oxidation and an over-reduction of the photosynthetic electron transport chain (Lucker and Kramer, 2013). A knock-on effect is the increased pressure on PSII excitation. To reduce this pressure at least two processes in addition to LHCSR/PSBS mediated photoprotection take place. One is a state transition from state I to state II where light harvesting complex II (LHCII) moves from PSII to PSI, which reduces PSII excitation (Goldschmidt-Clermont and Bassi, 2015). However, this appears to relax after approximately one hour even in limiting CO_2 conditions. The second and longer-term reduction of PSII excitation appears due to the translational repression of light-harvesting proteins (LHCBMs) by NAB1 (Berger et al., 2014). Upstream of NAB1 is the low CO_2 response factor (LCRF), a squamosa promoter-binding family transcription factor. LCRF is upregulated within 6 minutes of exposure to limiting CO_2, and in turn activates NAB1 that translationally represses the major light harvesting protein LHCBM6, decreasing PSII antenna size (Blifernez-Klassen et al., 2021). This minimizes overexcitation of PSII and potentially enables a new, longer-term ATP/NADPH ratio to be set for CCM function. LCRF regulation appears to be via a retrograde signal from the chloroplast and it has been proposed that over reduction of the plastoquinone pool that is important for initiating state transitions could also be the signal (Blifernez-Klassen et al., 2021).

Upon exposure to low Ci there is a rapid increase in CEF and decrease in linear electron flow (LEF) resulting in a CEF:LEF ratio change from ~1.5 to ~3.5 (Lucker and

Kramer, 2013). Although, a transition from state I to state II may support this change, it is unlikely to be the primary contributor due to a comparable CEF:LEF change in the state transition mutant (*stt7-9*), which is locked in state I (Lucker and Kramer, 2013). Lucker and Kramer (2013) propose that regulation by either redox or allosteric changes via metabolites (i.e. NADPH:ATP), ions such as Ca^{2+} or reactive oxygen species could induce the observed rapid CEF:LEF ratio changes. Understanding this trigger during the early stage of acclimation to limiting CO_2 could help shed light on Ci sensing and the rapid transcriptional responses seen upon a high to low CO_2 shift (Brueggeman et al., 2012; Blifernez-Klassen et al., 2021).

Work investigating the role of the Ca^{2+}-binding protein, CAS, in the CCM supports a regulatory link between photosynthetic processes in the thylakoid, and potentially the pyrenoid, with the nucleus via retrograde signaling (Wang et al., 2016). CAS has a Ca^{2+} binding N-terminal and upon limiting CO_2 moves from thylakoids outside of the pyrenoid to the pyrenoid tubules. This movement coincides with increased pyrenoid Ca^{2+} concentration. CAS mutants have a perturbed CCM and upon low CO_2 exposure fail to maintain upregulation of several core CCM genes including *LCIA* and *HLA3*. Interestingly in WT cells Ca^{2+} is also critical for HLA3 and LCIA induction (Wang et al., 2016). CAS has also been implicated in photoacclimation and CEF (Petroutsos et al., 2011; Terashima et al., 2012), again highlighting the interlinking of short-term photoacclimation, CEF and the CCM. Related to the above and in further support of a role for chloroplast to nucleus retrograde signaling for CCM control is the coregulation of *LCIA* and *HLA3* with the decreased *HLA3* transcripts in the LCIA mutant (Yamano et al., 2015) and the failure to accumulate LCI1 upon disruption of CEF and PCEF (Burlacot et al., 2021).

Rapid post-translational regulation of photosynthetic processes, including state transitions, is widely observed (Grabsztunowicz et al., 2017) and the regulation of the CCM by post-translation modification (PTM) has been suggested (Wang et al., 2015). It is of particular interest in relation to the low CO_2 to very low CO_2 acclimation transition that appears to be primarily independent of transcription (Fang et al., 2012) and the accumulating data indicating that many CCM related proteins relocate during CCM induction. Phosphorylation has been implicated in CAH3 relocation (Blanco-Rivero et al., 2012a), and has been suggested as a control mechanism for Rubisco condensation (Freeman Rosenzweig et al., 2017) based on the multiple phosphorylation sites on EPYC1 (Turkina et al., 2006) and is of interest with respect to LCIB/C regulation/relocalization since phosphorylation of LCIC has been detected (Wang et al., 2014). LCIB was also shown to be glutathionylated (Zaffagnini et al., 2012), suggesting a redox regulation role in LCIB function and CCM acclimation. However, to date no PTMs have been unambiguously linked to CCM protein function and CCM induction.

VII. Conclusions: A Rubisco centric view of the CCM

Rubisco assembly, structure and function is intricately linked to CCM operation. And vice-versa, CCM function is directly linked to Rubisco performance and enables algae to achieve high photosynthetic rates with considerably less Rubisco than non-CCM containing species (Bar-On and Milo, 2019). At the heart of this intertwined function is the pyrenoid, which enables the spatial separation of Rubisco from the bulk stroma in

an enriched CO_2 environment. Pyrenoid assembly, and hence CCM function, is directly dependent on Rubisco assembly and structure. The interaction of EPYC1 with specific residues in the SS ensures that only correctly assembled Rubisco holoenzymes are condensed into the pyrenoid. The identification of a conserved RBM that guides assembly and organization of the pyrenoid indicates a central role for Rubisco in pyrenoid assembly and CCM function. This Rubisco, and hence pyrenoid-centric view of the CCM is proving critical for our understanding of CCM function and the synthetic engineering of a CCM (Atkinson et al., 2020). It is envisioned that future discoveries will further interlink Rubisco assembly, structure and function with the CCM in *Chlamydomonas* and these discoveries will drive forward our knowledge across diverse algal lineages, many that contain diverse forms of Rubisco.

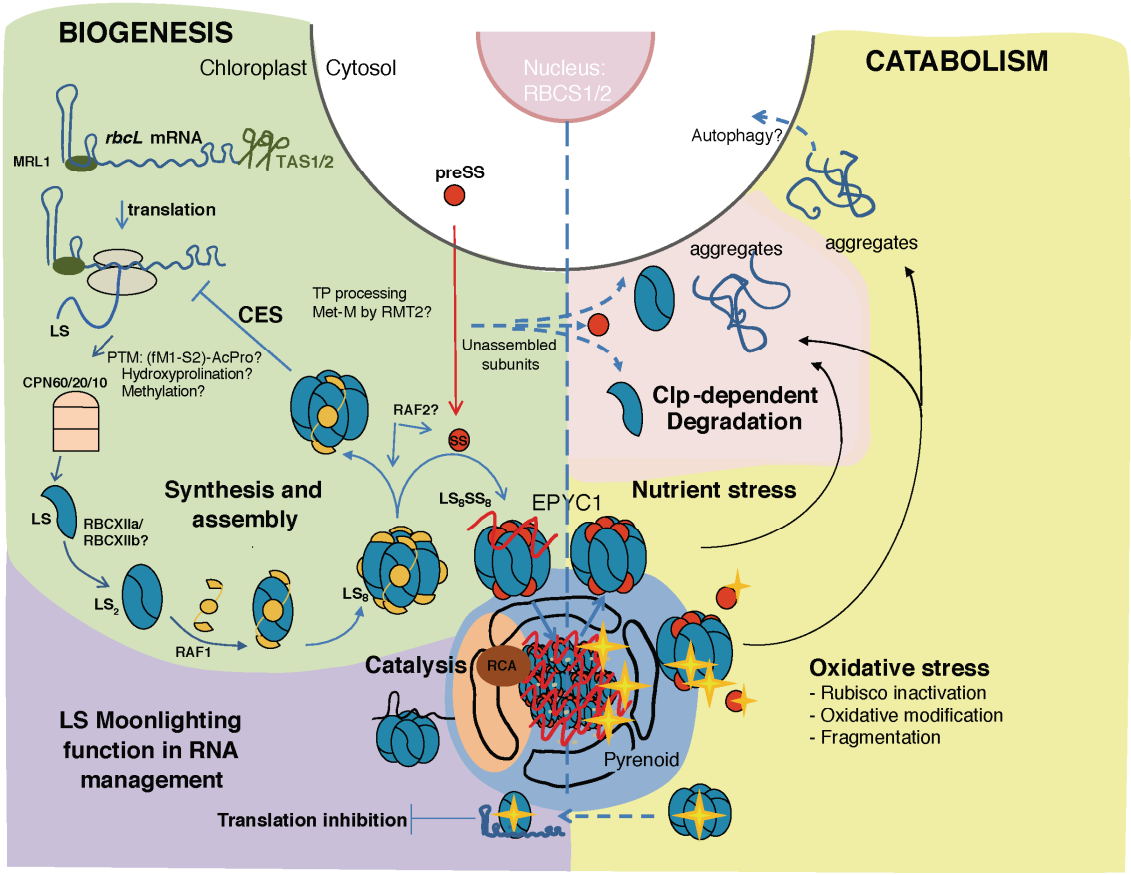

Figure 1. Main steps of Rubisco biogenesis and catabolism
Biogenesis starts with transcription of the *RBCS* genes in the nucleus, and of *rbcL* in the chloroplast. The *rbcL* mRNA is processed at the 3' end possibly by the TAS1/2 factors, and is stabilized by binding of the MRL1 factor onto *rbcL* 5'UTR. Nascent LS exiting from the ribosome will undergo N-terminal processing before being taking over by the Chaperonin (CPN60/20/10) for proper folding. It is not yet known at which step other PTM such as hydroxyprolination of residues P104 and P151 or methylation of Cys256 and 369 occur. LS dimerization will follow, maybe facilitated by the RbcX2A chaperone. Dimers will be stabilized by the RAF1 chaperone and will further oligomerize yielding a tetramer of dimers. After being translated in the cytoplasm and import into the chloroplast, the SS targeting signal is cleaved, followed by the methylation of its N-ter Methionine residue, possibly by the RMT2 methyltransferase. SS will displace RAF1 from the LS_8-$RAF1_8$ complexes, thereby yielding the LS_8SS_8 Rubisco holoenzyme. The RAF2 chaperone may be involved in this late assembly step, but its precise role remains to be characterized. Unassembled SS subunits are degraded by the Clp protease. Unassembled LS not stabilized by the RAF1 chaperone will be similarly degraded, while the presence of a LS_8-RAF1 complex will inhibit further LS synthesis through the Control by Epistasy of Synthesis (CES) process. The interaction of the SS within the assembled Rubisco with the EPYC1 protein will result in Rubisco condensation and pyrenoid formation. An LS fraction, not assembled within the holoenzyme, was shown to interact with RNA in the pyrenoid vicinity, which could provide a way to manage RNA from oxidative modifications. Oxidative stress induced Rubisco inactivation, oxidative modification and possibly fragmentation (yellow stars),

followed by enzyme disassembly and degradation. LS aggregates can form and in some cases are found associated to membranes, maybe in relation to the formation of autophagic vesicles. Nutrient stress induced Rubisco degradation through NO signaling, in a pathway involving Clp-dependent degradation.

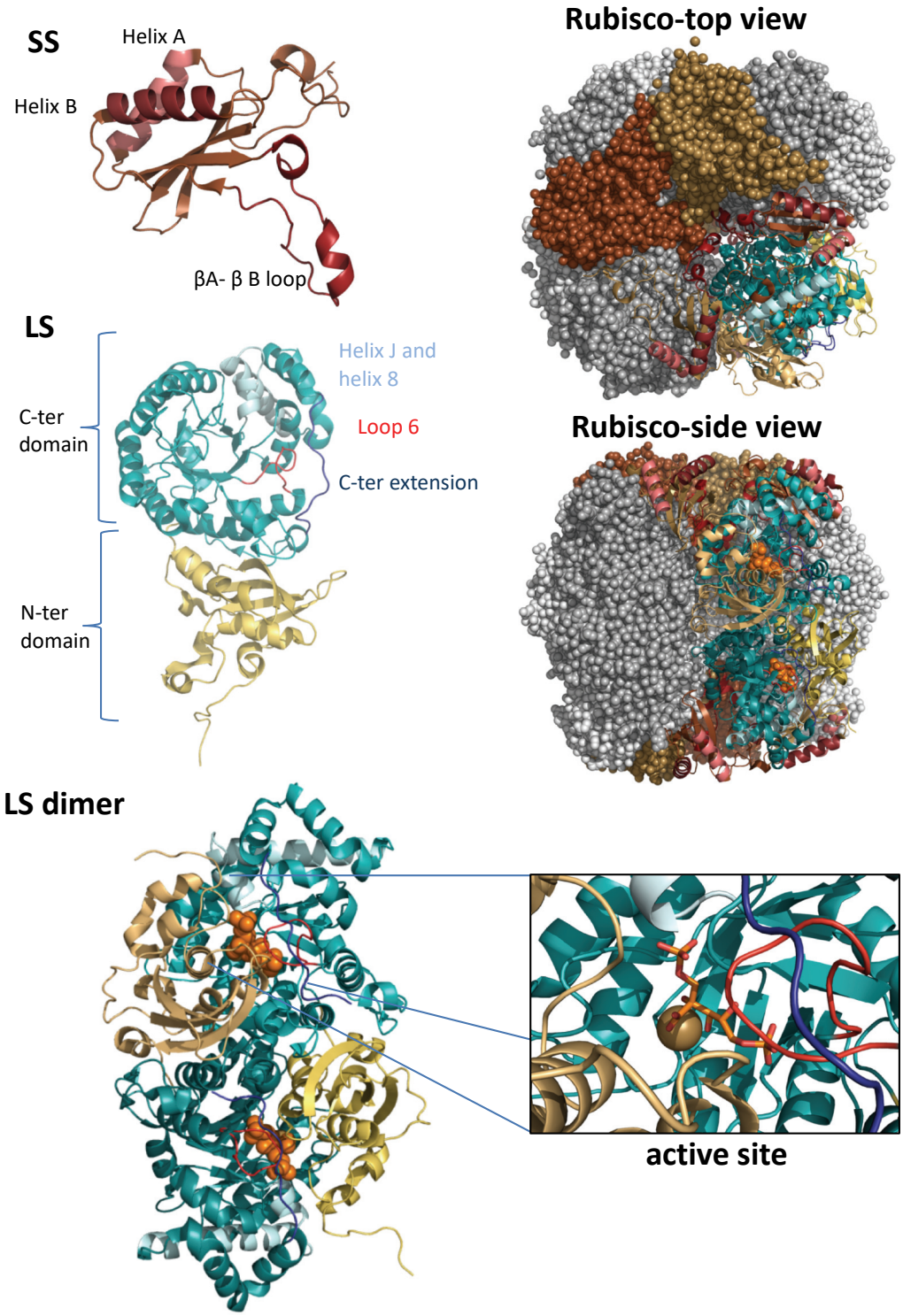

Figure 2. Rubisco subunits and holoenzyme structure in *Chlamydomonas* (from 1IR2, Mizohata et al., 2002). The eight LS are depicted in dark and light grey colors. Four SS cap the LS octamer on the top and bottom, as visible from the top and side view of Rubisco holoenzyme structure. SS monomers, depicted in brown and chocolate colors, consist in a 4-stranded β-sheet covered on one side by two helixes (helix A (salmon), helix B (ruby)). The variable βA- βB loops (firebrick), is buried in the central cavity formed by the LS octamer. LS monomers are composed of an N-ter domain (pale yellow) and C-ter domain adopting a TIM-barrel structure (blue). Specific features

mentioned in the main text are highlighted such as: loop 6 (red), the C-ter extension (dark blue) and helixes J and 8 (pale blue). The latter shows contact with SS. Two catalytic sites are formed at the dimer interface, as seen by the position of the CABP 6-carbon transition analog, represented in orange either as spheres in the LS dimer view or as sticks in the active side close-up view. The Mg ion binding to the carbamylated K201 residue is represented as a sphere in sand color.

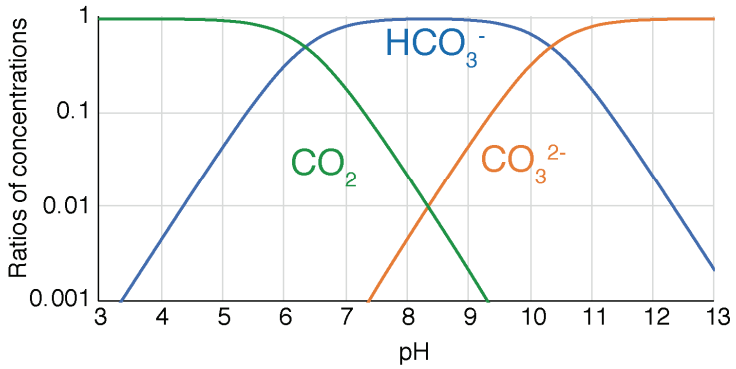

Figure 3. Bjerrum plot showing the relationship between dissolved inorganic carbon species as a function of pH. Note the logarithmic Y-axis. Plot is drawn using data from CO2SYS (Lewis and Wallace, 1998) with constants for freshwater (Millero, 1979).

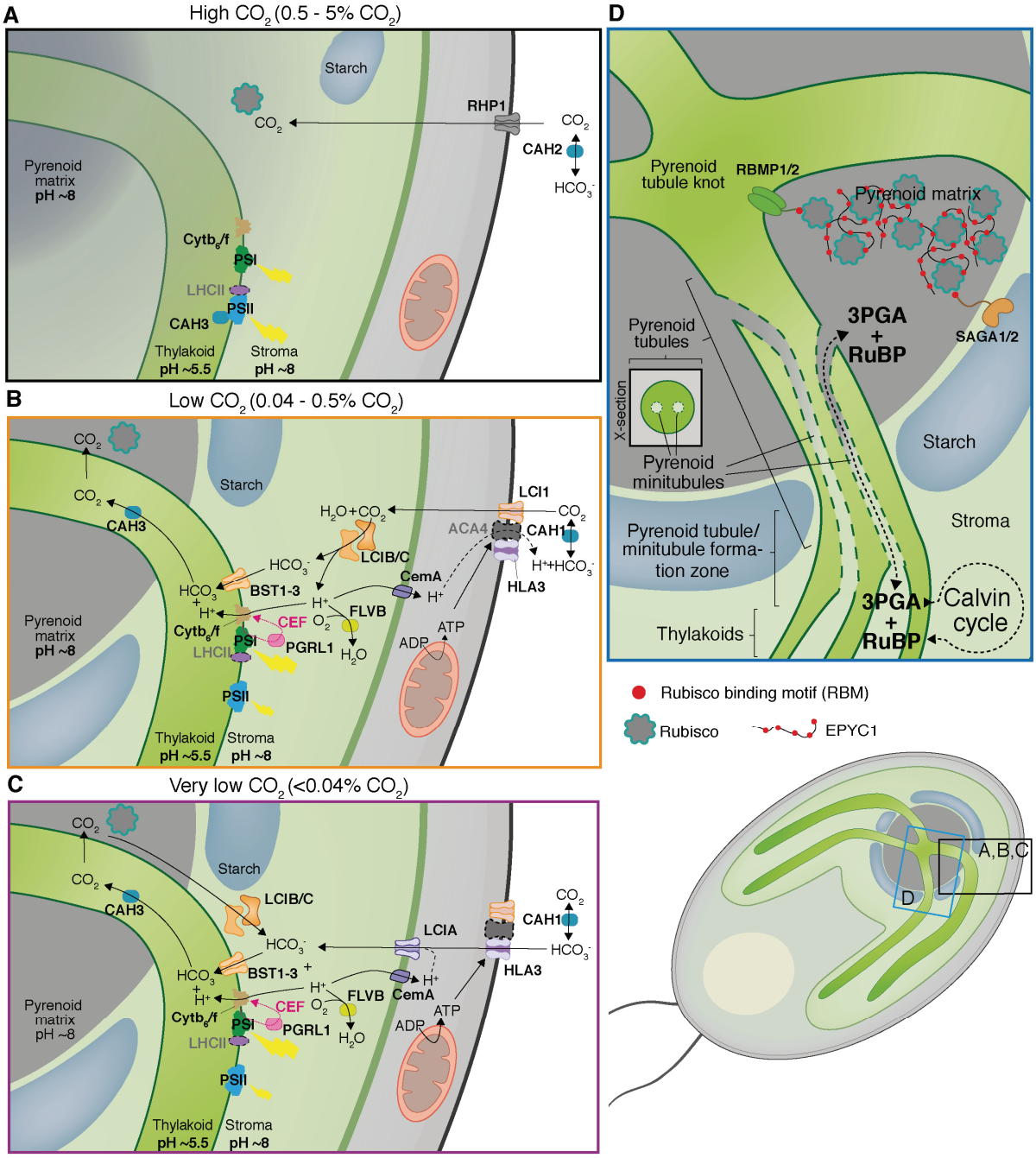

Figure 2. The different CO_2 acclimation states of Chlamydomonas and pyrenoid structural organization. (A-C) The three different acclimation states of the CCM. **A)** At high CO_2, the inwards CO_2 gradient is thought to be sufficient to enable Rubisco active site saturation. Potentially, the carbonic anhydrase CAH2 helps to replenish cell surface CO_2 and the CO_2 channel, RHP1, reduces resistance to CO_2 across the plasma membrane. **B)** At low CO_2 an LCIB carbonic anhydrase centric Ci uptake system dominates. CO_2 diffusion across the plasma membrane is assisted via the CO_2 channel LCI1, that could be enhanced via H^+ pumping of ACA4. The high pH of the stroma created via light driven H^+ pumping into the thylakoid lumen, and potentially the chloroplast envelope H^+ pump CemA, favours HCO_3^- over CO_2, creating an inwards CO_2 gradient. Once CO_2 enters the stroma, LCIB catalyzes CO_2 conversion to HCO_3^- which is then channeled into the thylakoid lumen via BST1-3.

Subsequently thylakoid lumen carbonic anhydrase, CAH3, localized in the pyrenoid tubules catalyzes HCO_3^- dehydration to CO_2 in the acidic thylakoid lumen that can leak into the pyrenoid matrix for fixation via Rubisco. Protons required for CAH3 mediated HCO_3^- dehydration are potentially supplied via increased cyclic electron flow (CEF) around PSI (shown in pink). The trigger and mechanism that results in increased CEF (and decreased linear electron flow) are unclear, however a state transition involving LHCII movement from PSII to PSI has been implicated to some degree. Starch sheath formation at the periphery of the pyrenoid creates a diffusion barrier to minimize CO_2 leakage away from Rubisco. **C)** At very low CO_2 a HCO_3^- based uptake system dominates. HCO_3^- is pumped across the plasma membrane via HLA3 most likely through ATP hydrolysis of mitochondrial supplied ATP and across the chloroplast envelope via LCIA that potentially acts as H^+/HCO_3^- symporter. Once in the stroma HCO_3^- follows the same route as at low CO_2. To minimize unwanted HCO_3^- to CO_2 conversion in the bulk stroma and to capture CO_2 leaking out of the pyrenoid matrix LCIB moves to the periphery of the pyrenoid.

Table 1: Gene-identifiers for Chlamydomonas candidate genes involved in Rubisco biogenesis, maintenance and pyrenoid organization

Name (alias)	Gene identifier	Involved in	Reference publication
RBCS1	Cre02.g120100	Rubisco holoenzyme subunit	Goldschmidt-Clermont and Rahire, 1986
RBCS2	Cre02.g120150	Rubisco holoenzyme subunit	Goldschmidt-Clermont and Rahire, 1986
rbcL	CreCp.g802313	Rubisco holoenzyme subunit	Dron et al., 1982
MRL1	Cre06.g298300	*rbcL* transcript stabilization	Johnson et al., 2010
RAF1	Cre06.g308450	Rubisco chaperone	Wietrzynski et al, 2021
RAF2 (CGL31)	Cre01.g049000	Rubisco chaperone	Not yet described in Cr
RBCX2A (CGL41/CrRbcXIIa)	Cre01.g030350	Rubisco chaperone	Bracher et al., 2015
RBCX2B (CrRbcXIIb)	Cre07.g339000	Rubisco chaperone	Bracher et al., 2015
CPN60A (CPN60 α)	Cre04.g231222	Rubisco chaperonin required for LS folding	Thompson et al., 1995
CPN60B1 (CPN60 β1)	Cre17.g741450	Rubisco chaperonin required for LS folding	Thompson et al., 1995
CPN60B2 (CPN60 β2)	Cre07.g339150	Rubisco chaperonin required for LS folding	Thompson et al., 1995
CPN20	Cre08.g358562	Rubisco chaperonin Cofactor required for LS folding	Schroda et al., 2004
CPN23	Cre12.g505850	Rubisco chaperonin Cofactor required for LS folding	Schroda et al., 2004
CPN11	Cre16.g673729	Rubisco chaperonin Cofactor required for LS folding	Schroda et al., 2004
EPYC1	Cre10.g436550	Pyrenoid formation	Mackinder et al., 2016
SAGA1	Cre11.g467712	Rubisco-interacting protein, pyrenoid organization	Itakura et al., 2019
RCA1	Cre04.g229300	Rubisco activase	Roesler and Ogren, 1990, Pollock et al., 2003
RCA2	Cre17.g718950	Rubisco activase-like protein	

Table 2: Lists of available Chlamydomonas Rubisco structures

Description	PDB ID:	L	S	Ref
CrRubisco with CAPB	1GK8, 1IR2	Cr-WT	Cr-WT	Taylor et al., 2001 ; Mizohata et al., 2002
Apo-Cr Rubisco	7JN4	Cr-WT	Cr-WT	He et al., 2020
C192S	2VDH, 2VDI	C192S	WT	Murria et al., 2008
L290F	1UWA	L290F	WT	Karkehabadi et al., 2005
L290F-A222T	1UW9	L290F-A222T	WT	Karkehabadi et al., 2005
V331A	2V63	V331A	WT	Karkehabadi et al., 2007
V331A-T342I	2V68	V331A-T342I	WT	Karkehabadi et al., 2007
T342I	2V67	T342I	WT	Karkehabadi et al., 2007
V331A-G344S	2V6A	V331A-G344S	WT	Karkehabadi et al., 2007
D473E	2V69	D473E	WT	Karkehabadi et al., 2007
Hybrid Cr-Syn Rubisco	1UZH	Cr-WT	Syn	Karkehabadi et al., 2005
Hybrid Cr-Sp Rubisco	1UZD	Cr-WT	spinach	Karkehabadi et al., 2005

Table 3 Large subunit mutants										
aa	**Mutation**	**Location**	**PS[a]**	**Holoenz acc.[b]**	**Thermal stability[c]**	**Ω[d,e]**	**V_c[e,f]**	**K_c[e,g]**	**K_o[e,h]**	**References**
WT*			+	100%	90% at 55°C	63	107	31	372	
					41% at 60°C					
					0% at 65°C					
M42	M42V	Nter	+			62	nd	nd	nd	(Du et al., 2003)
C53	C53A	Nter	+			62	nd	nd	nd	(Du et al., 2003)
	M42V-C53A	Nter	+			60	nd	nd	nd	(Du et al., 2003)
G54	G54D	Nter	-	0%						(Thow & Spreitzer, 1992)
G54	G54A	Nter	+	50%		60	100	32	360	(Spreitzer et al., 1995)
G54	G54V	Nter	+	25%		52	19	31	633	(Spreitzer et al., 1995)
N123	N123G	Nter-Cter interaction	-	100%		12	3	105	103	(Zhu and Spreitzer, 1994)
G171	G171D	β	-	100%						(Spreitzer & Mets, 1980)
C172	C172S*	β1	+	reduced	<WT	70	98	61	816	(Moreno and Spreitzer, 1999; Garcia-Murria et al., 2008)
T173	T173I	β1	-	100%						(Spreitzer et al., 1988)
C192	C192S*	α6	+			63	75	23	330	(Garcia-Murria et al., 2008)
R217	R217S	α2	-	5% est.						(Thow & Spreitzer, 1992)
R217	R217S-A242V	β3	+	25%		31	10	235	3778	(Thow et al., 1994)
V221	V221C-V235I	α2	+	100%		62	122	28	275	(Spreitzer et al., 2005)
Y226	Y226L	α2	+	80%						(Esquivel et al., 2006)
			+- at 35°C							
V235	V235I		+	100%		58	118	41	348	(Spreitzer et al., 2005)
L326	L326I	β6	+-	15%	25%	57	86	35	367	(Zhu & Spreitzer, 1996)
V331	V331A*	Loop 6	-	Near normal		40	7	166	2937	(Chen and Spreitzer, 1989) (Karkehabadi et al., 2007)
V331	V331A-T342I*	Loop 6	+			53	35	47	829	(Chen and Spreitzer, 1989) (Karkehabadi et al., 2007)
T342	T342I*	α6								(Karkehabadi et al., 2007)
V331	V331A-G344S*		+			46	27	73	1290	(Chen et al., 1991)
	L326I-M349L	Loop 6	+-	50%	55%	50	28	43	524	(Zhu & Spreitzer, 1996)
V341	V346I	α6	+	100%		61	103	36	390	(Zhu & Spreitzer, 1996)
M349	M349L	α6	+	75%	90%	59	97	33	379	(Zhu & Spreitzer, 1996)
S379	S379A	β7-Loop 6 interaction	-	100%		18	4	236	1673	(Zhu and Spreitzer, 1994)
C256	C256F	α3	+	100%	No effect	61	68	37	440	(Du et al., 2003)

K258	K258R	α3	+	100%	No effect	60	80	30	377	(Du et al., 2003)
I265	I265V	β4	+	100%	No effect	63	91	32	470	(Du et al., 2003)
	K258R-I265V		+-	25% est.	No effect					(Du et al., 2003)
	C256F-K258R-I265V		+-	25% est.	No effect	59	32	70	946	(Du et al., 2003)
						57	48	67	777	(Spreitzer et al., 2005)
	V221C-V235I-C256F-K258R-I265V		+,+- at 35°C	25% est.		64	48	67	1089	(Spreitzer et al., 2005)
L290	L290F*	B5	+	70%,	0% at 60°C	52	40	49	733	(Chen et al., 1988; Hong and Spreitzer, 1997)
			- at 35°C	10–17% at 35°C						(Du and Spreitzer, 2000)
						54	36	42	521	(Genkov et al., 2006)
						56	31	39	622	
L290	L290F-A222T*		+	42%,	0% at 60°C	61	77	40	651	(Hong and Spreitzer, 1997)
			+ at 35°C	27% at 35°C						
L290	L290F-V262L		+	50%,	61% at 60°C	62	72	68	1238	(Hong and Spreitzer, 1997)
			+ at 35°C	30% at 35°C						
A222	A222T	α2	+	100%	58% at 65°C	63	89	26	264	(Du and Spreitzer, 2000)
V262	V262L	Below β4	+	100%	93% at 65°C	62	78	45	484	(Du and Spreitzer, 2000)
C449	C449S	Cter	+							(Marin-Navarro and Moreno, 2006)
C459	C459S	Cter	+							(Marin-Navarro and Moreno, 2006)
	C449S-C459S		+							(Marin-Navarro and Moreno, 2006)
D470	D470P-T471A-I472M-K474T	Cter	+	100%	No effect	69	90	36	545	(Satagopan and Spreitzer, 2008)
D473	D473A*	Cter	+	100%	No effect	52	36	77	1931	(Satagopan and Spreitzer, 2004)
	D473E*	Cter	+	100%	No effect	54	34	87	1900	(Satagopan and Spreitzer, 2004), (Karkehabadi et al., 2007)

[a]Photosynthetic growth on minimal medium at 25°C, unless otherwise indicated.

[b]Percent of holoenzyme accumulation compared to WT as measured, or estimated from published immunoblots (est.).

[c]Thermal instability was measured by the amount of activity retained by the purified enzyme after 20 minutes exposure at different temperatures. Unless otherwise indicated, the values reported correspond to activity at 55°C.

[d] $\Omega = V_c K_0 / V_0 K_c$.

[e]Values indicated are tentatively normalized to the wild-type values reported. For actual values refer to the appropriate publication.

[f] V_c*, in µmol/h/mg*

[g] K_c*, in µM* CO_2.

[h] K_0*, in µM* O_2

**Mutants for which structures are available.*

Table 4: Small subunit mutants										
aa	**Mutation**	**Location**	**PS[a]**	**Holoenzyme acc.[b]**	**Thermal stability[c]**	**Ω[d,e]**	**V_c[e,f]**	**K_c[e,g]**	**K_o[e,h]**	**References**
C65	C65S-L290F	βA/βB	+	100%,.WT at 35°C	Less than L290F (20%) at 55°C,0% at 60°C	60	37	34	465	(Genkov et al., 2006)
	C65S	βA/βB	+	100%,.WT at 35°C	88% at 60°C	66	141	30	326	(Genkov et al., 2006)
	C65A	βA/βB	+		No effect	65	116	33	410	(Genkov et al., 2006)
	C65P	βA/βB	+		93% at 60°C	57	50	36	348	(Genkov et al., 2006)
Y67	Y67A	βA/βB	+,+- at 35° C	10%	WT		5% at 30° C			(Esquivel et al., 2006)
Y68	Y68A	βA/βB	+,+- at 35° C	100%	WT	62	31, 60% at 30° C	22	347	(Spreitzer et al., 2001)(Esquivel et al., 2006)
Y72	Y72A	βA/βB	+,-+- at 35° C	10%	WT		5% at 30° C			(Esquivel et al., 2006)
R71	R71A	βA/βB	- at 35° C	50% est.,5% at 35°C	,WT, 0% at 55°C	58	17	40	623	(Spreitzer et al., 2001)
D69	D69A	βA/βB	+		WT	62	46	20	318	(Spreitzer et al., 2001)
R59	R59E	βA/βB	- at 35° C	20% est.,0% at 35°C						(Spreitzer et al., 2001)
N54	N54S-L290F	βA/βB	+ at 35° C	66%,46% at 35°C	Comparable to L290F	63	67	32	489	(Du et al., 2000)
	N54S-RbcS1Δ	βA/βB	+		.WT, 35% at 65°C	64	77	25	331	(Du et al., 2000)
A57	A57V-L290F	βA/βB	+ at 35° C	57%,42% at 35°C		61	71	31	461	(Du et al., 2000)
	A57V-RbcS1Δ	βA/βB	+		.WT, 88% at 65°C	62	65	25	334	(Du et al., 2000)
spinach	ABSO*	βA/βB		60% est.	85% at 60°C	64	55	21	330	(Spreitzer et al., 2005)
						62	53	23	320	(Karkehabadi et al., 2005a)
	ABSO-V221C-V235I-C256F-K258R-I265V	βA/βB	+- at 35° C	40% est.		70	59	23	328	(Spreitzer et al., 2005)
Synechococcus	ABAN*	βA/βB	+- at 35° C	40% est.	0% at 60°C	56	58	32	260	(Karkehabadi et al., 2005a)
spinach	SSSO		+- in air,+ with CO_2	WT		65	97	34	539	Genkov et al., 2010
Arabidopsis	SSAT		+- in air,+ with CO_2	WT		68	105	30	547	Genkov et al., 2010

sunflower	SSHA		+- in air,+ with CO_2	WT		63	114	31	557	Genkov et al., 2010
Tobacco	SSNT		+- in air,+ with CO_2	WT		66	86	25	439	Wachter et al., 2013
S16	S16A	N-ter	+	Reduced at 35°C		59				Genkov et al., 2009
L18	L18A	N-ter	- at 35° C	0% at 35°C						Genkov et al., 2009
P19	P19A	N-ter	+	Reduced at 35°C		59				Genkov et al., 2009
Y32	Y32A	α helix A	+- at 35° C	0% at 35°C		54	23	30	383	Genkov et al., 2009
E43	E43A	βA strand	- at 35° C	0% at 35°C		55	10	64	162 4	Genkov et al., 2009
W73	W73A	βB strand	- at 35° C	Reduced at 35°C		58	28	46	115 9	Genkov et al., 2009
L78	L78A	βB-αB loop	- at 35° C			61	16	53	974	Genkov et al., 2009
P79	P79A	βB-αB loop	+			58	47	33	529	Genkov et al., 2009
F81	F81A	βB-αB loop	+- at 35° C			61	47	43	100 8	Genkov et al., 2009
E92	E92A	α helix B	+					0		Genkov et al., 2009
I58	I58W3	βA/βB	+- at 35° C	Reduced at 35°C		52	29	46	118 0	Esquivel et al., 2013

[a]Photosynthetic growth on minimal medium at 25°C, unless otherwise indicated.

[b]Percent of holoenzyme accumulation compared to WT as measured, or estimated from published immunoblots (est.).

[c]Thermal instability was measured by the amount of activity retained by the purified enzyme after -0 minutes exposure at different temperatures. Unless otherwise indicated, the values reported correspond to activity at 55°C.

[d]$\Omega = V_cK_0/V_0K_c$.

[e]Values indicated are tentatively normalized to the wild-type values reported. In case of the Y67, Y68, and Y7- mutants, the actual data do not figure in the publication, therefore the published percentages of V_c measured at 30°C compared to WT reported were indicated. For other cases, refer to the appropriate publication for actual values.

[f]V_c, in µmol/h/mg.

[g]K_c, in µM CO.

[h]K_0, in µM O.

**Mutants for which structures are available.*

REFERENCES

Abat, J.K., and Deswal, R. (2009). Differential modulation of S-nitrosoproteome of Brassica juncea by low temperature: change in S-nitrosylation of Rubisco is responsible for the inactivation of its carboxylase activity. Proteomics **9,** 4368-4380.

Aigner, H., Wilson, R.H., Bracher, A., Calisse, L., Bhat, J.Y., Hartl, F.U., and Hayer-Hartl, M. (2017). Plant RuBisCo assembly in *E. coli* with five chloroplast chaperones including BSD2. Science **358,** 1272-1278.

Amiya, R., and Shapira, M. (2021). ZnJ6 Is a Thylakoid Membrane DnaJ-Like Chaperone with Oxidizing Activity in Chlamydomonas reinhardtii. International journal of molecular sciences **22**.

Andersson, I. (2008). Catalysis and regulation in Rubisco. J Exp Bot **59,** 1555-1568.

Andersson, I., and Backlund, A. (2008). Structure and function of Rubisco. Plant Physiology and Biochemistry **46,** 275-291.

Anthonisen, I.L., Salvador, M.L., and Klein, U. (2001). Specific sequence elements in the 5' untranslated regions of rbcL and atpB gene mRNas stabilize transcripts in the chloroplast of Chlamydomonas reinhardtii. Rna **7,** 1024-1033.

Antonovsky, N., Gleizer, S., Noor, E., Zohar, Y., Herz, E., Barenholz, U., Zelcbuch, L., Amram, S., Wides, A., Tepper, N., Davidi, D., Bar-On, Y., Bareia, T., Wernick, D.G., Shani, I., Malitsky, S., Jona, G., Bar-Even, A., and Milo, R. (2016). Sugar Synthesis from CO_2 in Escherichia coli. Cell **166,** 115-125.

Atkinson, N., Mao, Y., Chan, K.X., and McCormick, A.J. (2020). Condensation of Rubisco into a proto-pyrenoid in higher plant chloroplasts. Nat. Commun. **11,** 6303.

Atkinson, N., Feike, D., Mackinder, L.C.M., Meyer, M.T., Griffiths, H., Jonikas, M.C., Smith, A.M., and McCormick, A.J. (2016). Introducing an algal carbon-concentrating mechanism into higher plants: location and incorporation of key components. Plant Biotechnol. J. **14,** 1302-1315.

Atkinson, N., Leitao, N., Orr, D.J., Meyer, M.T., Carmo-Silva, E., Griffiths, H., Smith, A.M., and McCormick, A.J. (2017). Rubisco small subunits from the unicellular green alga Chlamydomonas complement Rubisco-deficient mutants of Arabidopsis. The New Phytologist **214,** 655-667.

Atkovska, K., and Hub, J.S. (2017). Energetics and mechanism of anion permeation across formate-nitrite transporters. Scientific Reports **7,** 12027.

Badger, M. (1994). The Role of Carbonic Anhydrase in Photosynthesis. Annu. Rev. Plant Physiol. Plant Mol. Biol. **45,** 369-392.

Badger, M.R., Kaplan, A., and Berry, J.A. (1980). Internal inorganic carbon pool of Chlamydomonas reinhardtii Evidence for a carbon dioxide-concentrating mechanism. Plant Physiol. **66,** 407-413.

Badger, M.R., Andrews, T.J., Whitney, S.M., Ludwig, M., Yellowlees, D.C., Leggat, W., and Price, G.D. (1998). The diversity and coevolution of Rubisco, plastids, pyrenoids, and chloroplast-based CO2-concentrating mechanisms in algae. Can. J. Bot. **76,** 1052-1071.

Banda, D.M., Pereira, J.H., Liu, A.K., Orr, D.J., Hammel, M., He, C., Parry, M.A.J., Carmo-Silva, E., Adams, P.D., Banfield, J.F., and Shih, P.M. (2020). Novel bacterial clade reveals origin of form I Rubisco. Nature plants **6,** 1158-1166.

Bar-On, Y.M., and Milo, R. (2019). The global mass and average rate of rubisco. Proc. Natl. Acad. Sci. U. S. A.

Barrett, J., Girr, P., and Mackinder, L.C.M. (2021). Pyrenoids: CO2-fixing phase separated liquid organelles. Biochimica et biophysica acta. Molecular cell research **1868,** 118949.

Benlloch, R., Shevela, D., Hainzl, T., Grundström, C., Shutova, T., Messinger, J., Samuelsson, G., and Elisabeth Sauer-Eriksson, A. (2015). Crystal Structure and Functional Characterization of Photosystem II-Associated Carbonic Anhydrase CAH3 in Chlamydomonas reinhardtii. Plant Physiol. **167,** 950-962.

Berger, H., Blifernez-Klassen, O., Ballottari, M., Bassi, R., Wobbe, L., and Kruse, O. (2014). Integration of carbon assimilation modes with photosynthetic light capture in the green alga Chlamydomonas reinhardtii. Mol. Plant **7,** 1545-1559.

Bhat, J.Y., Thieulin-Pardo, G., Hartl, F.U., and Hayer-Hartl, M. (2017). Rubisco Activases: AAA+ Chaperones Adapted to Enzyme Repair. Front Mol Biosci **4,** 20.

Bienvenut, W.V., Espagne, C., Martinez, A., Majeran, W., Valot, B., Zivy, M., Vallon, O., Adam, Z., Meinnel, T., and Giglione, C. (2011). Dynamics of post-translational modifications and protein stability in the stroma of Chlamydomonas reinhardtii chloroplasts. Proteomics **11,** 1734-1750.

Bienvenut, W.V., Brunje, A., Boyer, J.B., Muhlenbeck, J.S., Bernal, G., Lassowskat, I., Dian, C., Linster, E., Dinh, T.V., Koskela, M.M., Jung, V., Seidel, J., Schyrba, L.K., Ivanauskaite, A., Eirich, J., Hell, R., Schwarzer, D., Mulo, P., Wirtz, M., Meinnel, T., Giglione, C., and Finkemeier, I. (2020). Dual lysine and N-terminal acetyltransferases reveal the complexity underpinning protein acetylation. Molecular systems biology **16,** e9464.

Blanco-Rivero, A., Shutova, T., Román, M.J., Villarejo, A., and Martinez, F. (2012a). Phosphorylation controls the localization and activation of the lumenal carbonic anhydrase in Chlamydomonas reinhardtii. PloS one **7,** e49063.

Blanco-Rivero, A., Shutova, T., Roman, M.J., Villarejo, A., and Martinez, F. (2012b). Phosphorylation controls the localization and activation of the lumenal carbonic anhydrase in Chlamydomonas reinhardtii. PloS one **7,** e49063.

Blifernez-Klassen, O., Berger, H., Mittmann, B.G.K., Klassen, V., Schelletter, L., Buchholz, T., Baier, T., Soleimani, M., Wobbe, L., and Kruse, O. (2021). A gene regulatory network for antenna size control in carbon dioxide-deprived Chlamydomonas reinhardtii cells. The Plant cell.

Blowers, A.D., Ellmore, G.S., Klein, U., and Bogorad, L. (1990). Transcriptional analysis of endogenous and foreign genes in chloroplast transformants of Chlamydomonas. The Plant cell **2,** 1059-1070.

Borkhsenious, O.N., Mason, C.B., and Moroney, J.V. (1998). The intracellular localization of ribulose-1, 5-bisphosphate carboxylase/oxygenase in Chlamydomonas reinhardtii. Plant Physiol. **116,** 1585-1591.

Bouchnak, I., and van Wijk, K.J. (2019). N-Degron Pathways in Plastids. Trends in plant science **24,** 917-926.

Boulouis, A., Drapier, D., Razafimanantsoa, H., Wostrikoff, K., Tourasse, N.J., Pascal, K., Girard-Bascou, J., Vallon, O., Wollman, F.A., and Choquet, Y. (2015). Spontaneous dominant mutations in chlamydomonas highlight ongoing evolution by gene diversification. The Plant cell **27,** 984-1001.

Bracher, A., Starling-Windhof, A., Hartl, F.U., and Hayer-Hartl, M. (2011). Crystal structure of a chaperone-bound assembly intermediate of form I Rubisco. Nature Structural & Molecular Biology **18,** 875-880.

Bracher, A., Whitney, S.M., Hartl, F.U., and Hayer-Hartl, M. (2017). Biogenesis and Metabolic Maintenance of Rubisco. Annual review of plant biology **68,** 29-60.

Bracher, A., Hauser, T., Liu, C., Hartl, F.U., and Hayer-Hartl, M. (2015). Structural Analysis of the Rubisco-Assembly Chaperone RbcX-II from Chlamydomonas reinhardtii. PloS one **10,** 1-17.

Brueggeman, A.J., Gangadharaiah, D.S., Cserhati, M.F., Casero, D., Weeks, D.P., and Ladunga, I. (2012). Activation of the carbon concentrating mechanism by CO2 deprivation coincides with massive transcriptional restructuring in Chlamydomonas reinhardtii. The Plant cell **24,** 1860-1875.

Brutnell, T.P., Sawers, R.J., Mant, A., and Langdale, J.A. (1999). BUNDLE SHEATH DEFECTIVE2, a novel protein required for post-translational regulation of the rbcL gene of maize. The Plant cell **11,** 849-864.

Burlacot, A., Dao, O., Auroy, P., Cuine, S., Li-Beisson, Y., and Peltier, G. (2021). Alternative electron pathways of photosynthesis drive the algal CO2 concentrating mechanism. Cold Spring Harbor Laboratory.

Cavaiuolo, M., Kuras, R., Wollman, F.A., Choquet, Y., and Vallon, O. (2017). Small RNA profiling in Chlamydomonas: insights into chloroplast RNA metabolism. Nucleic acids research **45,** 10783-10799.

Chen, B., Lee, K., Plucinak, T., Duanmu, D., Wang, Y., Horken, K.M., Weeks, D.P., and Spalding, M.H. (2017). A novel activation domain is essential for CIA5-mediated gene regulation in response to CO2 changes in Chlamydomonas reinhardtii. Algal Research **24,** 207-217.

Chen, Z.-Y., Lavigne, L., Mason, C.B., and Moroney, J.V. Cloning and Overexpression of Two cDNAs Encoding the Low-C0, -Inducible Chloroplast Envelope Protein LIP-36 from Chlamydomonas reinhardtii '.

Chen, Z.X., and Spreitzer, R.J. (1989). Chloroplast intragenic suppression enhances the low CO2/O2 specificity of mutant ribulose-bisphosphate carboxylase/oxygenase. The Journal of biological chemistry **264,** 3051-3053.

Chen, Z.X., Chastain, C.J., Al-Abed, S.R., Chollet, R., and Spreitzer, R.J. (1988). Reduced CO_2/O_2 specificity of ribulose-bisphosphate carboxylase/oxygenase in a temperature-sensitive chloroplast mutant of Chlamydomonas. Proceedings of the National Academy of Sciences of the United States of America **85,** 4696-4699.

Chen, Z.X., Yu, W.Z., Lee, J.H., Diao, R., and Spreitzer, R.J. (1991). Complementing amino acid substitutions within loop 6 of the alpha/beta-barrel active site influence the CO_2/O_2 specificity of chloroplast ribulose-1,5-bisphosphate carboxylase/oxygenase. Biochemistry **30,** 8846-8850.

Choi, H.I., Kim, J.Y.H., Kwak, H.S., Sung, Y.J., and Sim, S.J. (2016). Quantitative analysis of the chemotaxis of a green alga, Chlamydomonas reinhardtii, to bicarbonate using diffusion-based microfluidic device. Biomicrofluidics **10,** 014121.

Cohen, I., Sapir, Y., and Shapira, M. (2006). A conserved mechanism controls translation of Rubisco large subunit in different photosynthetic organisms. Plant Physiol **141,** 1089-1097.

Cohen, I., Knopf, J.A., Irihimovitch, V., and Shapira, M. (2005). A Proposed Mechanism for the Inhibitory Effects of Oxidative Stress on Rubisco Assembly and Its Subunit Expression. Plant Physiology **137,** 738-746.

Conlan, B., Birch, R., Kelso, C., Holland, S., De Souza, A.P., Long, S.P., Beck, J.L., and Whitney, S.M. (2019). BSD2 is a Rubisco-specific assembly chaperone, forms intermediary hetero-oligomeric complexes, and is nonlimiting to growth in tobacco. Plant, cell & environment **42,** 1287-1301.

Crozet, P., Navarro, F.J., Willmund, F., Mehrshahi, P., Bakowski, K., Lauersen, K.J., Perez-Perez, M.E., Auroy, P., Gorchs Rovira, A., Sauret-Gueto, S., Niemeyer, J., Spaniol, B., Theis, J., Trosch, R., Westrich, L.D., Vavitsas, K., Baier, T., Hubner, W., de Carpentier, F., Cassarini, M., Danon, A., Henri, J., Marchand, C.H., de Mia, M., Sarkissian, K., Baulcombe, D.C., Peltier, G., Crespo, J.L., Kruse, O., Jensen, P.E., Schroda, M., Smith,

A.G., and Lemaire, S.D. (2018). Birth of a Photosynthetic Chassis: A MoClo Toolkit Enabling Synthetic Biology in the Microalga Chlamydomonas reinhardtii. ACS synthetic biology **7,** 2074-2086.

Cummins, E.P., Selfridge, A.C., Sporn, P.H., Sznajder, J.I., and Taylor, C.T. (2014). Carbon dioxide-sensing in organisms and its implications for human disease. Cell. Mol. Life Sci. **71,** 831-845.

Cummins, P.L., Kannappan, B., and Gready, J.E. (2018). Revised mechanism of carboxylation of ribulose-1,5-biphosphate by rubisco from large scale quantum chemical calculations. Journal of computational chemistry **39,** 1656-1665.

Cummins, P.L., Kannappan, B., and Gready, J.E. (2019). Ab Initio Molecular Dynamics Simulation and Energetics of the Ribulose-1,5-biphosphate Carboxylation Reaction Catalyzed by Rubisco: Toward Elucidating the Stereospecific Protonation Mechanism. The journal of physical chemistry. B **123,** 2679-2686.

Da Silva, T.C., Polli, J.E., and Swaan, P.W. (2013). The solute carrier family 10 (SLC10): beyond bile acid transport. Molecular aspects of medicine **34,** 252-269.

Davidi, D., Shamshoum, M., Guo, Z., Bar-On, Y.M., Prywes, N., Oz, A., Jablonska, J., Flamholz, A., Wernick, D.G., Antonovsky, N., de Pins, B., Shachar, L., Hochhauser, D., Peleg, Y., Albeck, S., Sharon, I., Mueller-Cajar, O., and Milo, R. (2020). Highly active rubiscos discovered by systematic interrogation of natural sequence diversity. The EMBO journal **39,** e104081.

De Mia, M., Lemaire, S.D., Choquet, Y., and Wollman, F.A. (2019). Nitric Oxide Remodels the Photosynthetic Apparatus upon S-Starvation in *Chlamydomonas reinhardtii*. Plant Physiol **179,** 718-731.

Dent, R.M., Haglund, C.M., Chin, B.L., Kobayashi, M.C., and Niyogi, K.K. (2005). Functional genomics of eukaryotic photosynthesis using insertional mutagenesis of *Chlamydomonas reinhardtii*. Plant Physiology **137,** 545-556.

Desimone, M., Henke, A., and Wagner, E. (1996). Oxidative Stress Induces Partial Degradation of the Large Subunit of Ribulose-1,5-Bisphosphate Carboxylase/Oxygenase in Isolated Chloroplasts of Barley. Plant Physiol **111,** 789-796.

Doron, L., Goloubinoff, P., and Shapira, M. (2018). ZnJ2 Is a Member of a Large Chaperone Family in the Chloroplast of Photosynthetic Organisms that Features a DnaJ-Like Zn-Finger Domain. Frontiers in molecular biosciences **5,** 2.

Doron, L., Segal, N., Gibori, H., and Shapira, M. (2014). The BSD2 ortholog in *Chlamydomonas reinhardtii* is a polysome-associated chaperone that co-migrates on sucrose gradients with the rbcL transcript encoding the Rubisco large subunit. The Plant Journal **80,** 345-355.

Dron, M., Rahire, M., and Rochaix, J.D. (1982). Sequence of the chloroplast DNA region of Chlamydomonas reinhardii containing the gene of the large subunit of ribulose bisphosphate carboxylase and parts of its flanking genes. J Mol Biol **162,** 775-793.

Du, Y.C., Hong, S., and Spreitzer, R.J. (2000). RbcS suppressor mutations improve the thermal stability and CO_2/O_2 specificity of rbcL- mutant ribulose-1,5-bisphosphate carboxylase/oxygenase. Proceedings of the National Academy of Sciences of the United States of America **97,** 14206-14211.

Du, Y.C., Peddi, S.R., and Spreitzer, R.J. (2003). Assessment of structural and functional divergence far from the large subunit active site of ribulose-1,5-bisphosphate carboxylase/oxygenase. The Journal of biological chemistry **278,** 49401-49405.

Duanmu, D., and Spalding, M.H. (2011). Insertional suppressors of Chlamydomonas reinhardtii that restore growth of air-dier lcib mutants in low CO2. Photosynthesis research **109,** 123-132.

Duanmu, D., Wang, Y., and Spalding, M.H. (2009a). Thylakoid Lumen Carbonic Anhydrase (CAH3) Mutation Suppresses Air-Dier Phenotype of LCIB Mutant in Chlamydomonas reinhardtii. Plant Physiol. **149,** 929-937.

Duanmu, D., Miller, A.R., Horken, K.M., Weeks, D.P., and Spalding, M.H. (2009b). Knockdown of limiting-CO2–induced gene HLA3 decreases HCO3− transport and photosynthetic Ci affinity in Chlamydomonas reinhardtii. Proc. Natl. Acad. Sci. U. S. A. **106,** 5990-5995.

Duff, A.P., Andrews, T.J., and Curmi, P.M. (2000). The transition between the open and closed states of rubisco is triggered by the inter-phosphate distance of the bound bisphosphate. J Mol Biol **298,** 903-916.

Düner, M., Lambertz, J., Mügge, C., and Hemschemeier, A. (2018). The soluble guanylate cyclase CYG12 is required for the acclimation to hypoxia and trophic regimes in Chlamydomonas reinhardtii. The Plant Journal **93,** 311-337.

Durao, P., Aigner, H., Nagy, P., Mueller-Cajar, O., Hartl, F.U., and Hayer-Hartl, M. (2015). Opposing effects of folding and assembly chaperones on evolvability of Rubisco. Nature chemical biology **11,** 148-155.

Eberhard, S., Drapier, D., and Wollman, F.A. (2002). Searching limiting steps in the expression of chloroplast-encoded proteins: relations between gene copy number, transcription, transcript abundance and translation rate in the chloroplast of Chlamydomonas reinhardtii. The Plant journal : for cell and molecular biology **31,** 149-160.

Emlyn-Jones, D., Woodger, F.J., Price, G.D., and Whitney, S.M. (2006). RbcX can function as a rubisco chaperonin, but is non-essential in Synechococcus PCC7942. Plant & Cell Physiology **47,** 1630-1640.

Emrich-Mills, T.Z., Yates, G., Barrett, J., Girr, P., Grouneva, I., Lau, C.S., Walker, C.E., Kwok, T.K., Davey, J.W., Johnson, M.P., and Mackinder, L.C.M. (2021). A recombineering pipeline to clone large and complex genes in Chlamydomonas. The Plant cell.

Engel, B.D., Schaffer, M., Kuhn Cuellar, L., Villa, E., Plitzko, J.M., and Baumeister, W. (2015). Native architecture of the Chlamydomonas chloroplast revealed by in situ cryo-electron tomography. Elife **4**.

Engel, B.D., Ishikawa, H., Wemmer, K.A., Geimer, S., Wakabayashi, K.-I., Hirono, M., Craige, B., Pazour, G.J., Witman, G.B., and Kamiya, R. (2012). The role of retrograde intraflagellar transport in flagellar assembly, maintenance, and function. J. Cell Biol. **199,** 151-167.

Esquivel, M.G., Pinto, T.S., Marin-Navarro, J., and Moreno, J. (2006). Substitution of tyrosine residues at the aromatic cluster around the betaA-betaB loop of rubisco small subunit affects the structural stability of the enzyme and the in vivo degradation under stress conditions. Biochemistry **45,** 5745-5753.

Esquivel, M.G., Genkov, T., Nogueira, A.S., Salvucci, M.E., and Spreitzer, R.J. (2013). Substitutions at the opening of the Rubisco central solvent channel affect holoenzyme stability and CO_2/O_2 specificity but not activation by Rubisco activase. Photosynth Res **118,** 209-218.

Fang, W., Si, Y., Douglass, S., Casero, D., Merchant, S.S., Pellegrini, M., Ladunga, I., Liu, P., and Spalding, M.H. (2012). Transcriptome-wide changes in Chlamydomonas reinhardtii gene expression regulated by carbon dioxide and the CO2-concentrating mechanism regulator CIA5/CCM1. The Plant cell **24,** 1876-1893.

Fei, C., Wilson, A.T., Mangan, N.M., Wingreen, N.S., and Jonikas, M.C. (2021). Diffusion barriers and adaptive carbon uptake strategies enhance the

modeled performance of the algal CO2-concentrating mechanism. Cold Spring Harbor Laboratory.

Feiz, L., Williams-Carrier, R., Wostrikoff, K., Belcher, S., Barkan, A., and Stern, D.B. (2012). Ribulose-1,5-bis-phosphate carboxylase/oxygenase accumulation factor 1 is required for holoenzyme assembly in maize. The Plant cell **24,** 3435-3446.

Feiz, L., Williams-Carrier, R., Belcher, S., Montano, M., Barkan, A., and Stern, D.B. (2014). A protein with an inactive pterin-4a-carbinolamine dehydratase domain is required for Rubisco biogenesis in plants. The Plant Journal **80,** 862-869.

Feller, U., Anders, I., and Mae, T. (2008). Rubiscolytics: fate of Rubisco after its enzymatic function in a cell is terminated. J Exp Bot **59,** 1615-1624.

Flamholz, A.I., Prywes, N., Moran, U., Davidi, D., Bar-On, Y.M., Oltrogge, L.M., Alves, R., Savage, D., and Milo, R. (2019). Revisiting Trade-offs between Rubisco Kinetic Parameters. Biochemistry **58,** 3365-3376.

Flecken, M., Wang, H., Popilka, L., Hartl, F.U., Bracher, A., and Hayer-Hartl, M. (2020). Dual Functions of a Rubisco Activase in Metabolic Repair and Recruitment to Carboxysomes. Cell **183,** 457-473 e420.

Freeman Rosenzweig, E.S., Xu, B., Kuhn Cuellar, L., Martinez-Sanchez, A., Schaffer, M., Strauss, M., Cartwright, H.N., Ronceray, P., Plitzko, J.M., Förster, F., Wingreen, N.S., Engel, B.D., Mackinder, L.C.M., and Jonikas, M.C. (2017). The Eukaryotic CO2-Concentrating Organelle Is Liquid-like and Exhibits Dynamic Reorganization. Cell **171,** 148-162.e119.

Fristedt, R., Hu, C., Wheatley, N., Roy, L.M., Wachter, R.M., Savage, L., Harbinson, J., Kramer, D.M., Merchant, S.S., Yeates, T., and Croce, R. (2018). RAF2 is a RuBisCO assembly factor in Arabidopsis thaliana. The Plant Journal **94,** 146-156.

Fuhrmann, M., Stahlberg, A., Govorunova, E., Rank, S., and Hegemann, P. (2001). The abundant retinal protein of the Chlamydomonas eye is not the photoreceptor for phototaxis and photophobic responses. Journal of cell science **114,** 3857-3863.

Fujiwara, S., Fukuzawa, H., Tachiki, A., and Miyachi, S. (1990). Structure and differential expression of two genes encoding carbonic anhydrase in Chlamydomonas reinhardtii. Proc. Natl. Acad. Sci. U. S. A. **87,** 9779-9783.

Fukuzawa, H., Miura, K., Ishizaki, K., Kucho, K.I., Saito, T., Kohinata, T., and Ohyama, K. (2001). Ccm1, a regulatory gene controlling the induction of a carbon-concentrating mechanism in Chlamydomonas reinhardtii by sensing CO2 availability. Proc. Natl. Acad. Sci. U. S. A. **98,** 5347-5352.

Funke, R.P., Kovar, J.L., and Weeks, D.P. (1997). Intracellular carbonic anhydrase is essential to photosynthesis in Chlamydomonas reinhardtii at atmospheric levels of CO2. Demonstration via genomic complementation of the high-CO2-requiring mutant ca-1. Plant Physiol. **114,** 237-244.

Gao, H., Wang, Y., Fei, X., Wright, D.A., and Spalding, M.H. (2015). Expression activation and functional analysis of HLA3, a putative inorganic carbon transporter in Chlamydomonas reinhardtii. The Plant Journal **82,** 1-11.

Garcia-Murria, M.J., Sudhani, H.P.K., Marin-Navarro, J., Sanchez Del Pino, M.M., and Moreno, J. (2018). Dissecting the individual contribution of conserved cysteines to the redox regulation of RubisCO. Photosynth Res **137,** 251-262.

Garcia-Murria, M.J., Karkehabadi, S., Marin-Navarro, J., Satagopan, S., Andersson, I., Spreitzer, R.J., and Moreno, J. (2008). Structural and functional consequences of the replacement of proximal residues Cys(172) and Cys(192) in the large subunit of ribulose-1,5-bisphosphate carboxylase/oxygenase from *Chlamydomonas reinhardtii*. The Biochemical journal **411,** 241-247.

Genkov, T., and Spreitzer, R.J. (2009). Highly conserved small subunit residues influence rubisco large subunit catalysis. The Journal of biological chemistry **284,** 30105-30112.

Genkov, T., Du, Y.C., and Spreitzer, R.J. (2006). Small-subunit cysteine-65 substitutions can suppress or induce alterations in the large-subunit catalytic efficiency and holoenzyme thermal stability of ribulose-1,5-bisphosphate carboxylase/oxygenase. Archives of biochemistry and biophysics **451,** 167-174.

Genkov, T., Meyer, M., Griffiths, H., and Spreitzer, R.J. (2010). Functional hybrid rubisco enzymes with plant small subunits and algal large subunits: engineered rbcS cDNA for expression in chlamydomonas. The Journal of biological chemistry **285,** 19833-19841.

Geraghty, A.M., and Spalding, M.H. (1996). Molecular and Structural Changes in Chlamydomonas under Limiting CO2 (A Possible Mitochondrial Role in Adaptation). Plant Physiology **111,** 1339.

Giglione, C., and Meinnel, T. (2021). Evolution-Driven Versatility of N Terminal Acetylation in Photoautotrophs. Trends in plant science **26,** 375-391.

Giglione, C., Vallon, O., and Meinnel, T. (2003). Control of protein life-span by N-terminal methionine excision. The EMBO journal **22,** 13-23.

Giordano, M., Beardall, J., and Raven, J.A. (2005). CO2 concentrating mechanisms in algae: mechanisms, environmental modulation, and evolution. Annu. Rev. Plant Biol. **56,** 99-131.

Gleizer, S., Ben-Nissan, R., Bar-On, Y.M., Antonovsky, N., Noor, E., Zohar, Y., Jona, G., Krieger, E., Shamshoum, M., Bar-Even, A., and Milo, R. (2019). Conversion of Escherichia coli to Generate All Biomass Carbon from CO_2. Cell **179,** 1255-1263 e1212.

Goldschmidt-Clermont, M. (1986). The two genes for the small subunit of RuBP Carboxylase/oxygenase are closely linked in Chlamydomonas reinhardtii. Plant Mol Biol **6,** 13-21.

Goldschmidt-Clermont, M., and Bassi, R. (2015). Sharing light between two photosystems: mechanism of state transitions. Current Opinion in Plant Biology **25,** 71-78.

Goldschmidt-Clermont, M., Rahire, M., and Rochaix, J.D. (2008). Redundant cis-acting determinants of 3' processing and RNA stability in the chloroplast rbcL mRNA of Chlamydomonas. The Plant journal : for cell and molecular biology **53,** 566-577.

Gontero, B., and Salvucci, M.E. (2014). Regulation of photosynthetic carbon metabolism in aquatic and terrestrial organisms by Rubisco activase, redox-modulation and CP12. Aquatic Botany **118,** 14-23.

Grabsztunowicz, M., Koskela, M.M., and Mulo, P. (2017). Post-translational Modifications in Regulation of Chloroplast Function: Recent Advances. Frontiers in Plant Science **8**.

Grabsztunowicz, M., Górski, Z., Luciński, R., and Jackowski, G. (2015). A reversible decrease in ribulose 1,5-bisphosphate carboxylase/oxygenase carboxylation activity caused by the aggregation of the enzyme's large subunit is triggered in response to the exposure of moderate irradiance-grown plants to low irradiance. Physiologia plantarum **154,** 591-608.

Hammel, A., Zimmer, D., Sommer, F., Muhlhaus, T., and Schroda, M. (2018). Absolute Quantification of Major Photosynthetic Protein Complexes in *Chlamydomonas reinhardtii* Using Quantification Concatamers (QconCATs). Front Plant Sci **9,** 1265.

Harada, H., Nakajima, K., Sakaue, K., and Matsuda, Y. (2006). CO2 sensing at ocean surface mediated by cAMP in a marine diatom. Plant Physiol. **142,** 1318-1328.

Hasse, D., Larsson, A.M., and Andersson, I. (2015). Structure of Arabidopsis thaliana Rubisco activase. Acta crystallographica. Section D, Biological crystallography **71,** 800-808.
Hauser, T. (2016). Structural und functional characterization of Rubisco assembly chaperones. In Faculty of Chemistry and Pharmacy (Ludwig-Maximilians-Universität München).
Hauser, T., Bhat, J.Y., Milicic, G., Wendler, P., Hartl, F.U., Bracher, A., and Hayer-Hartl, M. (2015). Structure and mechanism of the Rubisco-assembly chaperone Raf1. Nature Structural & Molecular Biology **22,** 720-728.
Hayer-Hartl, M., and Hartl, F.U. (2020). Chaperone Machineries of Rubisco - The Most Abundant Enzyme. Trends in biochemical sciences **45,** 748-763.
He, S., Chou, H.-T., Matthies, D., Wunder, T., Meyer, M.T., Atkinson, N., Martinez-Sanchez, A., Jeffrey, P.D., Port, S.A., Patena, W., He, G., Chen, V.K., Hughson, F.M., McCormick, A.J., Mueller-Cajar, O., Engel, B.D., Yu, Z., and Jonikas, M.C. (2020). The structural basis of Rubisco phase separation in the pyrenoid. Nature plants**,** 1-11.
Henderson, J.N., Kuriata, A.M., Fromme, R., Salvucci, M.E., and Wachter, R.M. (2011). Atomic resolution x-ray structure of the substrate recognition domain of higher plant ribulose-bisphosphate carboxylase/oxygenase (Rubisco) activase. The Journal of biological chemistry **286,** 35683-35688.
Herrin, D.L., Michaels, A.S., and Paul, A.L. (1986). Regulation of genes encoding the large subunit of ribulose-1,5-bisphosphate carboxylase and the photosystem II polypeptides D-1 and D-2 during the cell cycle of Chlamydomonas reinhardtii. The Journal of cell biology **103,** 1837-1845.
Hicks, A., Drager, R.G., Higgs, D.C., and Stern, D.B. (2002). An mRNA 3' processing site targets downstream sequences for rapid degradation in Chlamydomonas chloroplasts. The Journal of biological chemistry **277,** 3325-3333.
Hong, S., and Spreitzer, R.J. (1997). Complementing substitutions at the bottom of the barrel influence catalysis and stability of ribulose-bisphosphate carboxylase/oxygenase. The Journal of biological chemistry **272,** 11114-11117.
Horst, B.G., Stewart, E.M., Nazarian, A.A., and Marletta, M.A. (2019). Characterization of a Carbon Monoxide-Activated Soluble Guanylate Cyclase from Chlamydomonas reinhardtii. Biochemistry **58,** 2250-2259.
Houtz, R.L., Magnani, R., Nayak, N.R., and Dirk, L.M. (2008). Co- and post-translational modifications in Rubisco: unanswered questions. Journal of Experimental Botany **59,** 1635-1645.
Houtz, R.L., Poneleit, L., Jones, S.B., Royer, M., and Stults, J.T. (1992). Posttranslational modifications in the amino- terminal region of the large subunit of ribulose- 1,5-bisphosphate carboxylase/oxygenase from several plant species. Plant Physiol **98,** 1170-1174.
Huang, F., Kong, W.-W., Sun, Y., Chen, T., Dykes, G.F., Jiang, Y.-L., and Liu, L.-N. (2020). Rubisco accumulation factor 1 (Raf1) plays essential roles in mediating Rubisco assembly and carboxysome biogenesis. Proceedings of the National Academy of Sciences **117,** 17418-17428.
Idoine, A.D., Boulouis, A., Rupprecht, J., and Bock, R. (2014). The diurnal logic of the expression of the chloroplast genome in Chlamydomonas reinhardtii. PloS one **9,** e108760.
Im, C.S., and Grossman, A.R. (2002). Identification and regulation of high light-induced genes in Chlamydomonas reinhardtii. The Plant Journal **30,** 301-313.
Im, C.S., Zhang, Z., Shrager, J., Chang, C.W., and Grossman, A.R. (2003). Analysis of light and CO_2 regulation in *Chlamydomonas reinhardtii* using genome-wide approaches. Photosynth Res **75,** 111-125.

Irihimovitch, V., and Shapira, M. (2000). Glutathione redox potential modulated by reactive oxygen species regulates translation of Rubisco large subunit in the chloroplast. The Journal of biological chemistry **275,** 16289-16295.

Irihimovitch, V., and Stern, D.B. (2006). The sulfur acclimation SAC3 kinase is required for chloroplast transcriptional repression under sulfur limitation in Chlamydomonas reinhardtii. Proceedings of the National Academy of Sciences of the United States of America **103,** 7911-7916.

Ishida, H., Yoshimoto, K., Izumi, M., Reisen, D., Yano, Y., Makino, A., Ohsumi, Y., Hanson, M.R., and Mae, T. (2008). Mobilization of rubisco and stroma-localized fluorescent proteins of chloroplasts to the vacuole by an ATG gene-dependent autophagic process. Plant Physiol **148,** 142-155.

Itakura, A.K., Chan, K.X., Atkinson, N., Pallesen, L., Wang, L., Reeves, G., Patena, W., Caspari, O., Roth, R., Goodenough, U., McCormick, A.J., Griffiths, H., and Jonikas, M.C. (2019). A Rubisco-binding protein is required for normal pyrenoid number and starch sheath morphology in Chlamydomonas reinhardtii. Proc. Natl. Acad. Sci. U. S. A.

Izumi, M., and Nakamura, S. (2018). Chloroplast Protein Turnover: The Influence of Extraplastidic Processes, Including Autophagy. International journal of molecular sciences **19**.

Jin, S., Sun, J., Wunder, T., Tang, D., Cousins, A.B., Sze, S.K., Mueller-Cajar, O., and Gao, Y.-G. (2016). Structural insights into the LCIB protein family reveals a new group of β-carbonic anhydrases. Proc. Natl. Acad. Sci. U. S. A. **113,** 14716–14721.

Johanningmeier, U. (1988). Possible control of transcript levels by chlorophyll precursors in Chlamydomonas. European journal of biochemistry **177,** 417-424.

Johnson, X. (2011). Manipulating RuBisCO accumulation in the green alga, Chlamydomonas reinhardtii. Plant molecular biology **76,** 397-405.

Johnson, X., Wostrikoff, K., Finazzi, G., Kuras, R., Schwarz, C., Bujaldon, S., Nickelsen, J., Stern, D.B., Wollman, F.A., and Vallon, O. (2010). MRL1, a conserved Pentatricopeptide repeat protein, is required for stabilization of rbcL mRNA in Chlamydomonas and Arabidopsis. The Plant cell **22,** 234-248.

Jordan, D.B., and Ogren, W.L. (1981). Species variation in the specificity of ribulose biphosphate carboxylase/oxygenase. Nature **291,** 513-515.

Kane Dickson, V., Pedi, L., and Long, S.B. (2014). Structure and insights into the function of a Ca(2+)-activated Cl(-) channel. Nature **516,** 213-218.

Kanevski, I., Maliga, P., Rhoades, D.F., and Gutteridge, S. (1999). Plastome engineering of ribulose-1,5-bisphosphate carboxylase/oxygenase in tobacco to form a sunflower large subunit and tobacco small subunit hybrid. Plant Physiol **119,** 133-142.

Karkehabadi, S., Satagopan, S., Taylor, T.C., Spreitzer, R.J., and Andersson, I. (2007). Structural analysis of altered large-subunit loop-6/carboxy-terminus interactions that influence catalytic efficiency and CO_2/O_2 specificity of ribulose-1,5-bisphosphate carboxylase/oxygenase. Biochemistry **46,** 11080-11089.

Karkehabadi, S., Peddi, S.R., Anwaruzzaman, M., Taylor, T.C., Cederlund, A., Genkov, T., Andersson, I., and Spreitzer, R.J. (2005). Chimeric small subunits influence catalysis without causing global conformational changes in the crystal structure of ribulose-1,5-bisphosphate carboxylase/oxygenase. Biochemistry **44,** 9851-9861.

Khrebtukova, I., and Spreitzer, R.J. (1996). Elimination of the Chlamydomonas gene family that encodes the small subunit of ribulose-1,5-bisphosphate carboxylase/oxygenase. Proceedings of the National Academy of Sciences **93,** 13689-13693.

Kim, J., and Mullet, J.E. (2003). A Mechanism for Light-Induced Translation of the rbcL mRNA Encoding the Large Subunit of Ribulose-1,5-bisphosphate Carboxylase in Barley Chloroplasts. Plant and Cell Physiology **44,** 491-499.

Kim, S.R., Yang, J.I., and An, G. (2013). OsCpn60alpha1, encoding the plastid chaperonin 60alpha subunit, is essential for folding of rbcL. Molecules and cells **35,** 402-409.

Klein, U., Salvador, M.L., and Bogorad, L. (1994). Activity of the Chlamydomonas chloroplast rbcL gene promoter is enhanced by a remote sequence element. Proceedings of the National Academy of Sciences of the United States of America **91,** 10819-10823.

Knight, S., Andersson, I., and Brändén, C.I. (1990). Crystallographic analysis of ribulose 1,5-bisphosphate carboxylase from spinach at 2·4 Å resolution: Subunit interactions and active site. Journal of Molecular Biology **215,** 113-160.

Knopf, J.A., and Shapira, M. (2005). Degradation of Rubisco SSU during oxidative stress triggers aggregation of Rubisco particles in Chlamydomonas reinhardtii. Planta **222,** 787-793.

Kohinata, T., Nishino, H., and Fukuzawa, H. (2008). Significance of zinc in a regulatory protein, CCM1, which regulates the carbon-concentrating mechanism in Chlamydomonas reinhardtii. Plant & Cell Physiology **49,** 273-283.

Kolesinski, P., Rydzy, M., and Szczepaniak, A. (2017). Is RAF1 protein from Synechocystis sp. PCC 6803 really needed in the cyanobacterial Rubisco assembly process? Photosynthesis research **132,** 135-148.

Kono, A., and Spalding, M.H. (2020). LCI1, a Chlamydomonas reinhardtii plasma membrane protein, functions in active CO2 uptake under low CO2. The Plant Journal.

Kono, A., Chou, T.-H., Radhakrishnan, A., Bolla, J.R., Sankar, K., Shome, S., Su, C.-C., Jernigan, R.L., Robinson, C.V., Yu, E.W., and Spalding, M.H. (2020). Structure and function of LCI1: a plasma membrane CO2 channel in the Chlamydomonas CO2 concentrating mechanism. The Plant Journal **102,** 1107-1126.

Kuchitsu, K., Tsuzuki, M., and Miyachi, S. (1988). Changes of Starch Localization within the Chloroplast Induced by Changes in CO2 Concentration during Growth of Chlamydomonas reinhardtii: Independent Regulation of Pyrenoid Starch and Stroma Starch. Plant & Cell Physiology **29,** 1269-1278.

Kucho, K.-I., Ohyama, K., and Fukuzawa, H. (1999). CO2-Responsive Transcriptional Regulation ofCAH1 Encoding Carbonic Anhydrase Is Mediated by Enhancer and Silencer Regions in Chlamydomonas reinhardtii. Plant Physiol. **121,** 1329-1337.

Kucho, K.-i., Yoshioka, S., Taniguchi, F., Ohyama, K., and Fukuzawa, H. (2003). Cis-acting elements and DNA-binding proteins involved in CO2-responsive transcriptional activation of Cah1 encoding a periplasmic Carbonic Anhydrase in *Chlamydomonas reinhardtii*. Plant Physiology **133,** 783.

Küken, A., Sommer, F., Yaneva-Roder, L., Mackinder, L.C., Höhne, M., Geimer, S., Jonikas, M.C., Schroda, M., Stitt, M., Nikoloski, Z., and Mettler-Altmann, T. (2018). Effects of microcompartmentation on flux distribution and metabolic pools in Chlamydomonas reinhardtii chloroplasts. Elife **7**.

Larson, E.M., O'Brien, C.M., Zhu, G., Spreitzer, R.J., and Portis, A.R., Jr. (1997). Specificity for activase is changed by a Pro-89 to Arg substitution in the large subunit of ribulose-1,5-bisphosphate carboxylase/oxygenase. The Journal of biological chemistry **272,** 17033-17037.

Lewis, E., and Wallace, D. (1998). Program developed for CO_2 system calculations (Environmental System Science Data Infrastructure for a Virtual Ecosystem).

Li, C., Salvucci, M.E., and Portis, A.R., Jr. (2005). Two residues of rubisco activase involved in recognition of the Rubisco substrate. The Journal of biological chemistry **280,** 24864-24869.

Li, X., Patena, W., Fauser, F., Jinkerson, R.E., Saroussi, S., Meyer, M.T., Ivanova, N., Robertson, J.M., Yue, R., Zhang, R., Vilarrasa-Blasi, J., Wittkopp, T.M., Ramundo, S., Blum, S.R., Goh, A., Laudon, M., Srikumar, T., Lefebvre, P.A., Grossman, A.R., and Jonikas, M.C. (2019). A genome-wide algal mutant library and functional screen identifies genes required for eukaryotic photosynthesis. Nature genetics **51,** 627-635.

Lin, M.T., Stone, W.D., Chaudhari, V., and Hanson, M.R. (2020). Small subunits can determine enzyme kinetics of tobacco Rubisco expressed in *Escherichia coli*. Nature plants **6,** 1289-1299.

Liu, C., Young, A.L., Starling-Windhof, A., Bracher, A., Saschenbrecker, S., Rao, B.V., Rao, K.V., Berninghausen, O., Mielke, T., Hartl, F.U., Beckmann, R., and Hayer-Hartl, M. (2010). Coupled chaperone action in folding and assembly of hexadecameric Rubisco. Nature **463,** 197-202.

Liu, J., Yang, H., Lu, Q., Wen, X., Chen, F., Peng, L., Zhang, L., and Lu, C. (2012). PsbP-domain protein1, a nuclear-encoded thylakoid lumenal protein, is essential for photosystem I assembly in Arabidopsis. The Plant cell **24,** 4992-5006.

Loizeau, K., Qu, Y., Depp, S., Fiechter, V., Ruwe, H., Lefebvre-Legendre, L., Schmitz-Linneweber, C., and Goldschmidt-Clermont, M. (2014). Small RNAs reveal two target sites of the RNA-maturation factor Mbb1 in the chloroplast of Chlamydomonas. Nucleic acids research **42,** 3286-3297.

Lorimer, G.H., and Miziorko, H.M. (1980). Carbamate formation on the epsilon-amino group of a lysyl residue as the basis for the activation of ribulosebisphosphate carboxylase by CO_2 and Mg^{2+}. Biochemistry **19,** 5321-5328.

Lü, W., Du, J., Schwarzer, N.J., Wacker, T., Andrade, S.L.A., and Einsle, O. (2013). The formate/nitrite transporter family of anion channels. Biological Chemistry **394,** 715-727.

Lucker, B., and Kramer, D.M. (2013). Regulation of cyclic electron flow in Chlamydomonas reinhardtii under fluctuating carbon availability. Photosynthesis research **117,** 449-459.

Lumbreras, V., and Purton, S. (1998). Recent advances in chlamydomonas transgenics. Protist **149,** 23-27.

Ma, S., Martin-Laffon, J., Mininno, M., Gigarel, O., Brugière, S., Bastien, O., Tardif, M., Ravanel, S., and Alban, C. (2016). Molecular Evolution of the Substrate Specificity of Chloroplastic Aldolases/Rubisco Lysine Methyltransferases in Plants. Molecular plant **9,** 569-581.

Ma, Y., Pollock, S.V., Xiao, Y., Cunnusamy, K., and Moroney, J.V. (2011). Identification of a Novel Gene, CIA6, Required for Normal Pyrenoid Formation in Chlamydomonas reinhardtii. Plant Physiol. **156,** 884-896.

Machingura, M.C., Bajsa-Hirschel, J., Laborde, S.M., Schwartzenburg, J.B., Mukherjee, B., Mukherjee, A., Pollock, S.V., Förster, B., Price, G.D., and Moroney, J.V. (2017). Identification and characterization of a solute carrier, CIA8, involved in inorganic carbon acclimation in Chlamydomonas reinhardtii. J. Exp. Bot. **68,** 3879-3890.

Mackinder, L.C., Meyer, M.T., Mettler-Altmann, T., Chen, V.K., Mitchell, M.C., Caspari, O., Freeman Rosenzweig, E.S., Pallesen, L., Reeves, G., Itakura, A., Roth, R., Sommer, F., Geimer, S., Muhlhaus, T., Schroda, M., Goodenough, U., Stitt, M., Griffiths, H., and Jonikas, M.C. (2016). A repeat protein links Rubisco to form the eukaryotic carbon-concentrating organelle. Proceedings of the National Academy of Sciences of the United States of America **113,** 5958-5963.

Mackinder, L.C.M., Chen, C., Leib, R.D., Patena, W., Blum, S.R., Rodman, M., Ramundo, S., Adams, C.M., and Jonikas, M.C. (2017). A Spatial Interactome Reveals the Protein Organization of the Algal CO2-Concentrating Mechanism. Cell **171,** 133-147 e114.

Majeran, W., Wostrikoff, K., Wollman, F.A., and Vallon, O. (2019). Role of ClpP in the Biogenesis and Degradation of RuBisCO and ATP Synthase in Chlamydomonas reinhardtii. Plants **8**.

Majeran, W., Olive, J., Drapier, D., Vallon, O., and Wollman, F.A. (2001). The light sensitivity of ATP synthase mutants of *Chlamydomonas reinhardtii*. Plant Physiol **126,** 421-433.

Marin-Navarro, J., and Moreno, J. (2003). Modification of the proteolytic fragmentation pattern upon oxidation of cysteines from ribulose 1,5-bisphosphate carboxylase/oxygenase. Biochemistry **42,** 14930-14938.

Marin-Navarro, J., and Moreno, J. (2006). Cysteines 449 and 459 modulate the reduction-oxidation conformational changes of ribulose 1.5-bisphosphate carboxylase/oxygenase and the translocation of the enzyme to membranes during stress. Plant Cell Environ **29,** 898-908.

Mariscal, V., Moulin, P., Orsel, M., Miller, A.J., Fernández, E., and Galván, A. (2006). Differential regulation of the Chlamydomonas Nar1 gene family by carbon and nitrogen. Protist **157,** 421-433.

Markelova, A.G., Sinetova, M.P., Kupriyanova, E.V., and Pronina, N.A. (2009). Distribution and functional role of carbonic anhydrase Cah3 associated with thylakoid membranes in the chloroplast and pyrenoid of Chlamydomonas reinhardtii. Russ. J. Plant Physiol. **56,** 761.

Martin, W., Stoebe, B., Goremykin, V., Hapsmann, S., Hasegawa, M., and Kowallik, K.V. (1998). Gene transfer to the nucleus and the evolution of chloroplasts. Nature **393,** 162-165.

Mastrobuoni, G., Irgang, S., Pietzke, M., Assmus, H.E., Wenzel, M., Schulze, W.X., and Kempa, S. (2012). Proteome dynamics and early salt stress response of the photosynthetic organism *Chlamydomonas reinhardtii*. BMC genomics **13,** 215.

Maul, J.E., Lilly, J.W., Cui, L., dePamphilis, C.W., Miller, W., Harris, E.H., and Stern, D.B. (2002). The Chlamydomonas reinhardtii plastid chromosome: islands of genes in a sea of repeats. The Plant cell **14,** 2659-2679.

McConnell, E.W., Werth, E.G., and Hicks, L.M. (2018). The phosphorylated redox proteome of *Chlamydomonas reinhardtii*: Revealing novel means for regulation of protein structure and function. Redox biology **17,** 35-46.

McKay, R.M.L., and Gibbs, S.P. (1991). Immunocytochemical Localization of Phosphoribulokinase in Microalgae. Botanica Acta **104,** 367-373.

Mehta, R.A., Fawcett, T.W., Porath, D., and Mattoo, A.K. (1992). Oxidative stress causes rapid membrane translocation and in vivo degradation of ribulose-1,5-bisphosphate carboxylase/oxygenase. The Journal of biological chemistry **267,** 2810-2816.

Meyer, M., and Griffiths, H. (2013). Origins and diversity of eukaryotic CO2-concentrating mechanisms: lessons for the future. J. Exp. Bot. **64,** 769-786.

Meyer, M.T., Goudet, M.M.M., and Griffiths, H. (2020a). The Algal Pyrenoid. In Photosynthesis in Algae: Biochemical and Physiological Mechanisms, A.W.D. Larkum, A.R. Grossmann, and J.A. Raven, eds (Cham: Springer International Publishing), pp. 179-203.

Meyer, M.T., Genkov, T., Skepper, J.N., Jouhet, J., Mitchell, M.C., Spreitzer, R.J., and Griffiths, H. (2012). Rubisco small-subunit α-helices control pyrenoid formation in Chlamydomonas. Proc. Natl. Acad. Sci. U. S. A. **109,** 19474-19479.

Meyer, M.T., Itakura, A.K., Patena, W., Wang, L., He, S., Emrich-Mills, T., Lau, C.S., Yates, G., Mackinder, L.C.M., and Jonikas, M.C. (2020b). Assembly

of the algal CO_2-fixing organelle, the pyrenoid, is guided by a Rubisco-binding motif. Science advances **6**.

Millero, F.J. (1979). The thermodynamics of the carbonate system in seawater. Geochimica et Cosmochimica Acta **43,** 1651-1661.

Mishkind, M.L., and Schmidt, G.W. (1983). Posttranscriptional Regulation of Ribulose 1,5-bisphosphate Carboxylase Small Subunit Accumulation in Chlamydomonas reinhardtii. Plant Physiol **72,** 847-854.

Mitchell, M.C., Meyer, M.T., and Griffiths, H. (2014). Dynamics of Carbon-Concentrating Mechanism Induction and Protein Relocalization during the Dark-to-Light Transition in Synchronized Chlamydomonas reinhardtii. Plant Physiol. **166,** 1073-1082.

Miura, K., Yamano, T., Yoshioka, S., Kohinata, T., Inoue, Y., Taniguchi, F., Asamizu, E., Nakamura, Y., Tabata, S., Yamato, K.T., Ohyama, K., and Fukuzawa, H. (2004). Expression profiling-based identification of CO_2-responsive genes regulated by CCM1 controlling a carbon-concentrating mechanism in *Chlamydomonas reinhardtii*. Plant Physiol. **135,** 1595-1607.

Mizohata, E., Matsumura, H., Okano, Y., Kumei, M., Takuma, H., Onodera, J., Kato, K., Shibata, N., Inoue, T., Yokota, A., and Kai, Y. (2002). Crystal structure of activated ribulose-1,5-bisphosphate carboxylase/oxygenase from green alga *Chlamydomonas reinhardtii* complexed with 2-carboxyarabinitol-1,5-bisphosphate. Journal of Molecular Biology **316,** 679-691.

Moreno, J., and Spreitzer, R.J. (1999). C172S substitution in the chloroplast-encoded large subunit affects stability and stress-induced turnover of ribulose-1,5-bisphosphate carboxylase/oxygenase. The Journal of biological chemistry **274,** 26789-26793.

Moreno, J., Garcia-Murria, M.J., and Marin-Navarro, J. (2008). Redox modulation of Rubisco conformation and activity through its cysteine residues. J Exp Bot **59,** 1605-1614.

Moroney, J.V., and Tolbert, N.E. (1985). Inorganic Carbon Uptake by Chlamydomonas reinhardtii. Plant Physiol. **77,** 253-258.

Moroney, J.V., Husic, H.D., and Tolbert, N.E. (1985). Effect of Carbonic Anhydrase Inhibitors on Inorganic Carbon Accumulation by *Chlamydomonas reinhardtii*. Plant Physiology **79,** 177.

Moroney, J.V., Tolbert, N.E., and Sears, B.B. (1986). Complementation analysis of the inorganic carbon concentrating mechanism of *Chlamydomonas reinhardtii*. Mol. Gen. Genet. **204,** 199-203.

Moroney, J.V., Husic, H.D., Tolbert, N.E., Kitayama, M., Manuel, L.J., and Togasaki, R.K. (1989). Isolation and Characterization of a Mutant of Chlamydomonas reinhardtii Deficient in the CO2 Concentrating Mechanism. Plant Physiology **89,** 897.

Moroney, J.V., Ma, Y., Frey, W.D., Fusilier, K.A., Pham, T.T., Simms, T.A., DiMario, R.J., Yang, J., and Mukherjee, B. (2011). The carbonic anhydrase isoforms of Chlamydomonas reinhardtii: intracellular location, expression, and physiological roles. Photosynthesis research **109,** 133-149.

Muhlbauer, S.K., and Eichacker, L.A. (1999). The stromal protein large subunit of ribulose-1,5-bisphosphate carboxylase is translated by membrane-bound ribosomes. European journal of biochemistry **261,** 784-788.

Mukherjee, A., Lau, C.S., Walker, C.E., Rai, A.K., Prejean, C.I., Yates, G., Emrich-Mills, T., Lemoine, S.G., Vinyard, D.J., Mackinder, L.C.M., and Moroney, J.V. (2019). Thylakoid localized bestrophin-like proteins are essential for the CO_2 concentrating mechanism of Chlamydomonas reinhardtii. Proc. Natl. Acad. Sci. U. S. A. **116,** 16915-16920.

Ng, J., Guo, Z., and Mueller-Cajar, O. (2020). Rubisco activase requires residues in the large subunit N terminus to remodel inhibited plant Rubisco. The Journal of biological chemistry **295,** 16427-16435.

Nott, A., Jung, H.S., Koussevitzky, S., and Chory, J. (2006). Plastid-to-nucleus retrograde signaling. Annual review of plant biology **57,** 739-759.

Ohad, I., Siekevitz, P., and Palade, G.E. (1967). Biogenesis of chloroplast membranes. II. Plastid differentiation during greening of a dark-grown algal mutant (Chlamydomonas reinhardi). J. Cell Biol. **35,** 553-584.

Ohkawa, H., Sonoda, M., Katoh, H., and Ogawa, T. (1998). The use of mutants in the analysis of the CO_2-concentrating mechanism in cyanobacteria. Can. J. Bot. **76,** 1035-1042.

Ohnishi, N., Mukherjee, B., Tsujikawa, T., Yanase, M., Nakano, H., Moroney, J.V., and Fukuzawa, H. (2010). Expression of a low CO_2-inducible protein, LCI1, increases inorganic carbon uptake in the green alga Chlamydomonas reinhardtii. The Plant cell **22,** 3105-3117.

Onizuka, T., Endo, S., Akiyama, H., Kanai, S., Hirano, M., Yokota, A., Tanaka, S., and Miyasaka, H. (2004). The rbcX gene product promotes the production and assembly of ribulose-1,5-bisphosphate carboxylase/oxygenase of *Synechococcus sp. PCC7002* in *Escherichia coli*. Plant & Cell Physiology **45,** 1390-1395.

Ott, C.M., Smith, B.D., Portis, A.R., Jr., and Spreitzer, R.J. (2000). Activase region on chloroplast ribulose-1,5-bisphosphate carboxylase/oxygenase. Nonconservative substitution in the large subunit alters species specificity of protein interaction. The Journal of biological chemistry **275,** 26241-26244.

Owji, A.P., Zhao, Q., Ji, C., Kittredge, A., Hopiavuori, A., Fu, Z., Ward, N., Clarke, O.B., Shen, Y., Zhang, Y., Hendrickson, W.A., and Yang, T. (2020). Structural and functional characterization of the bestrophin-2 anion channel. Nature Structural & Molecular Biology **27,** 382-391.

Parry, M.A., Andralojc, P.J., Mitchell, R.A., Madgwick, P.J., and Keys, A.J. (2003). Manipulation of Rubisco: the amount, activity, function and regulation. J Exp Bot **54,** 1321-1333.

Pazour, G.J., Agrin, N., Leszyk, J., and Witman, G.B. (2005). Proteomic analysis of a eukaryotic cilium. J. Cell Biol. **170,** 103-113.

Petroutsos, D., Busch, A., Janssen, I., Trompelt, K., Bergner, S.V., Weinl, S., Holtkamp, M., Karst, U., Kudla, J., and Hippler, M. (2011). The chloroplast calcium sensor CAS is required for photoacclimation in Chlamydomonas reinhardtii. The Plant cell **23,** 2950-2963.

Pollock, S.V., Colombo, S.L., Prout, D.L., Jr., Godfrey, A.C., and Moroney, J.V. (2003). Rubisco activase is required for optimal photosynthesis in the green alga Chlamydomonas reinhardtii in a low-CO_2 atmosphere. Plant Physiol **133,** 1854-1861.

Pollock, S.V., Prout, D.L., Godfrey, A.C., Lemaire, S.D., and Moroney, J.V. (2004). The Chlamydomonas reinhardtii proteins Ccp1 and Ccp2 are required for long-term growth, but are not necessary for efficient photosynthesis, in a low-CO2 environment. Plant molecular biology **56,** 125-132.

Portis, A.R., Jr., and Salvucci, M.E. (2002). The discovery of Rubisco activase - yet another story of serendipity. Photosynth Res **73,** 257-264.

Portis, A.R., Jr., Li, C., Wang, D., and Salvucci, M.E. (2008). Regulation of Rubisco activase and its interaction with Rubisco. J Exp Bot **59,** 1597-1604.

Poudel, S., Pike, D.H., Raanan, H., Mancini, J.A., Nanda, V., Rickaby, R.E.M., and Falkowski, P.G. (2020). Biophysical analysis of the structural evolution of substrate specificity in RuBisCO. Proceedings of the National Academy of Sciences of the United States of America **117,** 30451-30457.

Price, G.D. and Badger, M.R. (1989). Expression of human carbonic anhydrase in the cyanobacterium *Synechococcus* PCC7942 creates a high CO_2-requiring phenotype evidence for a central role for carboxysomes in the CO_2 Concentrating Mechanism, Plant physiology. **91**, 505–513.

Pronina, N.A., and Borodin, V.V. (1993). CO_2 stress and CO_2 concentration mechanism: investigation by means of photosystem-deficient and carbonic anhydrase-deficient mutants of Chlamydomonas reinhardtii. PHOTOSYNTHETICA **28,** 515-515.

Qu, Z., and Hartzell, H.C. (2008). Bestrophin Cl- channels are highly permeable to HCO3. Am. J. Physiol. Cell Physiol. **294,** C1371-1377.

Ramazanov, Z., Mason, C.B., Ceraghty, A.M., Spalding, M.H., and Moroney, J.V. (1993). The Low $C0_2$-Inducible 36-Kilodalton Protein is Localized to the chloroplast envelopeof *Chlamydomonas reinhardtii*. Plant Physiol. **101,** 1195-1199.

Ramazanov, Z., Rawat, M., Henk, M.C., Mason, C.B., Matthews, S.W., and Moroney, J.V. (1994). The induction of the CO2-concentrating mechanism is correlated with the formation of the starch sheath around the pyrenoid of Chlamydomonas reinhardtii. Planta **195,** 210–216.

Ramundo, S., and Rochaix, J.D. (2014). Chloroplast unfolded protein response, a new plastid stress signaling pathway? Plant signaling & behavior **9,** e972874.

Ranty, B., Lorimer, G., and Gutterridge, S. (1991). An intra-dimeric crosslink of large subunits of spinach ribulose-1,5-bisphosphate carboxylase/oxygenase is formed by oxidation of cysteine 247. European journal of biochemistry **200,** 353-358.

Rasineni, G.K., Loh, P.C., and Lim, B.H. (2017). Characterization of Chlamydomonas Ribulose-1,5-bisphosphate carboxylase/oxygenase variants mutated at residues that are post-translationally modified. Biochimica et biophysica acta. General subjects **1861,** 79-85.

Raunser, S., Magnani, R., Huang, Z., Houtz, R.L., Trievel, R.C., Penczek, P.A., and Walz, T. (2009). Rubisco in complex with Rubisco large subunit methyltransferase. Proceedings of the National Academy of Sciences of the United States of America **106,** 3160-3165.

Raven, J.A. (1997). CO2-concentrating mechanisms: a direct role for thylakoid lumen acidification? Plant, cell & environment **20,** 147-154.

Rawat, M., and Moroney S, J.V. Partial Characterization of New Isoenzyme of Carbonic Anhydrase Isolated from Chlumydomonas reinhurdtii.

Rawat, M., and Moroney, J.V. (1995). The Regulation of Carbonic Anhydrase and Ribulose-1,5-Bisphosphate Carboxylase/Oxygenase Activase by Light and CO_2 in Chlamydomonas reinhardtii. Plant Physiol **109,** 937-944.

Recuenco-Munoz, L., Offre, P., Valledor, L., Lyon, D., Weckwerth, W., and Wienkoop, S. (2015). Targeted quantitative analysis of a diurnal RuBisCO subunit expression and translation profile in *Chlamydomonas reinhardtii* introducing a novel Mass Western approach. Journal of proteomics **113,** 143-153.

Reinfelder, J.R. (2011). Carbon concentrating mechanisms in eukaryotic marine phytoplankton. Ann. Rev. Mar. Sci. **3,** 291-315.

Roesler, K.R., and Ogren, W.L. (1990). Primary Structure of Chlamydomonas reinhardtii Ribulose 1,5-Bisphosphate Carboxylase/Oxygenase Activase and Evidence for a Single Polypeptide. Plant Physiol **94,** 1837-1841.

Rolland, N., Dorne, A.J., Amoroso, G., Sültemeyer, D.F., Joyard, J., and Rochaix, J.D. (1997). Disruption of the plastid ycf10 open reading frame affects uptake of inorganic carbon in the chloroplast of Chlamydomonas. EMBO J. **16,** 6713-6726.

Rott, R., Drager, R.G., Stern, D.B., and Schuster, G. (1996). The 3' untranslated regions of chloroplast genes in Chlamydomonas reinhardtii do not serve as efficient transcriptional terminators. Molecular & general genetics : MGG **252,** 676-683.

Rowland, E., Kim, J., Bhuiyan, N.H., and van Wijk, K.J. (2015). The Arabidopsis Chloroplast Stromal N-Terminome: Complexities of Amino-Terminal Protein Maturation and Stability. Plant Physiol. **169,** 1881-1896.

Ruiz-Sola, A., Flori, S., Yuan, Y., Villain, G., Sanz-Luque, E., Redekop, P., Tokutsu, R., Kueken, A., Tsichla, A., Kepesidis, G., Allorent, G., Arend, M., Iacono, F., Finazzi, G., Hippler, M., Zoran, N., Jun, N., Grossman, A.R., and Petroutsos, D. (2021). Photoprotection is regulated by light-independent CO_2 availability. BioRxiv Preprint. https://doi.org/10.1101/2021.10.23.465040

Ruwe, H., Wang, G., Gusewski, S., and Schmitz-Linneweber, C. (2016). Systematic analysis of plant mitochondrial and chloroplast small RNAs suggests organelle-specific mRNA stabilization mechanisms. Nucleic acids research **44,** 7406-7417.

Rymarquis, L.A., Higgs, D.C., and Stern, D.B. (2006). Nuclear suppressors define three factors that participate in both 5' and 3' end processing of mRNAs in Chlamydomonas chloroplasts. The Plant journal : for cell and molecular biology **46,** 448-461.

Salvador, M.L., Klein, U., and Bogorad, L. (1993a). Light-regulated and endogenous fluctuations of chloroplast transcript levels in Chlamydomonas. Regulation by transcription and RNA degradation. The Plant journal : for cell and molecular biology **3,** 213-219.

Salvador, M.L., Klein, U., and Bogorad, L. (1993b). 5' sequences are important positive and negative determinants of the longevity of Chlamydomonas chloroplast gene transcripts. Proceedings of the National Academy of Sciences of the United States of America **90,** 1556-1560.

Salvador, M.L., Klein, U., and Bogorad, L. (1998). Endogenous fluctuations of DNA topology in the chloroplast of Chlamydomonas reinhardtii. Molecular and cellular biology **18,** 7235-7242.

Salvador, M.L., Suay, L., and Klein, U. (2011). Messenger RNA degradation is initiated at the 5' end and follows sequence- and condition-dependent modes in chloroplasts. Nucleic acids research **39,** 6213-6222.

Satagopan, S., and Spreitzer, R.J. (2004). Substitutions at the Asp-473 latch residue of chlamydomonas ribulosebisphosphate carboxylase/oxygenase cause decreases in carboxylation efficiency and CO_2/O_2 specificity. The Journal of biological chemistry **279,** 14240-14244.

Satagopan, S., and Spreitzer, R.J. (2008). Plant-like substitutions in the large-subunit carboxy terminus of Chlamydomonas Rubisco increase CO_2/O_2 specificity. BMC plant biology **8,** 85.

Savir, Y., Noor, E., Milo, R., and Tlusty, T. (2010). Cross-species analysis traces adaptation of Rubisco toward optimality in a low-dimensional landscape. Proceedings of the National Academy of Sciences of the United States of America **107,** 3475-3480.

Schmidt, G.W., and Mishkind, M.L. (1983). Rapid degradation of unassembled ribulose 1,5-bisphosphate carboxylase small subunits in chloroplasts. Proceedings of the National Academy of Sciences of the United States of America **80,** 2632-2636.

Schmollinger, S., Muhlhaus, T., Boyle, N.R., Blaby, I.K., Casero, D., Mettler, T., Moseley, J.L., Kropat, J., Sommer, F., Strenkert, D., Hemme, D., Pellegrini, M., Grossman, A.R., Stitt, M., Schroda, M., and Merchant, S.S. (2014). Nitrogen-Sparing Mechanisms in Chlamydomonas Affect the Transcriptome, the Proteome, and Photosynthetic Metabolism. The Plant cell **26,** 1410-1435.

Schroda, M. (2019). Good News for Nuclear Transgene Expression in Chlamydomonas. Cells **8**.

Schroda, M., Vallon, O., Wollman, F.A., and Beck, C.F. (1999). A chloroplast-targeted heat shock protein 70 (HSP70) contributes to the photoprotection and repair of photosystem II during and after photoinhibition. The Plant cell **11,** 1165-1178.

Serban, A.J., Breen, I.L., Bui, H.Q., Levitus, M., and Wachter, R.M. (2018). Assembly-disassembly is coupled to the ATPase cycle of tobacco Rubisco activase. The Journal of biological chemistry **293,** 19451-19465.

Shapira, M., Lers, A., Heifetz, P.B., Irihimovitz, V., Barry Osmond, C., Gillham, N.W., and Boynton, J.E. (1997). Differential regulation of chloroplast gene expression in Chlamydomonas reinhardtii during photoacclimation: light stress transiently suppresses synthesis of the Rubisco LSU protein while enhancing synthesis of the PS II D1 protein. Plant molecular biology **33,** 1001-1001.

Sinetova, M.A., Kupriyanova, E.V., Markelova, A.G., Allakhverdiev, S.I., and Pronina, N.A. (2012). Identification and functional role of the carbonic anhydrase Cah3 in thylakoid membranes of pyrenoid of Chlamydomonas reinhardtii. Biochim. Biophys. Acta **1817,** 1248–1255.

Singh, M., Boutanaev, A., Zucchi, P., and Bogorad, L. (2001). Gene elements that affect the longevity of rbcL sequence-containing transcripts in Chlamydomonas reinhardtii chloroplasts. Proceedings of the National Academy of Sciences of the United States of America **98,** 2289-2294.

Smythers, A.L., McConnell, E.W., Lewis, H.C., Mubarek, S.N., and Hicks, L.M. (2020). Photosynthetic Metabolism and Nitrogen Reshuffling Are Regulated by Reversible Cysteine Thiol Oxidation Following Nitrogen Deprivation in Chlamydomonas. Plants **9**.

Somerville, C.R., Portis, A.R., and Ogren, W.L. (1982). A Mutant of Arabidopsis thaliana Which Lacks Activation of RuBP Carboxylase In Vivo. Plant Physiol **70,** 381-387.

Soupene, E., Inwood, W., and Kustu, S. (2004). Lack of the Rhesus protein Rh1 impairs growth of the green alga *Chlamydomonas reinhardtii* at high CO_2. Proc. Natl. Acad. Sci. U. S. A. **101,** 7787-7792.

Spalding, M.H., Spreitzer, R.J., and Ogren, W.L. (1983a). Reduced inorganic carbon transport in a CO_2-requiring mutant of Chlamydomonas reinhardii. Plant Physiology **73,** 273-276.

Spalding, M.H., Spreitzer, R.J., and Ogren, W.L. (1983b). Carbonic Anhydrase-Deficient Mutant of *Chlamydomonas reinhardii* Requires Elevated Carbon Dioxide Concentration for Photoautotrophic Growth. Plant Physiol. **73,** 268-272.

Spreitzer, R.J. (2003). Role of the small subunit in ribulose-1,5-bisphosphate carboxylase/oxygenase. Archives of biochemistry and biophysics **414,** 141-149.

Spreitzer, R.J., and Salvucci, M.E. (2002). Rubisco: structure, regulatory interactions, and possibilities for a better enzyme. Annual review of plant biology **53,** 449-475.

Spreitzer, R.J., Peddi, S.R., and Satagopan, S. (2005). Phylogenetic engineering at an interface between large and small subunits imparts land-plant kinetic properties to algal Rubisco. Proceedings of the National Academy of Sciences of the United States of America **102,** 17225-17230.

Spreitzer, R.J., Esquivel, M.G., Du, Y.C., and McLaughlin, P.D. (2001). Alanine-scanning mutagenesis of the small-subunit beta A-beta B loop of chloroplast ribulose-1,5-bisphosphate carboxylase/oxygenase: substitution at Arg-71 affects thermal stability and CO_2/O_2 specificity. Biochemistry **40,** 5615-5621.

Stern, D.B., and Kindle, K.L. (1993). 3'end maturation of the Chlamydomonas reinhardtii chloroplast atpB mRNA is a two-step process. Molecular and cellular biology **13,** 2277-2285.

Stotz, M., Mueller-Cajar, O., Ciniawsky, S., Wendler, P., Hartl, F.U., Bracher, A., and Hayer-Hartl, M. (2011). Structure of green-type Rubisco activase from tobacco. Nat Struct Mol Biol **18,** 1366-1370.

Strenkert, D., Schmollinger, S., Gallaher, S.D., Salome, P.A., Purvine, S.O., Nicora, C.D., Mettler-Altmann, T., Soubeyrand, E., Weber, A.P.M., Lipton, M.S., Basset, G.J., and Merchant, S.S. (2019). Multiomics resolution of molecular events during a day in the life of Chlamydomonas. Proceedings of the National Academy of Sciences of the United States of America **116,** 2374-2383.

Studer, R.A., Christin, P.A., Williams, M.A., and Orengo, C.A. (2014). Stability-activity tradeoffs constrain the adaptive evolution of RubisCO. Proceedings of the National Academy of Sciences of the United States of America **111,** 2223-2228.

Suay, L., Salvador, M.L., Abesha, E., and Klein, U. (2005). Specific roles of 5' RNA secondary structures in stabilizing transcripts in chloroplasts. Nucleic acids research **33,** 4754-4761.

Sugiyama, T., Nakayama, N., Ogawa, M., and Akazawa, T. (1968). Structure and function of chloroplast proteins. II. Effect of p-chloromercuribenzoate treatment on the ribulose 1,5-diphosphate carboxylase activity of spinach leaf fraction I protein. Archives of biochemistry and biophysics **125,** 98-106.

Sun, Y., and Zerges, W. (2015). Translational regulation in chloroplasts for development and homeostasis. Biochimica et biophysica acta **1847,** 809-820.

Sun, Y., Valente-Paterno, M., Bakhtiari, S., Law, C., Zhan, Y., and Zerges, W. (2019). Photosystem Biogenesis Is Localized to the Translation Zone in the Chloroplast of Chlamydomonas. The Plant cell **31,** 3057-3072.

Taylor, T.C., Backlund, A., Bjorhall, K., Spreitzer, R.J., and Andersson, I. (2001). First crystal structure of Rubisco from a green alga, Chlamydomonas reinhardtii. The Journal of biological chemistry **276,** 48159-48164.

Tcherkez, G.G., Farquhar, G.D., and Andrews, T.J. (2006). Despite slow catalysis and confused substrate specificity, all ribulose bisphosphate carboxylases may be nearly perfectly optimized. Proceedings of the National Academy of Sciences of the United States of America **103,** 7246-7251.

Terashima, M., Specht, M., Naumann, B., and Hippler, M. (2010). Characterizing the anaerobic response of Chlamydomonas reinhardtii by quantitative proteomics. Molecular & cellular proteomics : MCP **9,** 1514-1532.

Terashima, M., Petroutsos, D., Hüdig, M., Tolstygina, I., Trompelt, K., Gäbelein, P., Fufezan, C., Kudla, J., Weinl, S., Finazzi, G., and Hippler, M. (2012). Calcium-dependent regulation of cyclic photosynthetic electron transfer by a CAS, ANR1, and PGRL1 complex. Proc. Natl. Acad. Sci. U. S. A. **109,** 17717-17722.

Terentyev, V.V., Shukshina, A.K., and Shitov, A.V. (2019). Carbonic anhydrase CAH3 supports the activity of photosystem II under increased pH. Biochim. Biophys. Acta Bioenerg.

Tirumani, S., Kokkanti, M., Chaudhari, V., Shukla, M., and Rao, B.J. (2014). Regulation of CCM genes in Chlamydomonas reinhardtii during conditions of light–dark cycles in synchronous cultures. Plant molecular biology **85,** 277-286.

Tourasse, N.J., Choquet, Y., and Vallon, O. (2013). PPR proteins of green algae. RNA biology **10,** 1526-1542.

Toyokawa, C., Yamano, T., and Fukuzawa, H. (2020). Pyrenoid Starch Sheath Is Required for LCIB Localization and the CO_2-Concentrating Mechanism in Green Algae. Plant Physiol.

Trosch, R., Barahimipour, R., Gao, Y., Badillo-Corona, J.A., Gotsmann, V.L., Zimmer, D., Muhlhaus, T., Zoschke, R., and Willmund, F. (2018).

Commonalities and differences of chloroplast translation in a green alga and land plants. Nature plants **4,** 564-575.

Turkina, M.V., Blanco-Rivero, A., Vainonen, J.P., Vener, A.V., and Villarejo, A. (2006). CO2 limitation induces specific redox-dependent protein phosphorylation in Chlamydomonas reinhardtii. Proteomics **6,** 2693-2704.

Uniacke, J., and Zerges, W. (2007). Photosystem II assembly and repair are differentially localized in Chlamydomonas. The Plant cell **19,** 3640-3654.

Uniacke, J., and Zerges, W. (2008). Stress induces the assembly of RNA granules in the chloroplast of Chlamydomonas reinhardtii. The Journal of cell biology **182,** 641-646.

Uniacke, J., and Zerges, W. (2009). Chloroplast protein targeting involves localized translation in Chlamydomonas. Proc. Natl. Acad. Sci. U S A **106,** 1439-1444.

Van, K., and Spalding, M.H. (1999). Periplasmic Carbonic Anhydrase Structural Gene (Cah1) Mutant in <em>Chlamydomonas reinhardtii</em&gt. Plant Physiology **120,** 757.

van Lun, M., van der Spoel, D., and Andersson, I. (2011). Subunit interface dynamics in hexadecameric rubisco. J Mol Biol **411,** 1083-1098.

van Lun, M., Hub, J.S., van der Spoel, D., and Andersson, I. (2014). CO_2 and O_2 distribution in Rubisco suggests the small subunit functions as a CO_2 reservoir. Journal of the American Chemical Society **136,** 3165-3171.

Vanzo, E., Ghirardo, A., Merl-Pham, J., Lindermayr, C., Heller, W., Hauck, S.M., Durner, J., and Schnitzler, J.P. (2014). S-nitroso-proteome in poplar leaves in response to acute ozone stress. PloS one **9,** e106886.

Villarejo, A., Martinez, F., Pino Plumed, M., and Ramazanov, Z. (1996). The induction of the CO2 concentrating mechanism in a starch-less mutant of Chlamydomonas reinhardtii. Physiol. Plant. **98,** 798-802.

Villarejo, A., Shutova, T., Moskvin, O., Forssén, M., Klimov, V.V., and Samuelsson, G. (2002). A photosystem II-associated carbonic anhydrase regulates the efficiency of photosynthetic oxygen evolution. EMBO J. **21,** 1930-1938.

Vitlin Gruber, A., and Feiz, L. (2018). Rubisco Assembly in the Chloroplast. Frontiers in molecular biosciences **5,** 24 (21-11).

Wachter, R.M., Salvucci, M.E., Carmo-Silva, A.E., Barta, C., Genkov, T., and Spreitzer, R.J. (2013). Activation of interspecies-hybrid Rubisco enzymes to assess different models for the Rubisco-Rubisco activase interaction. Photosynth Res **117,** 557-566.

Wakao, S., Shih, P.M., Guan, K., Schackwitz, W., Ye, J., Shih, R.M., Chovatia, M., Sharma, A., Martin, J., Wei, C.-L., and Niyogi, K.K. (2021). Discovery of photosynthesis genes through whole-genome sequencing of acetate-requiring mutants of *Chlamydomonas reinhardtii*. bioRxiv**,** 2021.2002.2017.431526.

Wang, H., Gau, B., Slade, W.O., Juergens, M., Li, P., and Hicks, L.M. (2014). The global phosphoproteome of Chlamydomonas reinhardtii reveals complex organellar phosphorylation in the flagella and thylakoid membrane. Molecular & cellular proteomics : MCP **13,** 2337-2353.

Wang, L., Yamano, T., Takane, S., Niikawa, Y., Toyokawa, C., Ozawa, S.-I., Tokutsu, R., Takahashi, Y., Minagawa, J., Kanesaki, Y., Yoshikawa, H., and Fukuzawa, H. (2016). Chloroplast-mediated regulation of CO_2-concentrating mechanism by Ca^{2+}-binding protein CAS in the green alga Chlamydomonas reinhardtii. Proc. Natl. Acad. Sci. U. S. A. **113,** 12586-12591.

Wang, Y., and Spalding, M.H. (2006). An inorganic carbon transport system responsible for acclimation specific to air levels of CO_2 in *Chlamydomonas reinhardtii*. Proceedings of the National Academy of Sciences **103,** 10110-10115.

Wang, Y., and Spalding, M.H. (2014a). Acclimation to very low CO_2: contribution of limiting CO2 inducible proteins, LCIB and LCIA, to inorganic carbon uptake in *Chlamydomonas reinhardtii*. Plant Physiol. **166,** 2040-2050.
Wang, Y., and Spalding, M.H. (2014b). LCIB in the Chlamydomonas CO_2-concentrating mechanism. Photosynthesis research **121,** 185-192.
Wang, Y., Stessman, D.J., and Spalding, M.H. (2015). The CO2 concentrating mechanism and photosynthetic carbon assimilation in limiting CO2 : how Chlamydomonas works against the gradient. The Plant Journal **82,** 429-448.
Wang, Z.Y., Snyder, G.W., Esau, B.D., Portis, A.R., and Ogren, W.L. (1992). Species-dependent variation in the interaction of substrate-bound ribulose-1,5-bisphosphate carboxylase/oxygenase (rubisco) and rubisco activase. Plant Physiol **100,** 1858-1862.
Wasmann, C.C., Ramage, R.T., Bohnert, H.J., and Ostrem, J.A. (1989). Identification of an assembly domain in the small subunit of ribulose-1,5-bisphosphate carboxylase. Proceedings of the National Academy of Sciences of the United States of America **86,** 1198-1202.
Wei, L., Derrien, B., Gautier, A., Houille-Vernes, L., Boulouis, A., Saint-Marcoux, D., Malnoe, A., Rappaport, F., de Vitry, C., Vallon, O., Choquet, Y., and Wollman, F.A. (2014). Nitric oxide-triggered remodeling of chloroplast bioenergetics and thylakoid proteins upon nitrogen starvation in *Chlamydomonas reinhardtii*. The Plant cell **26,** 353-372.
Westrich, L.D., Gotsmann, V.L., Herkt, C., Ries, F., Kazek, T., Trosch, R., Armbruster, L., Muhlenbeck, J.S., Ramundo, S., Nickelsen, J., Finkemeier, I., Wirtz, M., Storchova, Z., Raschle, M., and Willmund, F. (2021). The versatile interactome of chloroplast ribosomes revealed by affinity purification mass spectrometry. Nucleic acids research **49,** 400-415.
Whitney, S.M., and Andrews, T.J. (2001). Plastome-encoded bacterial ribulose-1,5-bisphosphate carboxylase/oxygenase (RubisCO) supports photosynthesis and growth in tobacco. Proceedings of the National Academy of Sciences of the United States of America **98,** 14738-14743.
Whitney, S.M., Birch, R., Kelso, C., Beck, J.L., and Kapralov, M.V. (2015). Improving recombinant Rubisco biogenesis, plant photosynthesis and growth by coexpressing its ancillary RAF1 chaperone. Proceedings of the National Academy of Sciences **112,** 3564-3569.
Wiechert, M., and Beitz, E. (2017). Mechanism of formate–nitrite transporters by dielectric shift of substrate acidity. The EMBO journal **36,** 949-958.
Wienkoop, S., Weiss, J., May, P., Kempa, S., Irgang, S., Recuenco-Munoz, L., Pietzke, M., Schwemmer, T., Rupprecht, J., Egelhofer, V., and Weckwerth, W. (2010). Targeted proteomics for *Chlamydomonas reinhardtii* combined with rapid subcellular protein fractionation, metabolomics and metabolic flux analyses. Molecular bioSystems **6,** 1018-1031.
Wietrzynski, W. (2017). Rubisco biogenesis and assembly in Chlamydomonas reinhardtii (Université Pierre et Marie Curie - Paris VI).
Wietrzynski, W., Traverso, E., Wollman, F.A., and Wostrikoff, K. (2021). The state of oligomerization of Rubisco controls the rate of synthesis of the Rubisco large subunit in Chlamydomonas reinhardtii. The Plant cell.
Wilson, R.H., Martin-Avila, E., Conlan, C., and Whitney, S.M. (2018). An improved Escherichia coli screen for Rubisco identifies a protein-protein interface that can enhance CO_2-fixation kinetics. The Journal of biological chemistry **293,** 18-27.
Wilson, R.H., Thieulin-Pardo, G., Hartl, F.U., and Hayer-Hartl, M. (2019). Improved recombinant expression and purification of functional plant Rubisco. FEBS letters **593,** 611-621.
Winder, T.L., Anderson, J.C., and Spalding, M.H. (1992). Translational Regulation of the Large and Small Subunits of Ribulose Bisphosphate

Carboxylase/Oxygenase during Induction of the CO_2-Concentrating Mechanism in Chlamydomonas reinhardtii. Plant Physiol **98,** 1409-1414.

Wunder, T., Cheng, S.L.H., Lai, S.-K., Li, H.-Y., and Mueller-Cajar, O. (2018). The phase separation underlying the pyrenoid-based microalgal Rubisco supercharger. Nat. Commun. **9,** 5076.

Xia, L.Y., Jiang, Y.L., Kong, W.W., Sun, H., Li, W.F., Chen, Y., and Zhou, C.Z. (2020). Molecular basis for the assembly of RuBisCO assisted by the chaperone Raf1. Nat. Plants **6,** 708-717.

Xiang, Y., Zhang, J., and Weeks, D.P. (2001). The Cia5 gene controls formation of the carbon concentrating mechanism in Chlamydomonas reinhardtii. Proc. Natl. Acad. Sci. U. S. A. **98,** 5341-5346.

Yamano, T., Sato, E., Iguchi, H., Fukuda, Y., and Fukuzawa, H. (2015). Characterization of cooperative bicarbonate uptake into chloroplast stroma in the green alga Chlamydomonas reinhardtii. Proceedings of the National Academy of Sciences **112,** 7315-7320.

Yamano, T., Tsujikawa, T., Hatano, K., Ozawa, S.-I., Takahashi, Y., and Fukuzawa, H. (2010). Light and Low-CO2-Dependent LCIB–LCIC Complex Localization in the Chloroplast Supports the Carbon-Concentrating Mechanism in Chlamydomonas reinhardtii. Plant & Cell Physiology **51,** 1453-1468.

Yang, T., Liu, Q., Kloss, B., Bruni, R., Kalathur, R.C., Guo, Y., Kloppmann, E., Rost, B., Colecraft, H.M., and Hendrickson, W.A. (2014). Structure and selectivity in bestrophin ion channels. Science **346,** 355-359.

Ynalvez, R.A., Xiao, Y., Ward, A.S., Cunnusamy, K., and Moroney, J.V. (2008). Identification and characterization of two closely related beta-carbonic anhydrases from Chlamydomonas reinhardtii. Physiol. Plant. **133,** 15-26.

Yosef, I., Irihimovitch, V., Knopf, J.A., Cohen, I., Orr-Dahan, I., Nahum, E., Keasar, C., and Shapira, M. (2004). RNA binding activity of the ribulose-1,5-bisphosphate carboxylase/oxygenase large subunit from Chlamydomonas reinhardtii. J. Biol. Chem. **279,** 10148-10156.

Yoshioka, S., Taniguchi, F., Miura, K., Inoue, T., Yamano, T., and Fukuzawa, H. (2004). The Novel Myb Transcription Factor LCR1 Regulates the CO_2-Responsive Gene Cah1, Encoding a Periplasmic Carbonic Anhydrase in *Chlamydomonas reinhardtii*. The Plant cell **16,** 1466-1477.

Yu, K., Lujan, R., Marmorstein, A., Gabriel, S., and Hartzell, H.C. (2010). Bestrophin-2 mediates bicarbonate transport by goblet cells in mouse colon. J. Clin. Invest. **120,** 1722-1735.

Zaffagnini, M., Bedhomme, M., Groni, H., Marchand, C.H., Puppo, C., Gontero, B., Cassier-Chauvat, C., Decottignies, P., and Lemaire, S.D. (2012). Glutathionylation in the photosynthetic model organism *Chlamydomonas reinhardtii:* a proteomic survey. Molecular & cellular proteomics : MCP **11,** M111 014142.

Zhan, Y., Dhaliwal, J.S., Adjibade, P., Uniacke, J., Mazroui, R., and Zerges, W. (2015). Localized control of oxidized RNA. J. Cell Sci. **128,** 4210-4219.

Zhan, Y., Marchand, C.H., Maes, A., Mauries, A., Sun, Y., Dhaliwal, J.S., Uniacke, J., Arragain, S., Jiang, H., Gold, N.D., Martin, V.J.J., Lemaire, S.D., and Zerges, W. (2018). Pyrenoid functions revealed by proteomics in *Chlamydomonas reinhardtii*. PloS one **13,** e0185039.

Zhang, S., Zhou, H., Yu, F., Gao, F., He, J., and Liu, C. (2016). Functional Partition of Cpn60alpha and Cpn60beta Subunits in Substrate Recognition and Cooperation with Co-chaperonins. Molecular plant **9,** 1210-1213.

Zhang, Z., Shrager, J., Jain, M., Chang, C.W., Vallon, O., and Grossman, A.R. (2004). Insights into the survival of *Chlamydomonas reinhardtii* during sulfur starvation based on microarray analysis of gene expression. Eukaryotic cell **3,** 1331-1348.

Zhao, Q., Zhang, X., Sommer, F., Ta, N., Wang, N., Schroda, M., Cong, Y., and Liu, C. (2019). Hetero-oligomeric CPN60 resembles highly symmetric group-I chaperonin structure revealed by Cryo-EM. The Plant journal : for cell and molecular biology **98,** 798-812.

Zhou, Y., and Whitney, S. (2019). Directed Evolution of an Improved Rubisco; In Vitro Analyses to Decipher Fact from Fiction. International journal of molecular sciences **20**.

Zhu, G., and Spreitzer, R.J. (1994). Directed mutagenesis of chloroplast ribulosebisphosphate carboxylase/oxygenase. Substitutions at large subunit asparagine 123 and serine 379 decrease CO_2/O_2 specificity. The Journal of biological chemistry **269,** 3952-3956.

Zones, J.M., Blaby, I.K., Merchant, S.S., and Umen, J.G. (2015). High-Resolution Profiling of a Synchronized Diurnal Transcriptome from Chlamydomonas reinhardtii Reveals Continuous Cell and Metabolic Differentiation. The Plant cell **27,** 2743-2769.

Zoschke, R., and Barkan, A. (2015). Genome-wide analysis of thylakoid-bound ribosomes in maize reveals principles of cotranslational targeting to the thylakoid membrane. Proceedings of the National Academy of Sciences of the United States of America **112,** E1678-1687.

Zybailov, B., Rutschow, H., Friso, G., Rudella, A., Emanuelsson, O., Sun, Q., and van Wijk, K.J. (2008). Sorting signals, N-terminal modifications and abundance of the chloroplast proteome. PloS one **3,** e1994.